2011

Characterization of Aminopeptidase PepZ in Staphylococcus aureus Virulence

Tiffany Marie Robison
University of South Florida, tmroger2@mail.usf.edu

Characterization of Aminopeptidase PepZ in *Staphylococcus aureus* Virulence

by

Tiffany M. Robison

A thesis submitted in partial fulfillment
of the requirements for the degree of
Master of Science
Department of Cell Biology, Microbiology, Molecular Biology
College of Arts and Sciences
University of South Florida

Major Professor: Lindsey N. Shaw, Ph.D.
James T. Riordan, Ph.D.
Stanley M. Stevens, Ph.D.

Date of Approval:
October 31, 2011

Keywords: CA-MRSA, Exopeptidase, Nutrition, Mass Spectrometry, 2D-DIGE

Acknowledgements

I owe my deepest gratitude to my mentor and advisor, Dr. Lindsey N. Shaw, for his encouragement, guidance and advice throughout my graduate studies and thesis writing. I would also like to thank my committee members, Dr. James T. Riordan and Dr. Stanley M. Stevens for their support and assistance throughout this project. Additionally, I am extremely grateful for all of the members of the Shaw, Riordan and Stevens labs for all of their assistance needed for the completion of this project as well. I am also very appreciative for all of the members and staff of the CMMB department for all of your encouragement and support while as a graduate student at USF.

Table of Contents

List of Figures iv

List of Tables vi

Abstract vii

Introduction 1
- *Staphylococcus aureus* is an Opportunistic Pathogen 1
- Manifestation of *S. aureus* Infection 1
- Antibiotic Resistance in *S. aureus* 2
- Community-Acquired *S. aureus* 4
- Toxin Production in *S. aureus* 5
- Proteolytic Enzymes 6
- Proteases of *S. aureus* 8
- Aminopeptidases 9
- Metalloaminopeptidases 10
- Leucine Specific Aminopeptidases 11
- Aminopeptidases of *S. aureus* 11
- Aminopeptidases in Bacterial Pathogenesis 13

Materials and Methods 15
- Culture Media 15
- Buffers and Reagents 20
- Bacterial Strains, Plasmids and Primers 24
- Transformations 24
- Electroporation of *S. aureus* 25
- Phage Transductions of *S. aureus* 25
- Construction of a *pepZ* mutant 25
- Construction of *pepZ-lacZ* Reporter Gene Fusions 26
- Transcriptional Analysis 26
  - Transcriptional Analysis of *pepZ* Expression 26
  - Transcriptional Disk Diffusion Assays 27
- Growth and Nutrition Profiling 27
  - Growth Analysis in Peptide Based Media 27
  - Long-Term Starvation Analysis 28
  - Competitive Growth Analysis 28
- Proteomic Analysis 29

Cytoplasmic Protein Extraction 29
Secreted Protein Extraction 29
Western Blot Detection 30
2D Difference Gel Electrophoresis (DIGE) 30
Trypsin Digestion 31
Desalt 31
Virulence Assays 32
Murine Model of Septic Arthritis 32
Biofilm Formation Analysis 32
Human Macrophage Survival and Clearance 33
Murine Model of Wound Formation 33
Murine Model of Bacterial Sepsis 33
Phenotypic Characterization 34
Growth Profiling using Chemically Defined Media 34
Evaluating Carbon Utilization 34
Lysis Kinetics 34
Heat Shock 35
Heat Stress 35
Oxidative Stress 35
Disk Diffusions 36

Results 37
Analysis of the Virulence of a *S. aureus pepZ* mutant using a Murine Model of Septic Arthritis 37
Profiling *pepZ* Expression using a *lacZ* Reporter Fusion 39
Evaluating the Effects of Environmental Stimuli of *pepZ* Transcription 41
Investigation of the Role of PepZ during *S. aureus* Growth in Peptide Rich Media 43
Investigating the Role of PepZ during Long-Term Starvation 45
Competitive Growth Analysis Reveals *pepZ* mutants are Impaired in their Ability to Compete with Wild-Type Strains 50
Anaerobic Stress Profiling of PepZ using Chemically Defined Media 55
Evaluating the Role of PepZ in *S. aureus* Carbon Utilization using Chemically Defined Media 57
Characterization of the Role of PepZ in Membrane Integrity and Autolysis 58
Evaluating the Role of PepZ in Cellular Survival Following Exposure to Elevated Temperature 59
Assessing the Role of PepZ in Response to Oxidative Stresses 61
General Stress Profiling of *pepZ* mutant Strains using a Modified Kirby-Bauer Assay 62
Characterization of the Subcellular Localization of PepZ 62
Exploring Potential Substrates for the PepZ Enzyme using 2D Difference Gel Electrophoresis (DIGE) and Tandem Mass Spectrometry 65
Exploring the Role of PepZ in the Formation of Biofilms 79
Analysis of the Importance of PepZ during Interaction with Components of the Human Immune System 80

Further Characterization of the Role of PepZ in *S. aureus* Virulence using a Murine Model of Wound Formation....81
Evaluating the Role of *pepZ* in CA-MRSA Sepsis using a Mouse Model....82

Discussion....84

Future Directions....95

References....97

Appendices....112

Appendix 1. Secreted Spots Determined by Mass Spectrometry Analysis to Have Undetectable Protein Levels....113

List of Figures

Figure 1. Characterization of the Role of PepZ in Systemic Dissemination using a Murine Model of Septic Arthritis 38

Figure 2. Physical Map of the Plasmid pAZ106 used to construct *pepZ-lacZ* Reporter Gene Fusions in *S. aureus* 39

Figure 3. Transcriptional Analysis of *pepZ* Expression in Liquid Media 40

Figure 4. Analysis of Growth in Peptide Based Media 45

Figure 5. Long-Term Starvation Response of *pepZ* mutants Grown in TSB 47

Figure 6. Starvation Response of Newman *pepZ* mutants Grown in Peptide Based Media 49

Figure 7. Starvation Response of CA-MRSA *pepZ* mutants in Peptide Based Media 49

Figure 8. Competitive Growth Analysis of a Newman *pepZ* mutant and Parent Strain in Peptide Based Media 51

Figure 9. Competitive Growth Analysis of a USA300 FPR *pepZ* mutant and Parental Strain in Peptide Based Media 52

Figure 10. Competitive Growth Analysis of a Newman *pepZ* mutant and Parent Strain in TSB 53

Figure 11. Competitive Growth Analysis of a USA300 FPR *pepZ* mutant and Parent Strains in TSB 53

Figure 12. Competitive Growth Analysis of a USA300 FPR *pepZ* mutant and Parent Strain 55

Figure 13. Competitive Growth Analysis of a Newman *pepZ* mutant and Parent Strain 55

Figure 14. Anaerobic Growth Analysis of *pepZ* mutants using Amino

Acid Limited Media....56

Figure 15. Anaerobic Growth Analysis of a USA300 FPR *pepZ* mutant Limited for Phosphate....57

Figure 16. Anaerobic Growth Analysis of a USA300 FPR *pepZ* mutant on Mannitol Salt Agar....57

Figure 17. The Role of PepZ in Membrane Integrity and Autolysis....59

Figure 18. The Role of PepZ in Response to Elevated Temperatures....61

Figure 19. Western Blot Detection of PepZ in Strain Newman....64

Figure 20. Western Blot Detection of PepZ in Strain USA300 FPR....64

Figure 21. Detection of PepZ during Continuous Growth of Strain Newman....65

Figure 22. Intracellular Proteome Analysis of *S. aureus* USA300 FPR and its *pepZ* mutant using 2D-DIGE....67

Figure 23. Secretome Analysis of *S. aureus* USA300 FPR and its *pepZ* mutant using 2D-DIGE....71

Figure 24. The Role of PepZ in the Formation of an *S. aureus* Biofilm....80

Figure 25. Characterization of the Role of PepZ in Human Immune System Interactions....81

Figure 26. PepZ is required for Full Virulence of CA-MRSA Strains in a Murine Model of Wound Formation....82

Figure 27. The Role of *pepZ* in CA-MRSA Sepsis....83

Figure 28. BLAST Analysis of PepZ Reveals Homology to Intracellular Leucine Specific Aminopeptidases from Other Organisms....85

List of Tables

Table 1. Bacterial Strains and Plasmids 24

Table 2. Primer Sequences 24

Table 3. Chemical Stress List 42

Table 4. Stressor Compounds Identified to Induce *pepZ* Transcription 43

Table 5. Intracellular Proteome Analysis of *S. aureus* USA300 FPR and its *pepZ* mutant using Mass Spectrometry 68

Table 6. Intracellular Protein Spots Identified by 2D-DIGE and Mass Spectrometry Analysis to Have Altered Protein Stability 70

Table 7. Secretome Analysis of *S. aureus* USA300 FPR and its *pepZ* mutant using Mass Spectrometry 72

Table 8. Secreted Protein Spots Identified by 2D-DIGE and Mass Spectrometry Analysis to Have Altered Protein Stability 75

Introduction

***Staphylococcus aureus* is an Opportunistic Pathogen.** *Staphylococcus aureus* is a Gram-positive, non-sporeforming bacteria, first observed in the 1880s [Ogston, 1984]. Cells of this organism arrange as clusters of round golden spheres, or cocci; and have a range in diameter of between 0.7 µm to 1.2 µm. The genome of *S. aureus* is approximately 2.8 Mbp with a G+C content of 33% [Gill et al., 2005; Kuroda et al., 2001]. As a facultative anaerobe, *S. aureus* can respire in the presence of oxygen, or undergo fermentation in the absence of oxygen. Optimal growth of *S. aureus* is achieved at temperatures of 25°C to 43°C and at pH levels of 4.8 to 9.4 [Novick, 2006].

Manifestation of *S. aureus* Infection. *S. aureus* is ubiquitous throughout nature as both a pathogen and commensal organism of humans, which are its natural reservoir [Lowry, 1998]. Approximately 30% of the adult population harbors this microbe asymptomatically in the anterior of their nares. This carrier population contributes to the transmission of *S. aureus* primarily through direct contact with sites of infection or areas of colonization [Wertheim et al., 2004]. The manifestation of *S. aureus* infection or disease is remarkably broad and diverse, ranging from localized acute soft tissue infections to life threating septicemia. Soft tissue or localized wound infections commonly begin as a small pimple at the site of infection. Often these lead to boils, carbuncles, or furuncles as the infection progresses [Lowry, 1998]. Further, these initial

foci of infection can rapidly lead to more invasive diseases, which can often result in the irreversible degradation of host tissues and muscle. Severe *S. aureus* infections can manifest as necrotizing diseases (e.g. necrotizing fasciitis and necrotizing pneumonia), systemic bacteremia, endocarditis, osteomyelitis and septic arthritis [Fowler et al., 2005]. The pathogenic success of *S. aureus* is largely based on regulatory networks that coordinate the expression of bacterial virulence factors. This is achieved by global regulators that modulate temporal gene expression according to changes in the environment [Chan and Foster, 1998; Novick, 2006; Yarwood et al., 2001].

Antibiotic Resistance in *S. aureus*. *S. aureus* is a remarkably successful pathogen, with overwhelming resistance to antibiotic therapies. The incidence of infections due to antibiotic resistant strains has achieved epidemic proportions, and is primarily the consequence of methicillin resistant *S. aureus*, or MRSA, strains [Chambers, 2001; Kaplan et al., 2005; Klevens et al., 2007]. In 2004, MRSA accounted for nearly 60% of all *S. aureus* infections reported for patients staying in intensive care units [National Nosocomial Infections Surveillance (NNIS) System Report, 2004. Methicillin resistant *S. aureus* is now believed to be the leading cause of death by a single infectious agent in the United States [Kobayashi and DeLeo, 2009]. The antibiotic penicillin was first introduced in the early 1940s, and by 1944, the first resistant isolates of *S. aureus* to emerged [Barber and Rozwadowska-Dowzenko, 1948]. These strains developed in healthcare settings from an acquired penicillinase encoded on a plasmid [Ridley et al., 1970]. Penicillinase inactivates the functional β-lactam ring though a targeted cleavage event, negating the activity of the drug [Discussion on Penicillin, 1994; Wu et al., 2001].

Despite these efforts, by 1960 80% of all *S. aureus* strains were penicillin resistant, and were spreading at pandemic proportions throughout both the community and hospital settings [Ridley et al., 1970]. As of 2008, more than 90% of all *S. aureus* isolates possessed penicillinase-mediated penicillin resistance [Tenover, 2008]. In 1959, methicillin was developed for the treatment of penicillin resistant *S. aureus* infections [Batchelor et al., 1959]. Methicillin is a semi-synthetic antimicrobial with an ortho-dimethoxyphenyl side group, which prevents penicillinase access to the β-lactam ring by steric hindrance [Klein and Finland, 1963]. The use of methicillin for treating penicillin resistant *S. aureus* infections was short lived, and within two years of its introduction the first resistant strain was isolated [Jevons, 1961]. In *S. aureus*, methicillin resistance occurs through the chromosomally encoded *mecA* gene, which specifies a low affinity binding protein PBP2a. The β-lactam activity of methicillin inactivates native penicillin binding proteins, which is counteracted through the transpeptidase activity of PBP2a. Thus, the controlled expression of PBP2a allows cell wall synthesis to continue even at high β-lactam concentrations [Ito et al., 1999; Wu et al., 2001]. The *mecA* gene resides on the mobile cassette element SCC*mec*, and integrates into the chromosome at a locus of unknown function, *orfX*. The procurement of SCC*mec* by *S. aureus* confers resistance to the entire class of β-lactam antibiotics, and is presumed to have initially evolved in *Staphylococcus sciuri* [Wu et al., 2001]. Therefore, glycopeptides are often the preferred therapy for severe MRSA infections and include the antibiotic vancomycin. Vancomycin targets cell wall transpeptidation by blocking or altering the D-Ala-D-Ala motif of the glycan chains. Isolation of *S. aureus* strains with reduced vancomycin susceptibility (VISA) was first reported in 1996 in Japan [Reduced susceptibility of *Staphylococcus*

aureus to vancomycin, 1997]. Reduced vancomycin susceptibility evolved in *S. aureus* according to the selective pressures associated with the over utilization of the antibiotic to treat *S. aureus* infections. Many studies attribute this to minor changes in key regulatory elements involved in cell wall metabolism [Cui et al., 2009; Meehl et al., 2007; Mwangi et al., 2007]. True vancomycin resistant *S. aureus* (VRSA) first surfaced in the United States in 2002, presenting a serious threat public health [*Staphylococcus aureus* resistant to vancomycin–United States, 2002, vancomycin-resistant *Staphylococcus aureus*–Pennsylvania, 2002]. Resistance in VRSA strains is primarily mediated by the *vanA* gene, which seems to be acquired through a conjugation event with enterococcal species [Evers et al., 1996].

Community-Acquired *S. aureus.* *S. aureus* infections have historically been confined to the hospital setting, largely populated with immunocompromised individuals [Deresinski, 2005]. However, in 1999 highly virulent MRSA strains were reported in the community, outside of the nosocomial setting [Four Pediatric Deaths From Community-Acquired Methicillin-Resistant *Staphylococcus aureus*—Minnesota and North Dakota, 1999; Fridkin et al., 2005]. Infections caused by Community-associated *S. aureus* strains (CA-MRSA) began emerging in healthy young adults, having no predisposing factors for *S. aureus* infections; including recent hospitalizations, underlying medical issues or history of *S. aureus* infection [Kobayashi and DeLeo, 2009]. These strains were highly virulent, causing severe necrotic skin and soft tissue infections, and demonstrated an affinity for individuals in highly populated or overcrowded areas, thereby contributing to increased rates of transmission. These areas include places such as jails and military barracks

[Aiello et al., 2006; Pan et al., 2003]. Factors contributing to the pathogenic success of CA-MRSA remain largely controversial and undefined; however two theories prevail regarding the virulent phenotype associated with these strains. In a study by Li et al., [Li et al., 2009], the virulent CA-MRSA phenotype was shown to be the result of differentially expressed intrinsic elements, largely attributable to an overactive *agr* locus. These findings differ from previous observations, in which acquired mobile genetic elements were implicated in the hyper-virulent phenotype, largely mediated through the pro-phage encoded Panton-Valentine leukocidin toxin (PVL), and the arginine catabolic mobile element. These mobile genetic elements have been suggested to aid in the increased rates of transmission observed in CA-MRSA strains, as well as immune evasion strategies associated through the cytolytic activity of the PVL toxin [Deresinski, 2005; Diep et al., 2008; Li et al., 2009]. CA-MRSA strains, while highly virulent, remain susceptible to many non β-lactam antibiotics [Chambers, 2001]. Treatment options are however limited, particularly in light of reported CA-MRSA isolates with decreased vancomycin susceptibility [Graber et al.].

Toxin Production in *S. aureus.* *S. aureus* is a highly ubiquitous organism that has been implicated in a wide spectrum of diseases ranging from skin and soft tissue infections to life threatening septicemia [Lowry, 1998]. These manifestations of disease are the result of virulence factors expressed by the organism, and include toxins, hemolysins, and proteases [Novick, 2006]. Typically, these are secreted factors which directly interact with the host during infection, and facilitate invasion and colonization [Cheung et al., 1992, 2008; Janzon et al., 1989; Peng et al., 1988]. The secretion of toxins in *S. aureus* is

controlled by global regulators that coordinate gene expression in a cell density and growth phase dependent manner. This is achieved through the upregulation of factors for invasion, adhesion and colonization, which facilitate the initial stages of infection. This differs from cells approaching later growth phases, in which factors for invasion are upregulated and those for colonization are down regulated. These later stages of growth utilize exotoxins to spread throughout host tissues; achieved through the activities of hemolysins, cytotoxins, proteases and leukocidins, etc. [Janzon et al., 1989; Novick, 2006, 1993; Peng et al., 1988].

Proteolytic Enzymes. Proteases function in a wide variety of essential regulatory and housekeeping functions. Their importance is demonstrated by the observation that 2-3% of the total gene products in all organisms are proteolytic enzymes [Rawlings et al., 2002]. Proteases are proteins that catalyze the cleavage of amide bonds in peptides via exopeptidase or endopeptidase activity [Sarnovsky et al., 1929; Rawlings and Barrett, 1995]. Exopeptidases cleave peptide bonds proximal to the amino or carboxy terminus, releasing free amino acids or small peptides [McDonald, 1986]. Endopeptidases cleave internal peptide bonds, and release oligopeptides. Protein hydrolysis is further defined according to the functional roles of active site residues [Taylor, 1993]. These functional groups required for catalysis consist of serine, aspartic, cysteine, prolyl or metal cofactor requiring metallo amino acid residues [Rawlings et al., 2002]. Serine proteases contain a serine residue at their active site that covalently binds and processes substrates of broad specificity [Rawlings and Barrett, 2004]. Aspartic proteases catalyze the hydrolysis of peptide bonds from each end of aromatic or bulky amino acid residue containing

substrates. These proteases catalyzed acid-base reactions by virtue of two aspartic residues located at their active site [Rawlings and Barrett, 1995]. Cysteine proteases contain an active site cysteine residue, which requires a reducing agent for enzymatic activity [Rawlings and Barrett, 2004]. Prolyl proteases are proline specific peptidases that catalyze the cleavage of amide bonds following a proline residue or an imide bond that precedes it. These proteases demonstrate full activity in the presence of manganese ions, and maintain substantial sequence homology to various peptidases that require divalent metal ions for catalysis [Bazan et al., 1994; Yaron and Naider, 1993]. Metalloproteases require divalent metal ions at their active site to drive peptide hydrolysis, and are highly diverse. These proteases are organized according to the conserved sequences that bind metal ions at their active sites, often HEXXH [Bazan et al., 1994; Rawlings et al., 2002; Taylor, 1993].

Proteases are further differentiated according to their cellular location, either intracellularly, membrane/wall associated or secreted into the external environment. This is largely dependent on the target substrates, enzymatic specificity and the fate of the peptides released during hydrolysis. Generally, intracellular proteases function in processes such as cell metabolism or sporulation [Dancer and Mandelstam, 1975; Sussman and Gilvarg, 1971]. For example, the Lon and ATP-dependent proteases of *Escherichia coli* regulate the destruction of damaged proteins in response to environmental stress [Chung and Goldberg, 1981]. This type of response is necessary to prevent the aggregation of hydrophobic residues that are exposed when proteins denature due to heat or acid shock. Endopeptidase activities mediated by outer membrane

permeases provide the required transport of oligopeptides into the cell, once produced by extracellular proteases. This activity is commonly vital for cell viability, and provides exogenous sources of amino acids [Sussman and Gilvarg, 1971]. In addition to nutritional roles, secreted proteases regulate protein maturation and activation events. This can be achieved at the post translational level, when proteins are secreted in inactive zymogen configurations [Drapeau et al., 1972; Rice et al., 2001; Schneewind et al., 1992; Shaw et al., 2004]. One such example is seen in the programmed cell death and/or apoptosis of eukaryotic cells. Apoptosis is mediated by caspase proteins that are synthesized and secreted in an inactive form. To achieve a functional state, post translational proteolytic processing must occur. This level of regulation ensures cell death signals are not prematurely released [Kerr et al., 1972]. Further, the secreted protease of *Pseudomonas aeruginosa*, elastase, has been implicated in the activation of host matrix metalloproteases, and ultimate deregulation of host tissue destruction [Sorsa, 1992]. Membrane bound proteases serve an array of functions in the microbial cell, including regulatory and nutritional roles, including the membrane bound protease of *E. coli*, RseP. RseP functions in a two-step proteolytic cleavage process, known as regulated intramembrane proteolysis, and assists in the induction process of σ^E under conditions of stress, allowing for the rapid modification of gene transcription profiles [Akiyama et al., 2004].

Proteases of *S. aureus*. The *S. aureus* genome encodes 132 putative proteases and 42 non-peptidase homologs [Merops]. Ten of the putative or characterized proteases are secreted into the external environment in a temporally-regulated manner; V8 serine-

protease (SspA), staphophain A (ScpA), staphophain B (SspB), aureolysin (Aur), and the serine-protease like enzymes (SplABCDEF) [Chan and Foster, 1998; Karlsson and Arvidson, 2002; Rice et al., 2001; Shaw et al., 2004]. Many of these secreted proteases have been characterized extensively and have been shown to contribute to the progression of disease in *S. aureus* [Karlsson and Arvidson, 2002; Lindsay and Foster, 1999; McAleese et al., 2001; McGavin et al., 1997]. The switch of infectious states from adhesion to invasion has been suggested to be primarily driven by the interplay of these secreted proteases, and cell adhesion and colonization factors [McGavin et al., 1997]. Indeed, multiple groups [Boles and Horswill, 2008; Beenken et al., 2010; Tsang et al., 2008] identified this kind of modification of protein profiles during the detachment stages of *S. aureus* biofilm. Specifically, an increase in the proteolytic activities of Aur and SplABCDEF was observed during detachment, whereas adhesion proteins were down regulated. These results are in accordance with the previously reported cleavage of an *S. aureus* adhesion protein clumping factor B, ClfB, by Aur [McAleese et al., 2001]. Moreover, bacterial sepsis, aided by the cysteine proteases ScpA and SspB, was shown to impact the severity and progression of infection and invasion [Imamura et al., 2005].

Aminopeptidases. Aminopeptidases are exopeptidases that liberate small peptides from oligopeptides providing cellular sources of energy and nutrition [Christensen et al., 1999; Li et al., 2009; Matsui et al., 2006]. This is typically achieved through the generation of free amino acids, which are later catabolized for use as intermediates in central metabolic pathways. Aminopeptidases are often substrate specific, and maintain conserved active site residues and folding patterns. These specific properties enable the sub-categorization

of proteolytic enzymes into the following evolutionary based clans according to the catalytic metals required for their active site residues, clans MF, MG, and MH, and are explained in further detail below [Rawlings et al., 2002, Rawlings and Barrett, 2004; Sussman and Gilvarg, 1971].

Metalloaminopeptidases. The metalloaminopeptidases are the largest and the most homogenous aminopeptidase family. They are arranged into 25 families according to the three conserved active site residues, histidine, glutamine, lysine and/or aspartate. These families are further defined by evolutionary derived clans; MF, MG, and MH respectively [Rawlings et al., 2002, Rawlings and Barrett, 2004]. Many of these peptidase families require divalent metal ions at their active site to drive catalysis; most commonly zinc. Metalloaminopeptidase clan MF is characterized by aminopeptidases that require two zinc ions at their active site for catalysis, and includes the leucine aminopeptidase from bovine lens [Kim and Lipscomb, 1993]. Clan MG metallopeptidases require either divalent cobalt or manganese ions for activity. One such example of peptidases typified by this clan is the highly conserved methionine aminopeptidases, which is required for the maturation of newly synthesized proteins [Bazan et al., 1994; Ben-Bassat et al., 1987]. The proteolytic enzymes characterized by clan MH represent a diverse mixture of aminopeptidases, carboxypeptidases and dipeptidases, and typically require divalent zinc ions at their active site, commonly aspartyl aminopeptidases [Russo and Baumann, 2004; Franzetti et al., 2002].

Leucine Specific Aminopeptidases. The M17 family of the metallopeptidases clan MF represents one of the most extensively studied classes of aminopeptidases. These are the leucyl aminopeptidases, and require divalent zinc ions for catalysis [Kim and Lipscomb, 1993]. These peptidases have distinct active sites, with paired lysine and aspartic residues for zinc ion binding, in addition to the catalytically active glutamic acid residues [Rawlings and Barrett, 2004]. Leucine specific aminopeptidases drive hydrolysis of the amide bonds from hydrophobic N-terminal amino acids, as well as di- and tripeptides. The best studied of these aminopeptidases is that from bovine lens, which assembles into a bilobal hexamer consisting of six 54 kDa subunits [Cuypers et al., 1982]. This structure is maintained by hydrogen bonds and van der walls interactions, and inhibited by metal chelating agents [Sussman and Gilvarg, 1971]. A homolog of the bovine leucine aminopeptidase was identified in *E. coli*, and is termed aminopeptidase A or PepA [Strater et al., 1999]. Protein sequence analysis reveals that PepA shares 31% amino acid identity overall, and a 52% amino acid identity at the carboxy terminus, with the bovine lens enzyme [Stirling et al., 1989]. *E. coli* aminopeptidase A is a multifunctional protease with DNA-binding activities, regulated by three distinct promoters [Woolwine and Wozniak, 1999]. It is catalytically activated in the presence of manganese and presumed to function in peptide turnover and/or metabolism [Miller, 1996]. In addition, the DNA-binding activities of PepA are essential to ColE1 plasmid inheritance and Xer site recombination [Cheung et al., 1992].

Aminopeptidases of *S. aureus.* Thirteen aminopeptidases are encoded in the genome of *S. aureus*, many of which remain uncharacterized. These include aminopeptidases: *pepA*$_1$,

pepA$_2$, *pepA*$_3$, *pepF*$_1$, *pepF*$_2$, *pepM*, *pepP*, *pepQ*, *pepS*, *pepT*$_1$, *pepT*$_2$, *pepV* and *pepZ* [Gill et al., 2005; Sobral et al., 2007; Shaw unpublished observation]. The peptidases PepA$_1$, PepA$_2$ and PepA$_3$ are glutamyl serine aminopeptidases, all of which are approximately 350 amino acids in length. Aminopeptidase PepM is an essential methionine aminopeptidase that modifies nascent polypeptides by removing the N-terminal methionine upon ribosomal release [Chang et al., 1989]. Crystal structure analysis of PepM performed by Oefner et al. [Oefner et al., 2003] reported the inhibition of this essential aminopeptidase by 1, 2, 4-triazols, thus presenting a possible new target for novel therapies against *S. aureus*. The catalytic and substrate processing activities of the proline dipeptidases PepP and PepQ, and peptidase PepT$_1$ have yet to be determined and remain uncharacterized. Aminopeptidase PepS is an intracellular aminopeptidase, with a substrate preference for the hydrophobic amino acid residues, Leu, Val, Phe, and Tyr. The crystal structure analysis of PepS identified impaired catalytic activity in the presence of the metal chelating agent EDTA, which was restored with the addition of zinc or cobalt ions [Odintsov et al., 2005]. Additionally, analysis using antisense RNA technology identified an impaired phenotype for growth in cells with reduced *pepS* mRNA transcript levels [Yinduo et al., 2001]. PepV, a dipeptidase in *S. aureus*, has been reported to vary among clonal variants of *S. aureus*, as peptidase activity was observed in methicillin resistant strains only, and was absent in methicillin susceptible strains [Staub and Sieber, 2009]. Additionally, the potential association for PepV and resistance in MRSA strain has been suggested as a result of activity-based protein profiling experiments, which identified the selective overexpression of dipeptidase activity in these strains [Staub and Sieber, 2009]. Aminopeptidase PepZ is a putative cytosolic leucine

specific aminopeptidase based on sequence homology with a leucine aminopeptidase of *E. coli*, PepA. A recent publication [Majerczyk et al., 2010] identified the decreased expression of *pepZ* in a *codY* deficient *S. aureus* strain. In bacteria such as *Lactococcus lactis*, CodY is a transcriptional regulator that senses available nutrients mediated through interactions with branch chain amino acids, and often regulates aminopeptidases for nutritional purposes accordingly [Majerczyk et al., 2010].

Aminopeptidases in Bacterial Pathogenesis. In addition to secreted toxins, there are a number of components within bacterial genomes that do not directly participate in host interactions, but still facilitate the infectious process. One such example is found within the proteolytic activities of aminopeptidases. The role for intracellular bacterial aminopeptidases in the aid and progression of disease remains largely uncharacterized; however, secreted or surface exposed aminopeptidases have been associated with virulence in some pathogens. In a study by Kumagai et al. [Kumagai et al., 1999], a secreted dipeptidyl aminopeptidase (DPPIV) from *Porphyromonas gingivalis* was found to be implicated in the formation of abscesses in mice. This was determined using a model of wound formation, which identified decreased wound formation and mortality in mice infected with aminopeptidase DPPIV deficient cells, compared to wild-type strain infections [Kumagai et al., 1999]. A later report corroborated these findings, in which the proteolytic activity of aminopeptidase DPPIV in *P. gingivalis* was shown to function in the degradation of collagen in host tissues [Kumagai et al., 2005]. Further, a proteomic analysis performed on membrane bound proteins from the zoonotic pathogen *Streptococcus suis* revealed increased levels of two aminopeptidases in virulent strain

proteomes: a leucine aminopeptidase and aminopeptidase T. Moreover, the leucine aminopeptidase was recently determined to have antigenic properties in immunoreactivity assays [Wang et al., 2011]. This differential protein analysis performed on proteomes from both virulent and avirulent strains of *S. suis* further substantiates the potential of aminopeptidases as virulence factors in bacteria.

Materials and Methods

Culture Media

All media was prepared using deionized water (diH_2O) and was sterilized by autoclaving at 121°C for 30 minutes unless otherwise indicated.

Tryptic soy broth (TSB)

3% tryptic soy

Luria-Bertani (LB) [Miller, 1972]

Tryptone	10 g L^{-1}
Yeast	5 g L^{-1}
NaCl	10 g L^{-1}

Top agar

0.7% agar in TSB

Biofilm broth

3%	TSB
0.5%	dextrose
3.0%	NaCl

B2

1% casein acid

2.5% yeast

0.1% K_2HPO_4

2.5% NaCl

Chemically defined limiting media

Solution 1

L-Aspartic acid	3 g
L-Alanine	2 g
L-Arginine	2 g
L-Cystiene	1 g
Glycine	2 g
L-Glutamic acid	3 g
L-Histidine	2 g
L-Isoleucine	3 g
L-Lysine	2 g
L-Leucine	3 g
L-Methionine	2 g
L-Phenylalanine	2 g
L-Proline	3 g
L-Serine	2 g

L-Threonine	3 g
L-Tryptophan	2 g
L-Tyrosine	2 g
L-Valine	3 g
Na_2HPO_4	140 g
KH_2PO_4	60 g
diH_2O	1400 ml

Solution 2

Biotin	0.4 mg
D-Pantothenic acid	8 mg
Pyridoxal	16 mg
Pyridoxamine diHCl	16 mg
Riboflavin	8 mg
Nicotinic acid	8 mg
Thiamine HCl	8 mg
diH_2O	400 ml

Sterilize by filter sterilization.

Solution 3

Adenine sulphate	400 mg L^{-1}
Guanine HCl	400 mg L^{-1}

HCl	0.1M

Solution 4

$CaCl_2 6H_2O$	1 g
$MnSO_4$	500 mg
Ferric Ammonium Sulphate	600 mg
HCl	0.1M
diH_2O	100 ml

Solution 5

Glucose	100 g L^{-1}
$MgSO_4 7H_2O$	5 g L^{-1}

Amino acid limiting

Combine the following solutions and filter sterilize:

Solution 1	0.07%
Solution 2	0.02%
Solution 3	0.05%
Solution 4	0.001%
Solution 5	0.1%

Glucose limiting

Prepare as indicated in the amino acid-limiting media protocol, with the exception of a ten-fold reduction of glucose in solution 5.

Phosphate limiting

Prepare as indicated in the amino acid-limiting media protocol, with the exception of a five-fold reduction of Na_2HPO_4 and KH_2PO_4 in solution 1.

Mannitol salt agar

Mannitol salt media was purchased from Fischer Scientific and prepared according to the manufactures specifications.

Milk broth

Dried skim milk was reconstituted in diH_2O at a 10% concentration and sterilized for 15 minutes by autoclaving

Purple broth

Purple both media was purchased from Fischer Scientific and prepared according to the manufacture's specifications.

Buffers and Reagents

PBS

0.8%	sodium chloride
0.14%	disodium phosphate
0.02%	potassium chloride
0.02%	potassium dihydrogen phosphate

pH 7.4

Phage buffer

1M	MgSO4
4mM	CaCl2
5.9 g L^{-1}	NaCl
1 g L^{-1}	gelatin
50mM	Tris-HCl, pH 7.8

UDS buffer

6M	urea
5mM	DTT
1%	SDS
50mM	Tris-HCl, pH8

2D-DIGE IEF buffer

7M	urea
2M	thiourea
4%	CHAPS
0.2%	SDS
0.1M	DTT
10mM	Tris-HCl, pH8.5

Laemmli buffer

diH_2O	4.0 ml
0.5M Tris-HCl, pH6.8	1.0 ml
10% SDS	1.6 ml
100% glycerol	0.8 ml
β-Mercaptoethanol	0.4 ml
Bromophenol blue	0.05%

Stacking gel

diH_2O	3.05 ml
10% SDS	50 µl
10% APS	25 µl
0.5M Tris-HCl, pH6.8	1.25 ml
TEMED	5 µl
Acrylamide	650 µl

Separating gel

diH_2O	3.35 ml
10% SDS	100 µl
10% APS	50 µl
1.5M Tris-HCl, pH8.8	2.5 ml
TEMED	7 µl
Acrylamide	4.0 ml

Destain solution

Methanol	10%
Acetic acid	5%

Coomassie blue stain

Methanol	50%
Acetic acid	10%
Coomassie blue	0.25%

10x electrophoresis buffer

Glycine	144 g L^{-1}
Tris base	30.3 g L^{-1}
SDS	10 g L^{-1}

Transfer buffer

Tris base, pH 8.5	5.8 g L^{-1}
Glycine	2.9 g L^{-1}
SDS	0.4 g L^{-1}
Methanol	200 ml

TBST

25mM Tris, pH 7.6

0.05% Tween-20

0.15M NaCl

Blocking reagent

TBST	7.5 ml
10 mg ml^{-1} BSA or 10% milk	3 ml

HisProbe working solution

TSBT	10 ml
His-probe	2 µl

SuperSignal®West Pico Substrate

SuperSignal®West Pico Substrate was purchased from Pierce and prepared according to the manufacture's specifications.

Bacterial Strains, Plasmids and Primers

Table 1. Bacterial Strains and Plasmids

Strain	Source	Characterisitics
S. aureus USA300 FPR3757 Erm S	Diep, 2006	CA-MRSA
S. aureus Newman	Duthie, 1952	Laboratory strain
S. aureus RN6390	Novick, 1990	Laboratory strain
S. aureus RN4220	Kreiswirth, 1983	Derivitive of 8325
S. aureus SH1000	Horsburgh, 2002	Derivitive of 8325-4
S. aureus RN4220 pAZ106::*pepZ-lacZ pepZ+*	This study	Reporter fusion
S. aureus Newman pAZ106::*pepZ-lacZ pepZ+*	This study	Reporter fusion
S. aureus SH1000 pAZ106::*pepZ-lacZ pepZ+*	This study	Reporter fusion
S. aureus USA300 FPR3757 Erm S pAZ106::*pepZ-lacZ pepZ+*	This study	Reporter fusion
S. aureus RN4220 pAZ106::*pepZ*	This study	Deficent in *pepZ*
S. aureus Newman pAZ106::*pepZ*	This study	Deficent in *pepZ*
S. aureus USA300 FPR3757 Erm S pAZ106::*pepZ*	This study	Deficiet in *pepZ*
S. aureus RN4220 pMK4::*pepZ*-6 His	This study	PepZ overexpression
S. aureus Newman pMK4::*pepZ*-6 His	This study	PepZ overexpression
S. aureus USA300 FPR3757 Erm S pMK4::*pepZ*-6 His	This study	PepZ overexpression
S. aureus USA300 FPR3757 Erm S pMK4	This study	Empty vector
S. aureus Newman pMK4	This study	Empty vector
plasmid pAZ106	Kemp, 1991	Amp^R, Ery^R
plasmid pMK4	Sullivan, 1984	Amp^R, Cm^R

**Cloning vectors pAZ106 and pMK4 where used for the molecular manipulation of bacterial strains constructed in this study. Cm^R, chloramphenicol resistance; Ery^R, erythromycin resistance and Amp^R, ampicillin resistance.*

Table 2. Primer Sequences

OL461	ATG TCT AGA CAG TTA GAG CGC ATT AGT	XbaI	F *pepZ*
OL462	ATG GGA TCC CAT TCG GTG GCA TAT TAC	BamHI	R *pepZ*
OL761	GAC CAT GCA GAG GAT GAT GC		R pAZ106
OL895	ATG TCT AGA GCT ACA CCA ATC GTT GCT TG	XbaI	F *pepZ lacZ*
OL958	ATG GGA TCC GGT TCA CAT GAC GGT GTA GG	BamHI	F *pepZ* for 6-HIS o/x
OL959	ATG CTG CAG TTA *ATG ATG ATG ATG ATG ATG* TTG TTG TTT TAA CCA TTG TAC	PstI	R *pepZ* for 6-HIS for o/x
OL1057	GTT AGC TCA CTC ATT AGG CAC CCC A		F pMK4 for 6-HIS o/x
OL1036	CCG CGC ACA TTT CCC CGA AA		R pMK4

**Underlined sequences identify cloning restriction sites. Italicized sequences represent histidine tags added for the construction of overexpression strains.*

Transformations. All molecular manipulations were performed as described by Sambrook and Russell [Sambrook et al., 2001].

Electroporation of *S. aureus*. 20 ng of plasmid DNA was extracted and resuspended in 70 µl of competent RN4220 cells and transferred to a 1 mm gapped electroporation cuvette. Electroporation was performed at room temperature using a BioRad Gene Pulser, followed by cell recovery at 37°C shaking in 1 ml of B2 media for 90 minutes. Cells were then plated onto TSA containing the correct antibiotic for selection, and incubated overnight at 37°C.

Phage Transductions of *S. aureus*. Transductions were performed using overnight bacterial cultures from transformants, combined with 1M $CaCl_2$ and previously prepared 80α phage lysate, which were incubated at in a 37°C water bath for 20 minutes. The cells were then recovered by centrifugation following the addition of 1% sodium citrate and resuspension in TSB containing 0.5% sodium citrate. Cells were then incubated for one hour in a 37°C water bath and centrifuged again prior to a second resuspension in TSB containing 0.5% sodium citrate and plating onto selective media for overnight incubation at 37°C [Mani et al., 1993].

Construction of a *pepZ* mutant. An *S. aureus pepZ* mutant was Available from laboratory stocks, which was made as follows. A PCR fragment was cloned into the vector pAZ106, which was purified and transformed into electrocompetent *S. aureus* RN4220 cells. Clones were selected for based on the plasmid encoded erythromycin resistance, and confirmed by PCR analysis. A representative clone was used to generate an 80α phage lysate for the transduction of *S. aureus* SH1000, Newman and USA300

FPR. Clones were then again selected for according to the erythromycin cassette and confirmed by PCR analysis.

Construction of *pepZ-lacZ* Reporter Gene Fusions. The reporter fusions were constructed from a 1211 bp fragment, which was PCR amplified using forward primer 895 located 626 bp upstream from the *pepZ* start codon and reverse primer 462 located 544 bp downstream of the start codon (Table 2). This fragment was then cloned into the suicide vector pAZ106, which contains a promoterless *lacZ* cassette located downstream of the multiple cloning site, for the construction of transcriptional fusions. Once this construct was confirmed in *E. coli*, purified plasmid was electroporated into the *S. aureus* strain RN4220 and a prepared lysate was then transduced into the wild-type strains SH1000, USA300 FPR and Newman for characterization experiments [Mani et al., 1993; Sambrook et al., 2001; Schenk and Laddaga, 1992].

Transcriptional Analysis

Transcriptional Analysis of *pepZ* Expression. Exponentially growing *pepZ-lacZ* reporter fusion cells were standardized to an OD_{600} of 0.05 in TSB and returned to 37°C shaking. Optical density measurements and 1 ml sample collections were obtained hourly for eight hours, with a final measurement and collection at 24 hours. A standard β-galactosidase assay was then performed from duplicate samples to determine the expression profile of *pepZ* under standard conditions and values averaged [Sambrook et

al., 2001]. One unit of β-galactosidase activity was defined as the amount of enzyme that catalyzed the production of 1 pmol MU min^{-1} OD_{600} $unit^{-1}$.

Transcriptional Disk Diffusion Assays. Sterile filter disks (7 mm, 3MM Whatman Paper) were placed onto of a TSA plate overlayed with TSA top agar (0.7% w/v), containing *pepZ-lacZ* reporter strain fusion cells and 40 µg ml^{-1} X-GAL [Cao et al., 2002]. Chemical stressors were then applied to the filter disks in volumes of 10 µl and incubated overnight at 37°C (hydrochloric acid, phosphoric acid, trichloroacetic acid, formic acid, acetic acid, sulfuric acid, nitric acid, sodium hydroxide, sodium chloride, glucose, ethanol, methanol, isopropanol, SDS, Triton X-100, Tween-20, N-lauroyl sarcosine, hydrogen peroxide, menadione, pyrogall, sodium nitroprusside, 4-methylmethanesulfonate, penicillin-G, vancomycin, phosphomycin, spectinomycin, ampicillin, tetracycline, erythromycin, lincomycin, kanamycin, neomycin, rifampicin, chloramphenicol, puromycin, oxacillin, bacitracin, mupirocin, diamide, berberine Cl, peracetic acid, EDTA, DTT and triclosan). The upregulation of *pepZ* expression was determined by screening for blue color changes in the media [Sambrook et al., 2001].

Growth and Nutrition Profiling

Growth Analysis in Peptide Based Media. Bacterial cells were grown to exponential phase at 37°C while shaking, washed in PBS and resuspended in 10% autoclaved milk to an OD_{600} of 0.05. Viable cell counts were performed in PBS every hour for 30 hours by

serial plating onto TSA. Plates were incubated overnight at 37°C and measured the following day by exact colony counts to determine CFU ml^{-1}.

Long-Term Starvation Analysis. Starvation analysis was examined from three independent cultures prepared using exponentially growing cells, which were washed in PBS and resuspended in 10% autoclaved milk or sterile TSB to an OD_{600} of 0.05. Cultures were grown shaking or static at 37°C and monitored by viable cell counts performed daily for seven days (shaking and static) cultures or weekly for four weeks (static cultures). Data was analyzed using a Student's *t* test with a 5% confidence limit to determine statistical significance

Competitive Growth Analysis. Competitive growth analysis was performed by inoculating sterile 10% reconstituted dried skim milk and TSB with exponentially growing wild-type and *pepZ* mutant cells in a 1:1 ratio, following PBS washes. Cocultures were grown shaking or static at 37°C and monitored by viable cell counts performed daily for seven days (shaking and static cultures) or weekly for four weeks (static cultures). Viable cell counts were performed by serial plating onto both TSA, and TSA containing erythromycin, which were incubated overnight at 37°C. The exact enumeration of both viable wild-type and *pepZ* mutant cells was used to calculate the competitive index (CI) [Shaw et al., 2008]. Data was analyzed using a Student's *t* test with a 5% confidence limit to determine statistical significance.

Proteomic Analysis

Cytoplasmic Protein Extraction. Synchronized cultures were harvested from cultures grown continuously while shaking at 37°C, hours 1 through 8 and 15. Cultures were centrifuged for ten minutes at 4150 RPM and the resulting pellet was washed three times in PBS. The final pellet was resuspended in either 750 µl UDS buffer for subcellular localization profiling or 200 µl of IEF buffer for 2D-DIGE. Cells were then lysed using a BioSpec Mini-BeadBeater, with 0.1 mm glass disruption beads for a total of four minutes in one minute intervals. Lysed cells were then centrifuged at 4°C for ten minutes at 13,300 RPM and the protein fractions were transferred into new tubes and measured for protein concentration using a Pierce 660 nm protein assay kit.

Secreted Protein Extraction. Proteins were harvested from synchronized cultures grown continuously at 37°C shaking at hours: 1 through 8 and 15. Cultures were centrifuged for ten minutes at 4150 RPM and the remaining supernatants were filter sterilized to remove residual whole bacterial cells. Supernatants were then precipitated at final concentrations of 10% trichloroacetic acid overnight at 4°C. The following day, precipitated secreted proteins were centrifuged for ten minutes at 4150 RPM at 4°C and washed with 100% ice cold ethanol three times. Protein pellets were then air dried and resuspended in either 750 µl UDS buffer for subcellular localization profiling or 200 µl of IEF buffer for 2D-DIGE, and measured for protein concentration using a Pierce 660 nm protein assay kit.

Western Blot Detection. Western blot detection of *pepZ* 6-His tagged proteins was performed using a Pierce PVDF Transfer Membrane and SuperSignal West HisProbe Kit. Intracellular and secreted proteins were extracted at various time points from cultures containing standardized pMK4::*pepZ* 6-His tagged cells. As a negative control, proteins were extracted from cells containing the pMK4 vector only, concurrently. Protein concentrations were quantified and then resolved using SDS-PAGE and transferred onto a polyvinylidene diflouride membrane. Following protein transfer, the membrane was blocked for one hour at room temperature or overnight at 4°C, washed in TBST, and probed for 6-His tagged proteins. Chemoluminescent substrate detection was then performed using horse radish peroxidase and hydrogen peroxide in equal volumes and proteins were visualized by X-ray detection.

2D Difference Gel Electrophoresis (DIGE). Intracellular and secreted protein fractions were extracted from continuously grown USA300 FPR wild-type and *pepZ* mutant strain cultures after three hours and prepared as previously described. The purified protein fractions were then transferred to the ICBR facility at the University of Florida for 2D-DIGE CyDyeTM analysis. 50 ug of protein from the *pepZ* mutant and wild-type samples, and internal standard were labeled with either, Cy5, Cy2 and Cy3 CyeDyeTM, and separated based on charge using two dimensional isoelectric focusing. The proteins were then further separated by molecular weight using SDS-PAGE. This was followed by the in-gel analysis of wild-type and *pepZ* mutant labeled samples using a Typhoon 9600 Variable Mode Imager. Changes in protein abundance were determined by DeCyderTM v.7.0 Differential Analysis Software and then extracted by ProPicTM. The extracted

proteins were then digested with trypsin and analyzed for identification using mass spectrometry and MASCOT software.

Trypsin Digestion. Trypsin digestion was performed using 100 µg of standardized protein. Protein samples were reduced at room temperature for one hour using 50 µl of 200mM dithiothreitol (DTT). Alkylation was then performed for one hour in the dark using 200 µl of 200mM iodoacetamide (IAA). An additional 200 µl of 200mM DTT was added to the samples to consume residual IAA. The samples were then diluted with 25mM ammonium bicarbonate to 5 ml, and digested with trypsin in a ratio of 1: 30 of trypsin weight to protein for 16 hours at 37˚C, and desalted the following day.

Desalt. Peptide desalting was performed using C-18 Vydac columns. The columns were activated with the addition of 1 ml of 100% acetonitrile, and repeated once. Column equilibration was carried out by applying 1 ml of 0.1% formic acid in diH_2O to the columns, and repeated once. The peptides were then applied to the columns and washed two times with 1 ml of 0.1% formic acid in diH_2O. Peptides were then eluted from the columns using 300 µl of 0.1% formic acid in acetonitrile, and repeated two times. The peptide samples were dried using SpeedVac centrifugation and resuspended in 100 µl of 0.1% formic acid in diH_2O. Peptides were further prepared by sonication for ten minutes and then analyzed using mass spectrometry.

Virulence Assays

Murine Model of Septic Arthritis. Female NRMI mice, 6 to 8 weeks old were inoculated intravenously with either 1 x 10^7 Newman wild-type or Newman *pepZ* mutant bacterial cells via tail vein injection, and evaluated for 12 days for the progression and severity of infection. Following animal sacrifice, septic dissemination and persistence was quantified as CFU ml^{-1} from kidney cellular homogenates harvested twelve days post inoculation, which were serial diluted in PBS and plated on horse blood agar plates and incubated for 24 hours. Clinical arthritic index measurements ranging from 0 to 3 were used to define the severity of erythema and/or swelling of at least one joint resulting from systemic infections using a double blind method. Each mouse limb was evaluated and scored for septic arthritis severity according to the following criteria: 1, mild swelling and/or erythema; 2, moderate swelling and erythema; 3, marked swelling and erythema. The sum of these scores corresponds to an arthritic index value used to quantify the severity of arthritis for each animal [Calander et al., 2004; Shaw et al., 2008].

Biofilm Formation Analysis. Biofilm formation was examined in triplicate from bacterial cells grown overnight in sterile biofilm media. The following day, 200 µl of culture was resuspended in sterile biofilm media to an OD_{600} of 0.1 and used to inoculate wells of a 96 well microtiter plate previously overlain with 20% human plasma. The microtiter plate was then incubated overnight at 37°C, before the culture was carefully removed and washed three times with PBS and allowed to air dry the following day. The biofilms were then fixed with 100% ethanol, air dried, stained with 10% crystal violet

and washed with PBS again. The plate was dried overnight at room temperature, and with the addition and removal of 100% ethanol, biofilm formation was measured via absorbance readings at 610 nm using a microtiter plate reader the following day [Beenken et al., 2003].

Human Macrophage Survival and Clearance. A human model of macrophage survival and clearance was performed in two independent experiments using Newman wild-type or *pepZ* mutant cells to inoculate wells of a microtiter plate containing human macrophages, in a ratio of 1: 50. Cell viability per well was monitored by quantitative plating at hours 0, 2, 24, 48, 72 and 96 post-inoculum [Koziel et al., 2009].

Murine Model of Wound Formation. Ten hairless, SKH-1 immunocompetent mice were inoculated subcutaneously in the right flank with 1.00 x 10^8 USA300 FPR wild-type or *pepZ* mutant cells for each strain. Infection was monitored for seven days and any abscesses formed were harvested following animal euthanasia [Bunce et al., 1992; Chan and Foster, 1998]. Viable *S. aureus* cells were quantified by serial diluting harvested abscess homogenates in PBS, and plating onto TSA. Plates were incubated overnight at 37°C, and CFU per abscess and percent recovery was determined the following day by colony enumeration. Data was analyzed using a Student's *t* test with a 5% confidence limit to determine statistical significance.

Murine Model of Bacterial Sepsis. Twenty female six-week old CD-1 Swiss, outbred and immunocompetent mice (Charles River Laboratories) were inoculated via tail vein

injection with 100 µl of 1.00 x 10^8 CFU ml^{-1} USA300 FPR wild-type or *pepZ* mutant cells in PBS for each strain. Mouse survival was monitored daily for seven days.

Phenotypic Characterization

Growth Profiling using Chemically Defined Media. Agar plates (amino acid limiting, mannitol salt agar, and phosphate limiting) were inoculated using three single wild-type or *pepZ* mutant colonies, and grown in parallel, aerobically and anaerobically overnight at 37°C. The following day, changes in growth patterns were observed for the various conditions.

Evaluating Carbon Utilization. Carbon utilization was explored in triplicate using 5 µl of standardized bacterial culture to inoculate wells of a microtiterplate containing 250 µl of sterile purple broth enriched with 2.5 µg ml^{-1} of; galactose, ribose, lactose, mannose, fructose, trehalose, raffinose, D-glucosamine or xylose. The plate was covered and incubated overnight at 37°C, and the following day, color changes from purple to yellow were used to determine utilization of the carbon sources.

Lysis Kinetics. Conditions of cell lysis were explored using exponentially growing bacterial cells washed in PBS, and resuspended to an OD_{600} of 2.0, in either sterile TSB containing 0.4 ug ml^{-1} penicillin-G or 0.05M Tris-HCl (pH7.6) containing 0.05% Triton-X-100. Cell lysis was measured by changes in turbidity every 30 minutes [Fujimoto and

Bayles, 1998; Mani et al., 1993; Shaw et al., 2005]. Data was analyzed using a Student's *t* test with a 5% confidence limit to determine statistical significance.

Heat Shock. Exponentially growing bacterial cells were resuspended in sterile TSB to OD_{600} of 0.2. Heat shock was induced by placing cultures in a 55°C water bath for 30 minutes, which were promptly returned to standard growth conditions at 37°C shaking. Cell viability was monitored in 30 minute intervals by optical density readings at OD_{600} [Shaw et al., 2008].

Heat Stress. Exponentially growing bacterial cells were resuspended in sterile TSB to OD_{600} of 0.05. Bacterial cells were assayed for adaptation to heat stress at 55°C shaking, which was measured by viable cell counts performed every 20 minutes for two hours. Serial diluted TSA plates were incubated at 37°C overnight and observed for CFU ml^{-1} percent survival the following day [Shaw et al., 2008]. Data was analyzed using a Student's *t* test with a 5% confidence limit to determine statistical significance.

Oxidative Stress. Exponentially growing bacterial cells were washed and resuspended in sterile PBS containing 7.5mM hydrogen peroxide. Cultures were incubated while shaking at 37°C and monitored in 20 minute intervals by viable cell counts diluted in PBS containing 10 mg^{-1} catalase, for hydrogen peroxide inactivation. Serial diluted plates were incubated at 37°C overnight and observed for CFU ml^{-1} percent survival the following day [Watson et al., 1998].

Disk Diffusions. General stress profiling was investigated using a modified Kirby-Bauer Assay performed in triplicate. As described previously, sterile filter disks (7 mm, 3MM Whatman Paper) were placed onto of a TSA plate overlayed with TSA top agar (0.7% w/v), containing wild-type or *pepZ* mutant strain cells [Cao et al., 2002]. Chemical stressors were then applied to the filter disks in volumes of 10 µl and incubated overnight at 37°C without the addition of X-GAL [Shaw et al., 2008]. Zones of inhibition were measured to identify changes in susceptibility to the various chemical compounds: hydrochloric acid, phosphoric acid, trichloroacetic acid, formic acid, acetic acid, sulfuric acid, nitric acid, sodium hydroxide, sodium chloride, glucose, ethanol, methanol, isopropanol, SDS, Triton X-100, Tween-20, N-lauroyl sarcosine, hydrogen peroxide, menadione, pyrogall, sodium nitroprusside, 4-methylmethanesulfonate, penicillin-G, vancomycin, phosphomycin, spectinomycin, ampicillin, tetracycline, erythromycin, lincomycin, kanamycin, neomycin, rifampicin, chloramphenicol, puromycin, oxacillin, bacitracin, mupirocin, diamide, berberine Cl, peracetic acid, EDTA, DTT and triclosan.

Results

Analysis of the Virulence of a *S. aureus pepZ* mutant using a Murine Model of Septic Arthritis. During a previous screen in our laboratory focused on the role of proteases in *S. aureus* virulence, we identified a mutant in aminopeptidase Z as being attenuated in disease causation. Specifically, the role of PepZ in *S. aureus* virulence was examined using a murine model of septic arthritis, in collaboration with Dr. Andrej Tarkowski from the University of Goteborg, Sweden. Female NRMI mice, 6 to 8 weeks old were inoculated intravenously with either the Newman wild-type or Newman *pepZ* mutant strain, and evaluated over twelve days for the progression and severity of infection. Mice infected with *pepZ* mutant cells displayed markedly reduced levels of septic dissemination, weight loss, and severity of infection. Septic dissemination and persistence within the host was quantified as CFU ml^{-1} from kidney cellular homogenates, harvested twelve days post inoculation. Dissemination of the *pepZ* mutant was severely attenuated compared to the wild-type (Fig. 1A), with an approximate one log reduction of mutant cells recovered from the kidneys of infected mice. In addition, infection associated weight loss was strikingly reduced in the *pepZ* mutant (Fig. 1B). Twelve days post inoculation, mice infected with *pepZ* mutant cells averaged a decline in weight of 10%, varying considerably from the average 27% weight loss in wild-type infections. Clinical arthritic index measurements ranging from 0 to 3 were used to define the severity of erythema and/or swelling of at least one joint resulting from systemic

infection. Each mouse limb was evaluated and scored for septic arthritis severity according to the following criteria: 1, mild swelling and/or erythema; 2, moderate swelling and erythema; 3, marked swelling and erythema. The sum of these scores corresponds to an arthritic index value used to quantify the severity of septic arthritis for each animal [Calander et al., 2004]. Symptoms of clinical arthritis measured at five and twelve days post infection showed significant reductions in *pepZ* mutant strain infections (Fig. 1C). Histological evaluation of athritic synovitis and erosion of bone and cartilage showed decreases in serverity in mutant strain infections as well (Fig. 1D).

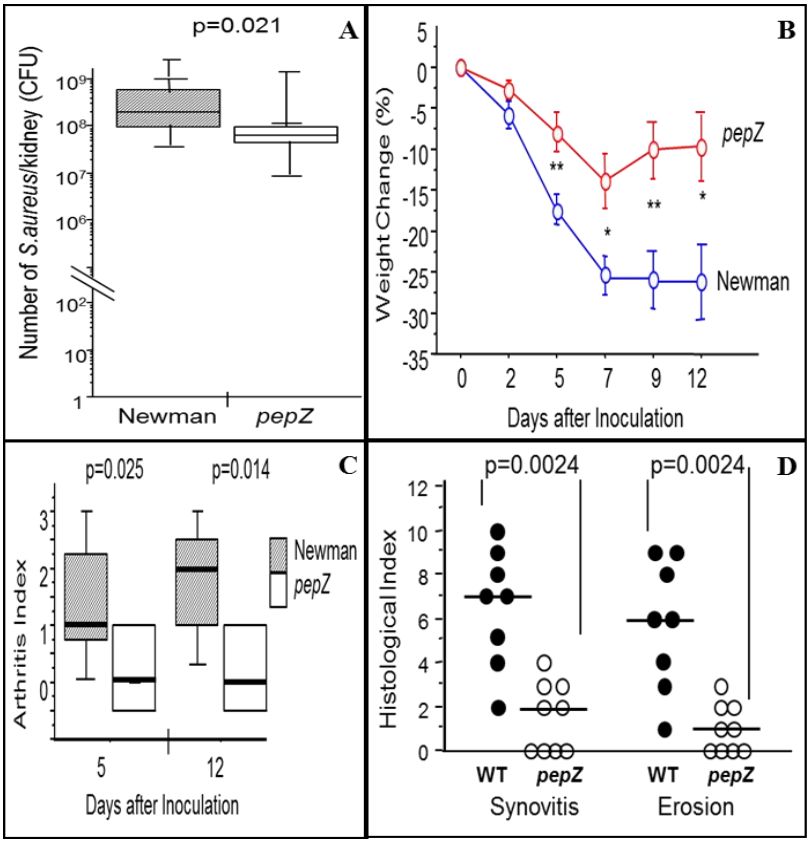

Figure 1. Characterization of the Role of PepZ in Systemic Dissemination using a Murine Model of Septic Arthritis. *S. aureus* strain Newman and its *pepZ* mutant were injected into 10 mice per strain and evaluated for 12 days to identify variations in pathogenesis. **(A)** Septic dissemination to the kidneys represented as CFU/ml. **(B)** Weight loss over 12 days **(C)** Arthritic index measurements 5 and 12 days post inoculation. **(D)** Histological index.

Profiling *pepZ* Expression using a *lacZ* Reporter Fusion. Given the obvious importance of aminopeptidase Z in *S. aureus* infection, we set out to characterize *pepZ* expression to further understand the way in which the cell employs this enzyme. This was achieved using *pepZ-lacZ* reporter fusion strains. These were constructed from a 1211 bp fragment, which was PCR amplified using a forward primer located 626 bp upstream from the *pepZ* start codon and a reverse primer located 544 bp downstream of the start codon. This fragment was then cloned into the suicide vector pAZ106, which contains a promoterless *lacZ* cassette located downstream of a multiple cloning site, for the construction of transcriptional fusions (Fig. 2).

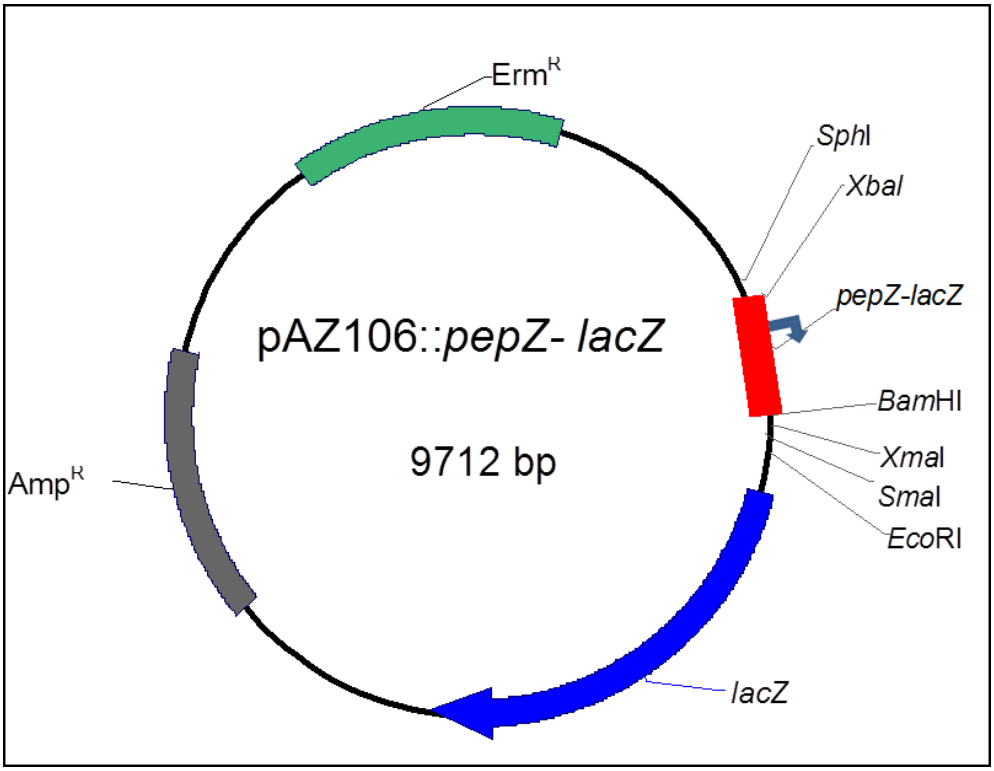

Figure. 2. Physical Map of the Plasmid pAZ106 used to construct *pepZ-lacZ* Reporter Gene Fusions in *S. aureus*. Restriction sites within the multiple cloning site upstream of the *lacZ* gene are shown on the map. The *pepZ* promoter fragment was inserted at the *XbaI* and *BamHI* restriction sites, in which the promoter region is indicated by a blue arrow. The pAZ106 vector contains ampicillin and erythromycin antibiotic resistance genes for selection in *E. coli* and *S. aureus*, respectively, as shown.

This construct was confirmed in *E. coli*, with purified plasmid then being electroporated into the *S. aureus* strain RN4220. Clones were selected via the erythromycin resistance cassette, and confirmed by PCR using forward primer 895 located 626 bp upstream from the *pepZ* start codon and reverse primer 761 located at 7458 bp on the suicide vector pAZ106 (Table 2). A confirmed clone was then used to generate an 80α phage lysate, for the transduction of the wild-type *S. aureus* strains SH1000, USA300 FPR and Newman. These *pepZ-lacZ* reporter fusion strains were again, selected for based on erythromycin resistance and confirm by PCR. The activity of the *pepZ* promoter was quantified using fluorescent light absorbance assays, which were achieved using 4-MUG as a substrate for β-galactosidase activity. We determined maximal levels of *pepZ* expression are achieved consistently during exponential growth (2-3h) in all backgrounds tested (Fig. 3).

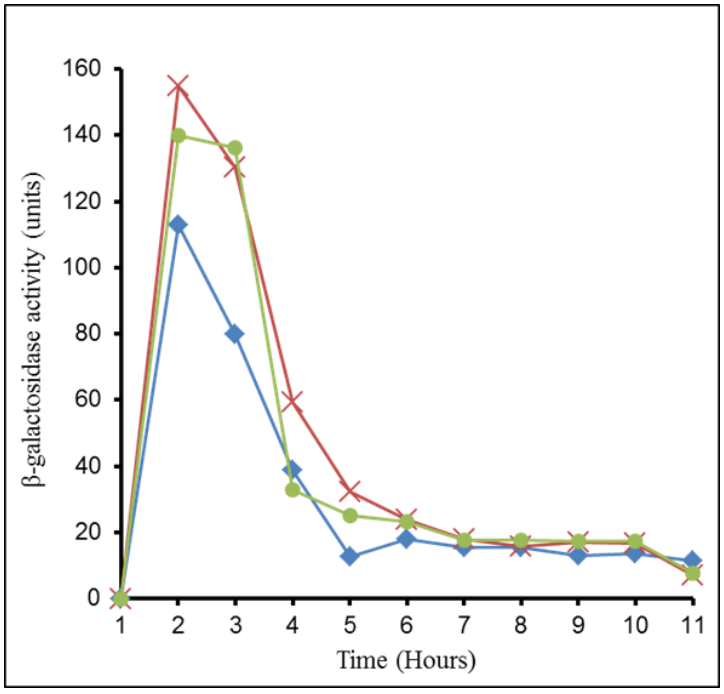

Figure 3. Transcriptional Analysis of *pepZ* Expression in Liquid Media. Expression analysis using *pepZ-lacZ* fusion strains grown in TSB, in SH1000 (◆), Newman (**X**) and USA300 FPR (●). Maximal expression of *pepZ* occurs consistently during exponential growth (2-3h), regardless of the strain tested.

Evaluating the Effects of Environmental Stimuli of *pepZ* Transcription. To further characterize the transcriptional regulation of *pepZ,* we employed transcriptional disk diffusion assays. This allowed us to identify changes in *pepZ* expression in response to a variety of chemical stressor compounds (Table 3). This was performed using *pepZ-lacZ* fusion strains in the SH1000, USA300 FPR and Newman backgrounds. Briefly, sterile filter disks (7 mm, 3M Whatman Paper) were placed on a TSA plate previously overlayed with TSA top agar (0.7%), containing 4 µg ml^{-1} X-GAL, and reporter fusion cells grown overnight, and diluted 1: 1000 [Cao et al., 2002]. Chemical stressors were then applied to the filter disks in a volume of 10 µl, and incubated overnight at 37°C. The upregulation of *pepZ* expression was determined by screening for blue color changes in the media, resulting from the cleavage of X-Gal by β-galactosidase [Sambrook et al., 2001]. This method of analysis identified the induction of *pepZ* in response to oxidative stress, cell wall perturbation and protein synthesis disruption. Specifically, the Newman *pepZ-lacZ* strain demonstrated *pepZ* expression in response to: hydrogen peroxide, oxacillin, rifampicin and bacitracin. Similar results were observed from the SH1000 *pepZ-lacZ* fusion strain, in which hydrogen peroxide, oxacillin, rifampicin, bacitracin, penicillin-G, peracetic acid and N-lauroyl sarcosine upregulated *pepZ* expression. The upregulation of *pepZ* in response to sulfuric acid, Triton X-100, N-lauroyl sarcosine, hydrogen peroxide, vancomycin, ampicillin, oxacillin, triclosan and bacitracin was identified in the USA300 FPR reporter fusion strain (Table 4).

Table 3. Chemical Stress List

Stress	Agent	Concentration
Acid	HCl	1M
	Phosphoric Acid	85%
	TCA	100%
	Formic Acid	88%
	Acetic Acid	12M
	Sulphuric Acid	12M
	Nitric Acid	12M
Alkaline	Sodium Hydroxide	3M
Osmotic	NaCl	1M
	Glucose	1M
Alcohol	Ethanol	100%
	Methanol	100%
	Isopropanol	100%
Detergent	SDS	10%
	Triton X-100	1%
	Tween-20	1%
	N-lauroyl sarcosine	
Oxidative	Hydrogen peroxide	30%
	Menadione	1%
	Pyrogall	400 mg/ml
Nitrostative	Sodium Nitroprusside	2.5M
DNA Damaging	4-methyl methanesulfonate	1M
Antibiotic	Penicillin-G	2 mg/ml
	Vancomycin	2 mg/ml
	Phosphomycin	2 mg/ml
	Spectinomycin	5 mg/ml
	Ampicillin	100 mg/ml
	Tetracycline	5 mg/ml
	Erythromycin	5 mg/ml
	Lincomycin	5 mg/ml
	Kanamycin	50 mg/ml
	Neomycin	50 mg/ml
	Rifampicin	5 mg/ml
	Chloramphenicol	10 mg/ml
	Puromycin	20 mg/ml
	Oxacillin	5 mg/ml
	Bacitracin	5 mg/ml
	Mupirocin	2 mg/ml
Disulfide	Diamide	500mM
Misc.	Berberine Cl	12.8 mg/ml
	Peracetic Acid	4.2M
	EDTA	0.1M
	DTT	1mM
	Triclosan	10%

**Stressor compounds used for general stress profiling of pepZ mutant strains, and transcriptional profiling for the activity of the pepZ promoter using reporter fusion strains.*

Table 4. Stressor Compounds Identified to Induce *pepZ* Transcription

Stress	SH1000	USA300 FPR	Newman
Ampicillin		X	
Bactitracin	X	X	X
Hydrogen peroxide	X	X	X
N-lauroyl sarcosine		X	
Oxacillin	X		X
Peracetic acid	X		
Penicillin-G	X		
Rifampicin	X		X
Sulphuric acid		X	
Triclosan		X	
Triton-X 100		X	
Vancomycin		X	

**Transcriptional disk diffusion assays using pepZ-lacZ reporter fusion strains were performed in triplicate and identified compounds associated with oxidative stress and cell wall synthesis disruption induced pepZ expression.*

Investigation of the Role of PepZ during *S. aureus* Growth in Peptide Rich Media.

Aminopeptidases commonly have a role in cellular nutrition, resulting from their cleavage of imported oligopeptides [Linderstrom-Lang, 1929; McDonald, 1986; Rawlings and Barrett, 2004]. The resulting free amino acids can then be utilized as intermediates in central metabolic pathways required for continued cell growth and propagation [Sussman and Gilvarg, 1971]. Accordingly, the potential role of PepZ in *S. aureus* nutrition was explored in peptide based media (dried skimmed milk) using wild-type strains USA300 FPR and Newman, and their *pepZ* mutant derivatives. Dried skimmed milk contains limited free amino acids, and abundant amounts of casein, a milk protein cleaved by aminopeptidases in other bacterial species. As such, strains deficient in aminopeptidases, such as PepZ, might perhaps be expected to have a reduced capacity for nutrient acquisition when grown under such conditions, resulting in decreased survival and viability. Experiments were performed with Newman and USA300 FPR

wild-types and *pepZ* mutant strains grown continuously in 10% milk for 30 hours, with shaking at 37°C. Cell viability was measured hourly and quantified by viable cell counts, plated in duplicate. In this experiment we identified similar peptide utilization profiles across all strains assayed (Fig. 4). Interestingly, at later time points, both the Newman wild-type and Newman *pepZ* mutant cells were identified to reach higher population densities when compared to USA300 FPR wild-type and USA300 FPR *pepZ* mutant cells. Specifically, the USA300 FPR wild-type and *pepZ* mutant strains both achieved an approximately 5-fold increase in cell density after 30 hours of continuous growth in milk media, when compared to their starting inocula. Viable cell counts from the Newman lineage strains, however, revealed a 28-fold increase from the initial inoculum of the parent, and a similar 29-fold increase for the mutant. These results suggest that Newman lineage strains are perhaps better adapted for growth in peptide rich environments than USA300 FPR strains; and that, more generally, PepZ is dispensable for growth in media where peptides form the sole carbon and nitrogen source.

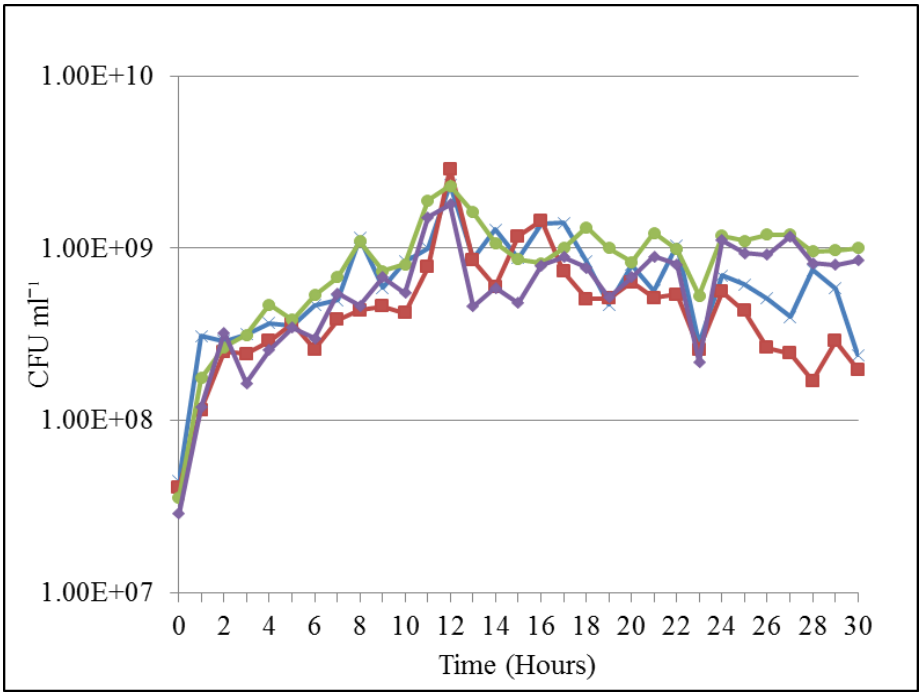

Figure 4. Analysis of Growth in Peptide Based Media. Growth analysis was performed over thirty hours in sterile 10% reconstituted milk media and monitored by duplicate CFU ml^{-1} plating hourly in strains: USA300 FPR (X), USA300 FPR *pepZ* (■), Newman (●) and Newman *pepZ* (◆). In this experiment we identified similar peptide utilization profiles across all strains assayed. Data is expressed as CFU ml^{-1} averages from serial plating at the indicated time intervals.

Investigating the Role of PepZ during Long-Term Starvation. The potential role for PepZ in long-term starvation survival was then explored using milk media and TSB, under both static and shaking conditions at 37°C. TSB is a complex medium containing abundant free amino acids, as well as carbon sources; differing significantly in composition from the peptide-rich milk media. Starvation analysis was examined from three independent cultures of TSB or milk containing exponentially growing Newman, USA300 FPR, Newman *pepZ* or USA300 FPR *pepZ* mutant cells. Cultures were grown shaking or static at 37°C and monitored by viable cell counts performed daily for seven days (shaking and static cultures) or weekly for four weeks (static cultures only). Shaking and static growth conditions were both used for analysis to determine changes in cell

viability while limited for oxygen in static culture, or in environments rich in oxygen, in shaking cultures. Cultures grown aerobically in TSB for one week resulted in similar cell death patterns across all strains tested (data not shown). Viable cell counts showed peak cell densities were achieved at day one, and steadily declined through day seven of the experiment. These results differ from TSB cultures grown under static conditions. Newman strains grown statically in TSB showed no distinct alterations between mutant and wild-type following one week of growth. At two weeks of static growth, we identified a 5% cell survival for the Newman *pepZ* mutant cells and a 24% cell survival for the Newman wild-type cells (Fig. 5A). At three weeks of starvation, a 15% cell survival for the Newman wild-type cells was determined; corresponding to an increase of 4.59-fold in growth when compared to the 7% survival of the mutant. Even larger variations were observed at four weeks of starvation, in which the 12% Newman wild-type cell survival measured 4-fold greater than that of the 3% cell survival identified for the mutant. Interestingly, viable cell counts from USA300 FPR wild-type and *pepZ* mutant cells grown statically in TSB identified a consistently larger viable cell population in *pepZ* mutant cells, compared to the wild-type (Fig. 5B). The USA300 FPR *pepZ* mutant was determined to remain at viable cell densities approximately 2.45-fold greater than the wild-type throughout the first three weeks of the experiment, which decreased to 1.75 after four weeks. The USA300 FPR wild-type cells resulted in cell survivals of 11% at one week of growth, 7% at two weeks of growth, 5% at three weeks of growth and 4% following four weeks of growth. In comparison, USA300 FPR *pepZ* mutant cell survival was determined to be 27% after one week of growth, 18% at two weeks of growth, 12% at three weeks of growth and 7% following four weeks of static growth in TSB.

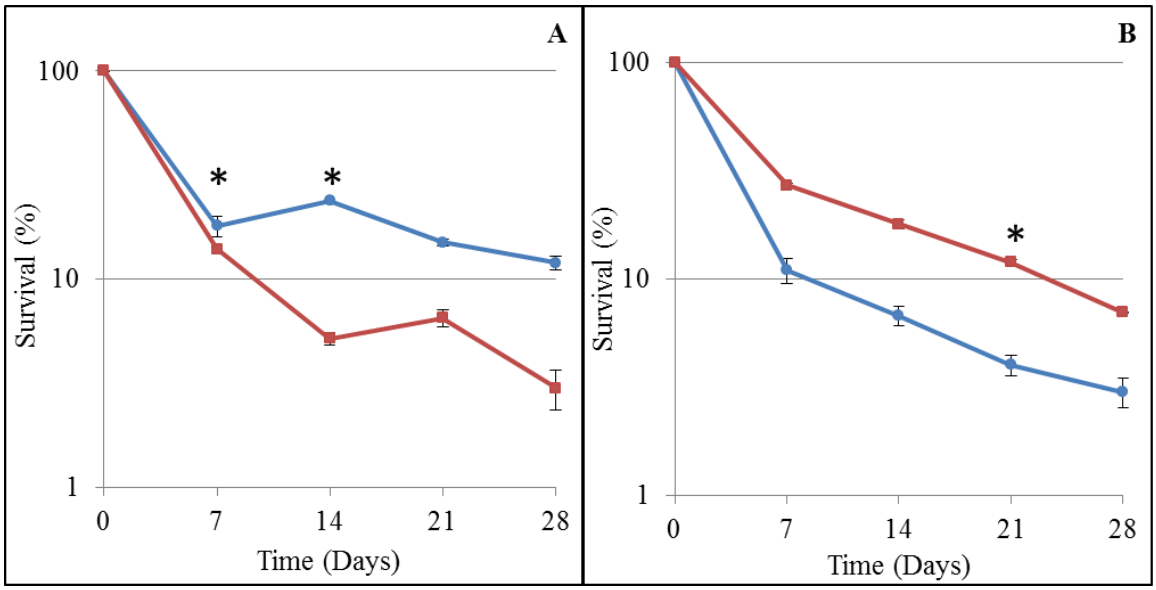

Figure 5. Long-Term Starvation Response of *pepZ* mutants Grown in TSB. (A) Newman wild-type (●) and *pepZ* mutant (■), and **(B)** USA300 **FPR** wild-type (●) and *pepZ* mutant (■) cells were grown statically in complex media at 37˚C. Viable cell counts were measured weekly at the specified time intervals. At four weeks of static starvation Newman wild-type cell survival measured 4-fold greater than that of the mutant. Viable cell counts from the USA300 cultures identified a consistently larger viable cell population in *pepZ* mutant cells, compared to the wild-type. Data is represented as percent survival from the inoculum from 3 independent experiments (+/- SD). Significant values (*) were determined using a Student's *t* test ($p<0.05$).

Starvation experiments performed in peptide based media for one week identified decreased survival of Newman *pepZ* mutant cells when cultured in static or shaking milk media, when compared to the parent. Static starvation assays performed in milk media revealed wild-type cell recovery was 3.7-fold greater than the mutant at day five, and 4-fold larger at day six (Fig. 6A). At seven days post inoculation we determined viable cell densities of 118% for Newman wild-type cells and 65% for *pepZ* mutant cells, representing a 1.8-fold change. The percent recovery for aerated milk cultures seven days post inoculation was determined to be 18% for Newman wild-type cells and 7% for Newman *pepZ* mutant cells, representing an approximately 4.5-fold change. Similar fold changes were observed between these two strains between days 3-6 (Fig. 6B). Starvation

analysis of USA300 FPR wild-type and *pepZ* mutant strains cultured in static peptide based media failed to identify any changes in cell fitness or survival, suggesting no apparent role for PepZ under these conditions (data not shown). In contrast, phenotypic variations were identified between the two USA300 FPR strains when cultured in peptide based media with shaking (Fig. 7). USA300 FPR *pepZ* mutant cells demonstrated an impaired cell survival of approximately 6.41-fold when compared to wild-type cells after only four days of growth under these conditions. The percent survival of viable cells remaining in cultures after seven days was determined to be 37% for wild-type cells and 5% for *pepZ* mutant cell cultures, representing an almost 8.9-fold change.

Analysis of *pepZ* mutants during long-term starvation was carried out for four weeks, and failed to provide any additional insights beyond the seven day starvation experiments (data not shown). This suggests that the aminopeptidase activity of PepZ is most important during initial periods of long-term starvation.

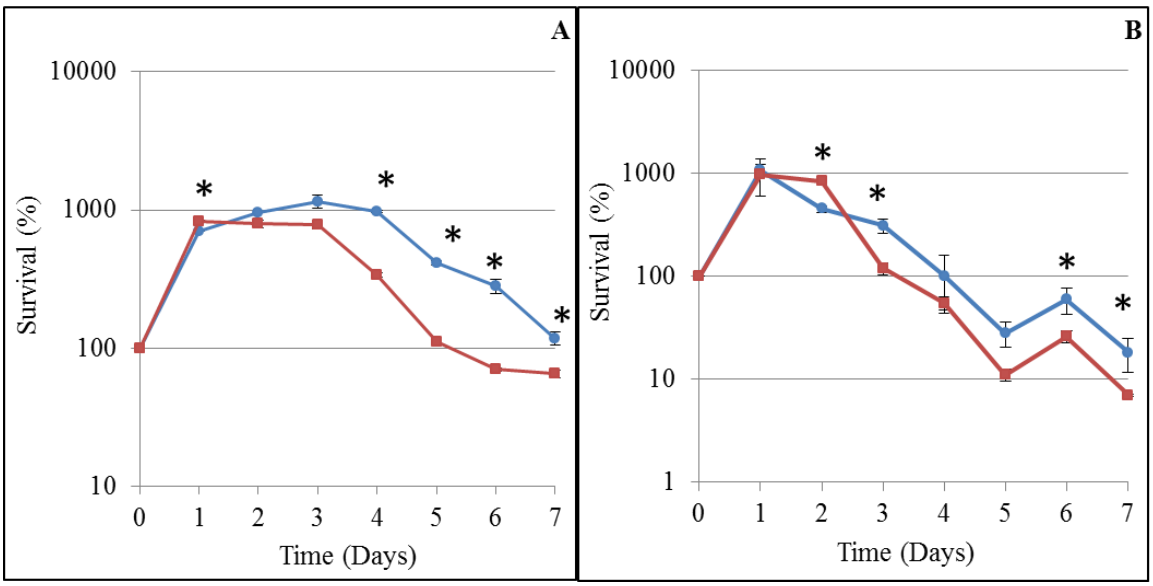

Figure 6. Starvation Response of Newman *pepZ* mutants Grown in Peptide Based Media. Newman wild-type (●) and *pepZ* mutant (■) strains grown (**A**) statically in 10% milk media at 37˚C or **(B)** in milk media with shaking at 37°C. At seven days of growth, static milk cultures demonstrated a 1.8-fold change in cell viabilities between mutant and wild-type, whereas aerated cultures identified a 4.5-fold change between the two strains. Data is represented as an average percent survival of the inoculum from 3 independent experiments (+/- SD)**.** Significant values (*) were determined using a Student's *t* test ($p<0.05$).

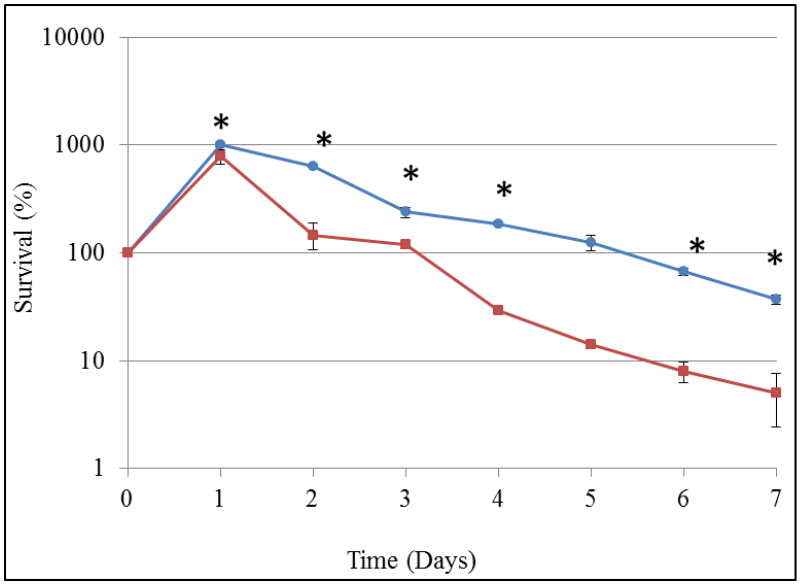

Figure 7. Starvation Response of CA-MRSA *pepZ* mutants in Peptide Based Media. USA300 **FPR** wild-type (●) and *pepZ* mutant (■) cells were grown in 10% milk media at 37°C with shaking. Viable cell counts were measured daily at the specified time intervals and the *pepZ* mutant cells demonstrated an impaired cell survival of approximately 6.41-fold when compared to wild-type cells consistently observed after only four days of growth. Data is represented as average percent survival of the inoculum from 3 independent experiments (+/- SD)**.** Significant values (*) were determined using a Student's *t* test ($p<0.05$).

Competitive Growth Analysis Reveals *pepZ* mutants are Impaired in their Ability to Compete with Wild-Type Strains. In order to further explore the hypothesis that the aminopeptidase activity of PepZ is important for nutrient acquisition in *S. aureus* we next performed coculture experiments in either TSB or 10% milk media. These were inoculated in a 1:1 ratio with either exponentially growing Newman wild-type and Newman *pepZ* mutant cells, or with USA300 FPR wild-type and USA300 FPR *pepZ* mutant cells. Cocultures were grown at 37°C and monitored by viable cell counts performed daily for seven days (shaking and static cultures) or weekly for four weeks (static cultures). Viable cell counts were performed by serial plating onto both TSA, and TSA containing erythromycin. In doing so, the exact enumeration of both viable wild-type and *pepZ* mutant cells was obtained to determine the competitive index (CI). This was achieved via the erythromycin resistance cassette carried on the pAZ106 plasmid used to generate the *pepZ* mutant strains, creating a method for selection of *pepZ* mutant cells only [Shaw et al., 2008].

From these experiments, we derived significant impairment in the ability of *pepZ* mutant strains to compete for nutrients while in coculture with *S. aureus* wild-types. This phenotype was observed in both backgrounds when cultured either static or shaking in peptide based media or TSB. Newman wild-type strains inoculated with its *pepZ* mutant in a 1:1 ratio in 10% milk media resulted in a 1: 0.37 ratio after 24 hours of static growth, which declined further to 1: 0.14 after 48 hours, 1: 0.011 days 5-6 and 1: 0.009 following seven days of competitive growth (Fig 8A). A similar phenotype, although not as pronounced, was observed when the Newman wild-type and *pepZ* mutant were

cocultured with shaking in peptide based media. The ratio of *pepZ* mutant to parent cells recovered after 24 hours of growth was 1: 0.68, which steadily decreased to 1: 0.43 at day 5, and 1: 0.283 following seven days of growth (Fig. 8B). Competitive growth analysis of the USA300 FPR wild-type and *pepZ* mutant strain inoculated together in 10% milk media in 1:1 ratio resulted in a ratio of 1: 0.125 after 24 hours of static growth (Fig. 9A). This was followed by a continual decline of viable *pepZ* mutant cells recovered over seven days of competitive growth; resulting in a ratio of 1: 0.01 at day 7. Further coculture analysis of the USA300 FPR strains performed in aerated milk media showed an impaired phenotype for the *pepZ* mutant as well, in which the ratio of parent to mutant cells was 1: 0.49 after 24 hours, 1: 0.17 at day 3, 1: 0.13 at day 4, and approximately 1: 0.01 days 5-7 (Fig. 9B).

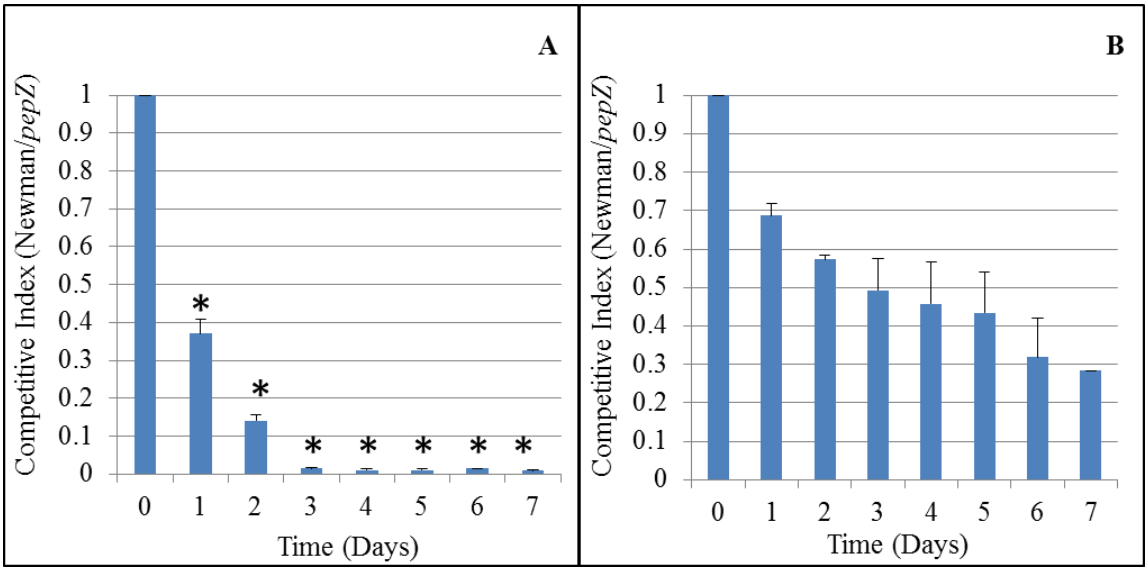

Figure 8. Competitive Growth Analysis of a Newman *pepZ* mutant and Parent Strain in Peptide Based Media. Newman wild-type and *pepZ* mutant strains were cocultured in 10% milk media at 37˚C **(A)** static and **(B)** shaking. The competitive index was derived from daily viable cell counts relative to the initial 1:1 inoculum. The standard deviation of 3 independent experiments is shown. Significant values (*) were determined using a Student's *t* test ($p<0.05$).

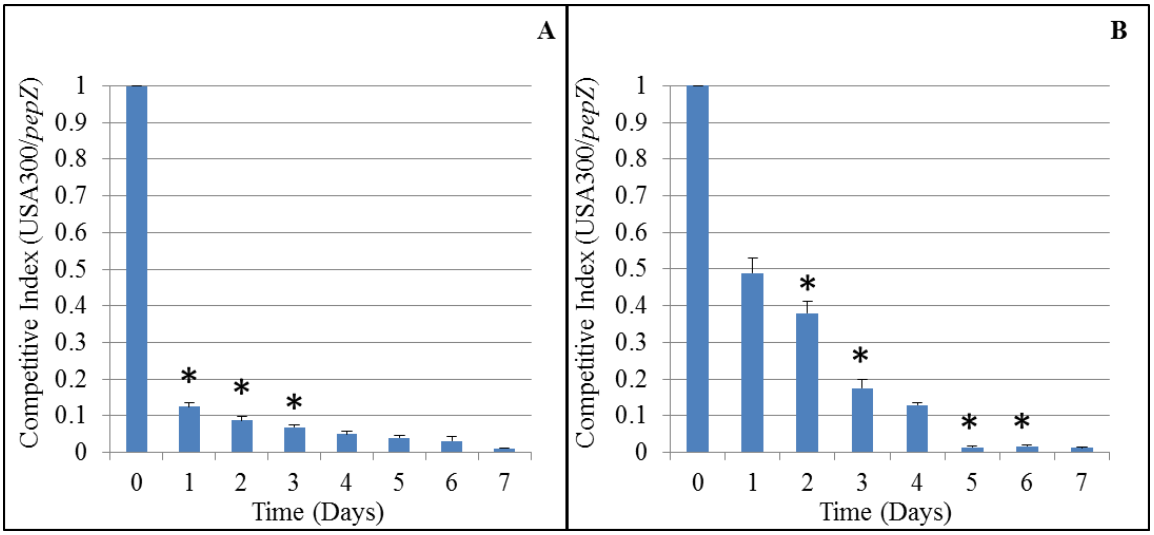

Figure 9. Competitive Growth Analysis of a USA300 FPR *pepZ* mutant and Parental Strain in Peptide Based Media. USA300 FPR wild-type and *pepZ* mutant strains were cocultured in 10% milk media at 37˚C **(A)** static and **(B)** shaking. The competitive index was derived from daily viable cell counts relative to the initial 1:1 inoculum. The standard deviation of 3 independent experiments is shown. Significant values (*) were determined using a Student's *t* test ($p<0.05$).

When grown statically in TSB, the Newman wild-type and *pepZ* mutant resulted in a growth ratio of 1: 0.311 after 24 hours, and a final ratio of 1: 0.052 after seven days (Fig 10A). Newman wild-type and *pepZ* mutant strains grown in aerated TSB coculture showed a decrease in viable *pepZ* mutant cells after 24 hours (ratio of 1: 0.516) followed by six and seven day ratios of 1: 0.03 (Fig. 10B). In the USA300 FPR wild-type and *pepZ* mutant static TSB cocultures, growth ratios of 1: 0.09 after 24 hours, and 1: 0.003 after seven days of competitive growth, were identified (Fig. 11A). USA300 FPR wild-type and *pepZ* mutant cocultures grown in aerated TSB yielded impaired mutant cell viability after 24 hours, resulting in a growth ratio of 1: 0.405. Further loss of viability was demonstrated in the *pepZ* mutant following seven days of competitive growth, declining to a ratio of 1: 0.018 (Fig. 11B).

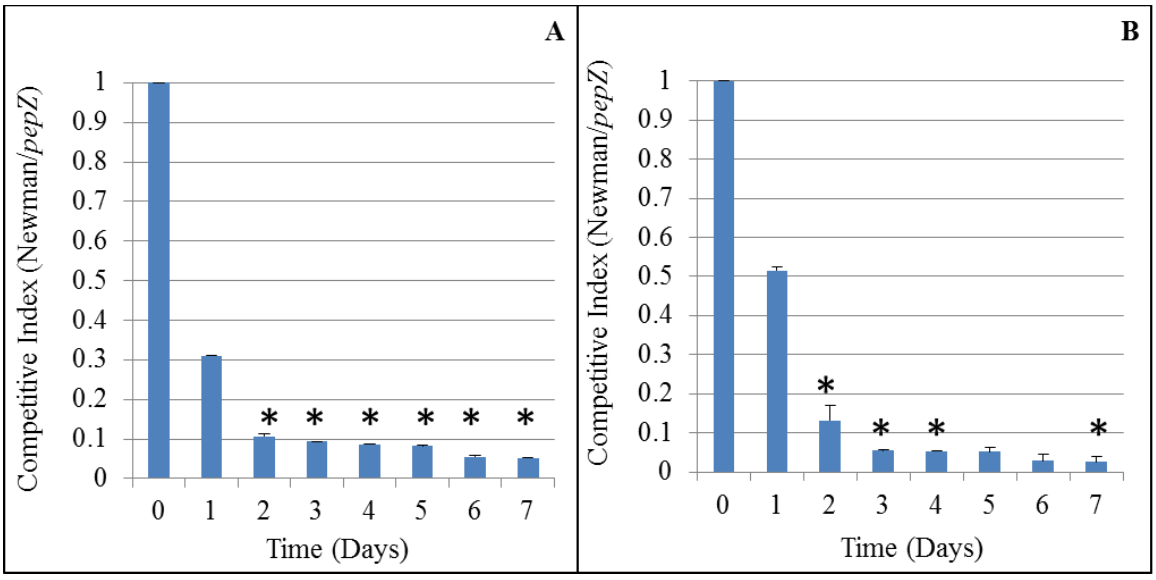

Figure 10. Competitive Growth Analysis of a Newman *pepZ* mutant and Parent Strain in TSB. Newman wild-type and *pepZ* mutant strains were cocultured in TSB at 37°C **(A)** static and **(B)** shaking. The competitive index was derived from daily viable cell counts relative to the initial 1:1 inoculum. The standard deviation of 3 independent experiments is shown. Significant values (*) were determined using a Student's *t* test ($p<0.05$).

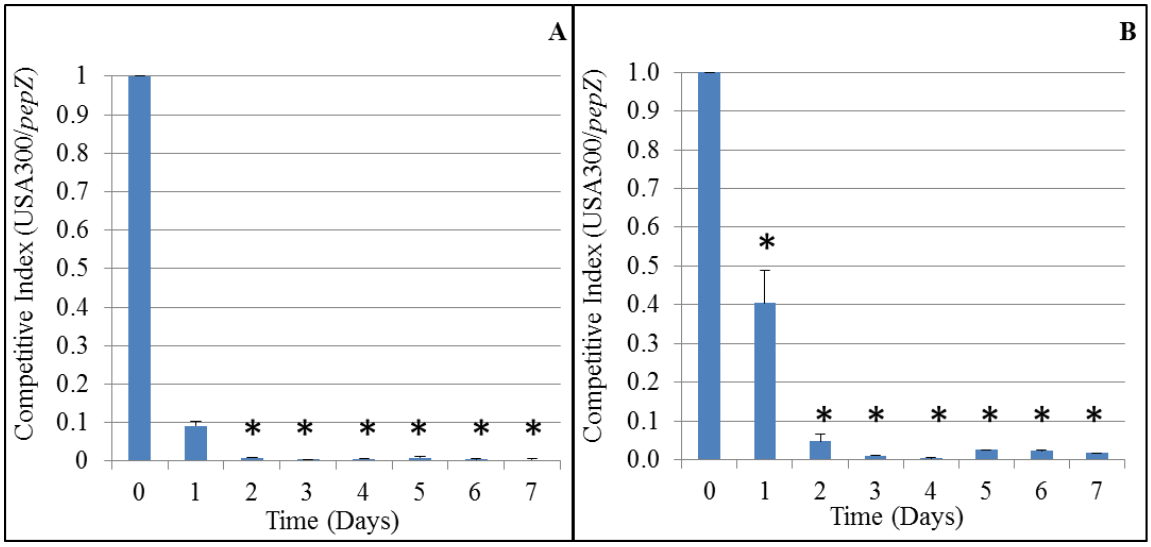

Figure 11. Competitive Growth Analysis of a USA300 FPR *pepZ* mutant and Parent Strain in TSB. USA300 FPR wild-type and *pepZ* mutant strains were cocultured in TSB at 37°C **(A)** static and **(B)** shaking. The competitive index was derived from daily viable cell counts relative to the initial 1:1 inoculum. The standard deviation of 3 independent experiments is shown. Significant values (*) were determined using a Student's *t* test ($p<0.05$).

USA300 FPR wild-type and *pepZ* mutant cocultures exploring long-term competitive growth under static growth conditions identified that maximum loss of viability in the mutant occurs after one week in both TSB and peptide based media. When cultured in TSB, USA300 FPR wild-type and *pepZ* mutant growth ratios of 1: 0.118 after one week, 1: 0.036 after three weeks of growth and 1: 0.129 after four weeks of static growth (Fig. 12A). Growth ratios observed of 1: 0.01 were determined after one week of growth for the USA300 FPR cocultures in milk media, which continued through week four (Fig 12B). In the Newman wild-type and *pepZ* mutant cocultures, a growth ratio of 1: 0.025 was identified after one week of competitive growth in static peptide based media, with an apparent recovery (CI=1: 0.161) after two weeks (Fig. 13A). This was followed by a decline in *pepZ* mutant cells to a ratio of 1: 0.08 following competitive growth after three weeks and, 1: 0.06 after four weeks. Competitive growth analysis of Newman wild-type and *pepZ* mutant cocultures grown under static growth conditions in TSB resulted in an average growth ratio of 1: 0.05 following one week of competitive growth, slightly decreasing to growth ratios of 1: 0.04 weeks 2-4 (Fig. 13B).

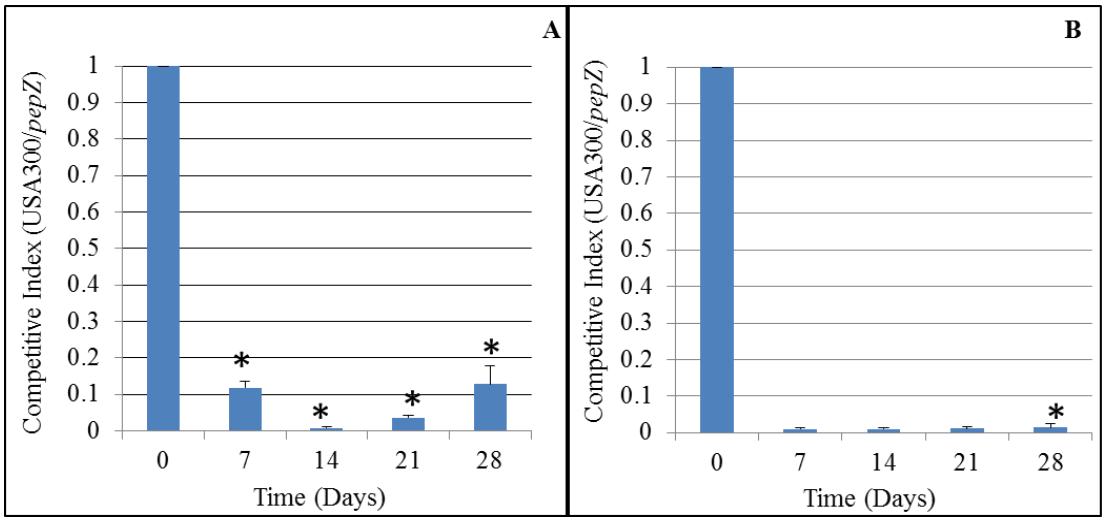

Figure 12. Competitive Growth Analysis of a USA300 FPR *pepZ* mutant and Parent Strain. USA300 FPR wild-type and *pepZ* mutant strains were cocultured together in **(A)** TSB and **(B)** 10% milk media at 37˚C static. The competitive index was derived from weekly viable cell counts relative to the initial 1:1 ratio inoculum. The standard deviation of 3 independent experiments is shown. Significant values (*) were determined using a Student's *t* test ($p<0.05$).

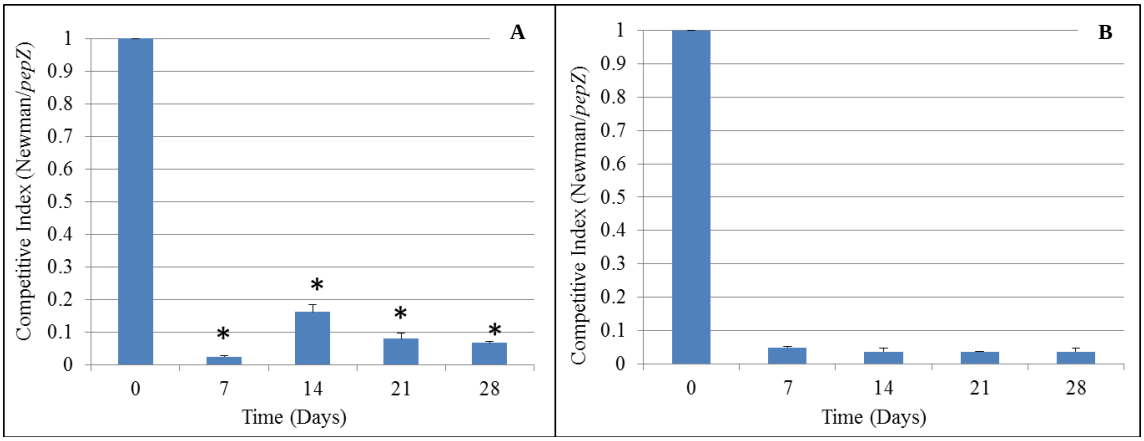

Figure 13. Competitive Growth Analysis of a Newman *pepZ* mutant and Parent Strain. Newman wild-type and *pepZ* mutant strains were cocultured together in (**A**) 10% milk media and (**B**) TSB while grown at 37˚C static. The competitive index was derived from weekly viable cell counts relative to the initial 1:1 ratio inoculum. The standard deviation of 3 independent experiments is shown. Significant values (*) were determined using a Student's *t* test ($p<0.05$).

Anaerobic Stress Profiling of PepZ using Chemically Defined Media. The role of PepZ in response to anaerobic conditions was assessed using chemically defined media, to identify changes in growth patterns when limited for both oxygen and a variety of

nutrient sources. This was performed using amino acid limiting media**,** mannitol salt agar (MSA)**,** phosphate limiting media**,** and glucose limiting media. Agar plates for each of these conditions were inoculated using three single Newman or USA300 FPR wild-type or *pepZ* mutant colonies, and grown in parallel, aerobically and anaerobically, overnight at 37°C. We identified that, in the absence of oxygen, the Newman and USA300 FPR *pepZ* mutant strains fail to proliferate when limited for amino acids (Fig. 14). The USA300 FPR *pepZ* mutant also showed impairment when grown under anaerobic conditions limited for phosphate, when compared to the wild-type (Fig. 15). Furthermore, the USA300 FPR *pepZ* mutant also failed to grow under anaerobic conditions when grown on MSA, suggesting impaired mannitol utilization when grown in oxygen limited conditions (Fig. 16).

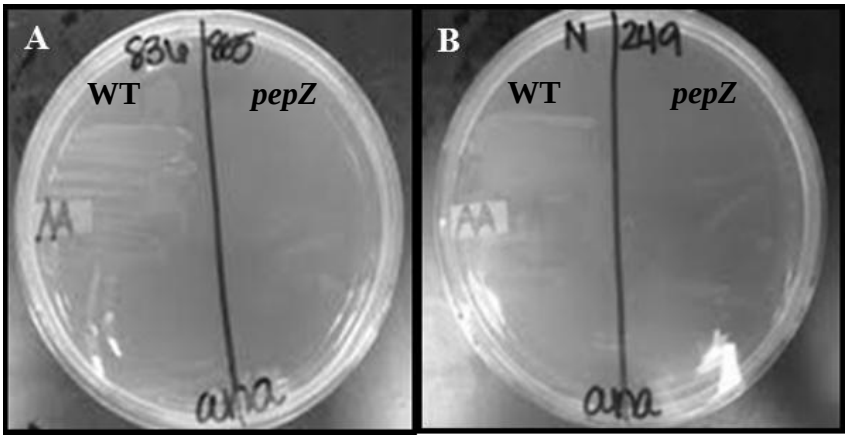

Figure 14. Anaerobic Growth Analysis of *pepZ* mutants using Amino Acid Limited Media. Anaerobic growth comparison on chemically defined media limited for amino acids demonstrated an impaired ability in the mutant strains **(A)** USA300 FPR *pepZ* and **(B)** Newman *pepZ* to grow. WT refers to wild-type, and the associated *pepZ* mutant is indicated as *pepZ* on the figure.

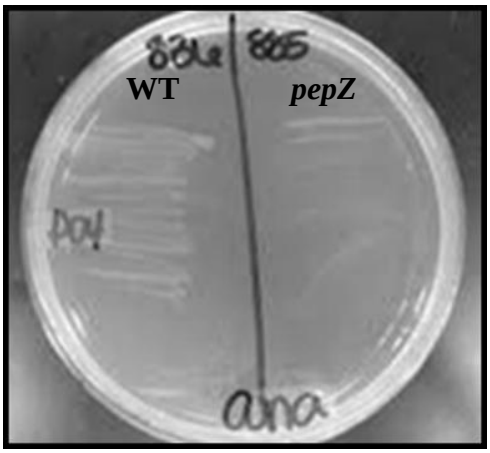

Figure 15. Anaerobic Growth Analysis of a USA300 FPR *pepZ* mutant Limited for Phosphate. Anaerobic growth comparison of USA300 FPR and its *pepZ* mutant on phosphate limiting media identified an impaired ability in the mutant strain to grow. USA300 FPR wild-type is shown as WT and the associated *pepZ* mutant is indicated as *pepZ* on the figure.

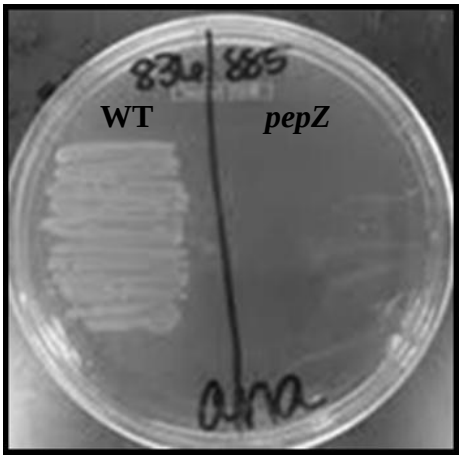

Figure 16. Anaerobic Growth Analysis of a USA300 FPR *pepZ* mutant on Mannitol Salt Agar. Anaerobic growth comparison of USA300 FPR and its *pepZ* mutant on MSA demonstrates a decreased ability in the mutant strain to utilize mannitol. USA300 FPR wild-type is shown as WT and the associated *pepZ* mutant is indicated as *pepZ* on the figure.

Evaluating the Role of PepZ in *S. aureus* Carbon Utilization using Chemically Defined Media. The proteolytic activity of aminopeptidases in part provides cellular sources of energy and nutrition. This is often achieved through the catabolism of amino acids, which result in metabolic by-products that converge as intermediates in central metabolic pathways. We therefore explored the role of PepZ in carbon utilization using

chemically defined liquid media, enriched with 100 µg ml^{-1} of galactose, ribose, lactose, mannose, fructose, trehalose, raffinose, D-glucosamine or xylose. Exponentially growing cells of USA300 FPR, SH1000 and Newman were assessed in parallel with their *pepZ* mutants. In this experiment, identical carbon utilization profiles and patterns of growth were identified across all strains (data not shown). These results suggest no direct role for PepZ in the carbon based cellular energy status of *S. aureus*.

Characterization of the Role of PepZ in Membrane Integrity and Autolysis. The intracellular processing of damaged proteins is vital to cell stability in all organisms [Nandi et al., 2006]. As such, peptide turnover is often mediated through the proteolytic activities of aminopeptidases, which may be crucial to cell wall degradation and biosynthesis as a result of cell autolysis [Rawlings and Barrett, 2004]. We therefore sought to characterize the role of PepZ in cell wall stability. This was examined using penicillin-G and Triton X-100 to induce cell lysis in the parent strains USA300 FPR and Newman, and their respective *pepZ* mutants. Penicillin-G induced cell lysis was assayed using exponentially growing cells in TSB containing 0.4 ug ml^{-1} penicillin-G [Fujimoto and Bayles, 1998]. Cell lysis, monitored in 30 minute intervals by turbidity change, did not reveal any alterations in either background between the *pepZ* mutant and wild-type strains (data not shown). Triton X-100 cell lysis experiments were carried out using exponentially growing cells resuspended in 0.05M Tris-HCl (pH 7.6) containing 0.05% Triton X-100. Cultures were incubated at 30°C shaking and measured for changes in turbidity in 30 minute intervals [Mani et al., 1993; Shaw et al., 2005]. In this experiment we identified an increase in parent strain viability when compared to the mutants (Fig.

17). This phenotype was more prominent in Newman, in which mutant strain survival decreased by approximately 2-fold at 60, 90 and 120 minutes. This was followed by a 3.86-fold final reduction of *pepZ* mutant cells when compared to the parent. As for the USA300 FPR strains, a decrease in survival of 1.2-fold was identified at 30 minutes for the mutant, followed by decreases of 1.4-fold at 60 minutes, 1.3-fold at 90 minutes, 1.2-fold at 120 minutes and 1.4-fold at 150 minutes when compared to the parent strain after exposure to cell lysis inducing conditions.

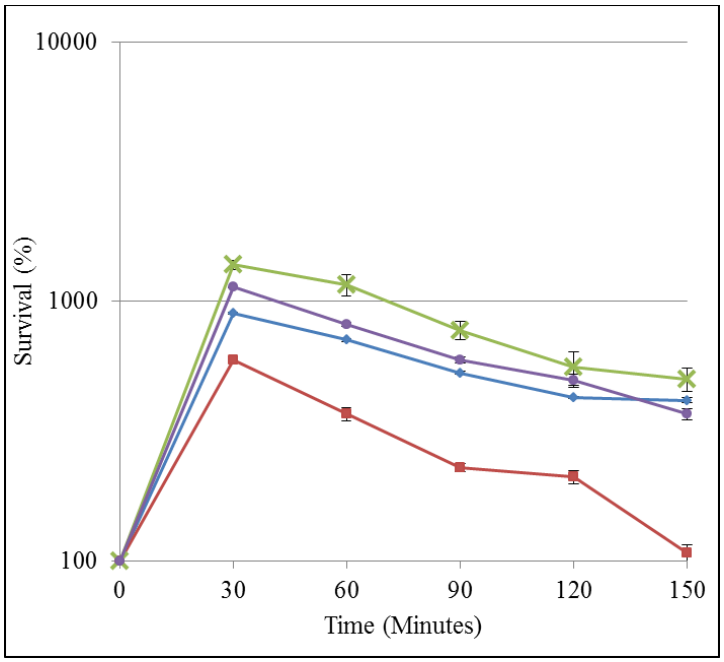

Figure 17. The Role of PepZ in Membrane Integrity and Autolysis. The effect of Triton X-100 mediated cell lysis on parent strains Newman (◆) and USA300 FPR (X), and their mutant derivatives Newman *pepZ* (■) and USA300 FPR *pepZ* (●). Results are represented as percent survival measured as OD600 at the specified time intervals from 3 independent experiments (+/- SD). Significant values (*) were determined using a Student's *t* test ($p<0.05$).

Evaluating the Role of PepZ in Cellular Survival Following Exposure to Elevated Temperature. We next sought to investigate the role of PepZ in response to increased temperatures, using heat shock and adaptation experiments, as proteolytic processing or

turnover of misfolded proteins due to increased temperatures is a common function of aminopeptidases. These experiments were performed at temperatures of 55°C using cells resuspended in sterile TSB at an OD_{600} of 0.2. Heat shock was induced by placing cultures in a 55°C water bath for 30 minutes and before returning them to standard growth conditions at 37°C, with shaking. Cell viability was monitored in 30 minute intervals by optical density readings at OD_{600} [Shaw et al., 2008]. We identified no alteration in either background between the *pepZ* mutant and wild-type strain when grown under these conditions (data not shown). A role for PepZ in heat adaptation was assessed using exponentially growing cells in TSB, incubated at 55°C with shaking. Cell death was monitored by viable cell counts performed in 20 minute intervals for two hours from two independent experiments [Shaw et al., 2008]. What we identified was a decreased capacity for survival in the Newman *pepZ* mutant strain compared to the wild-type (Fig. 18). Following 20 minutes of incubation at 55˚C, Newman *pepZ* mutant cells decreased by 60-fold when compared to the parent, followed by undetectable levels of the mutant at 40 minutes. The USA300 FPR wild-type and *pepZ* mutant strains lost viability at equivalent rates, and were undetectable after 60 minutes of incubation at 55°C.

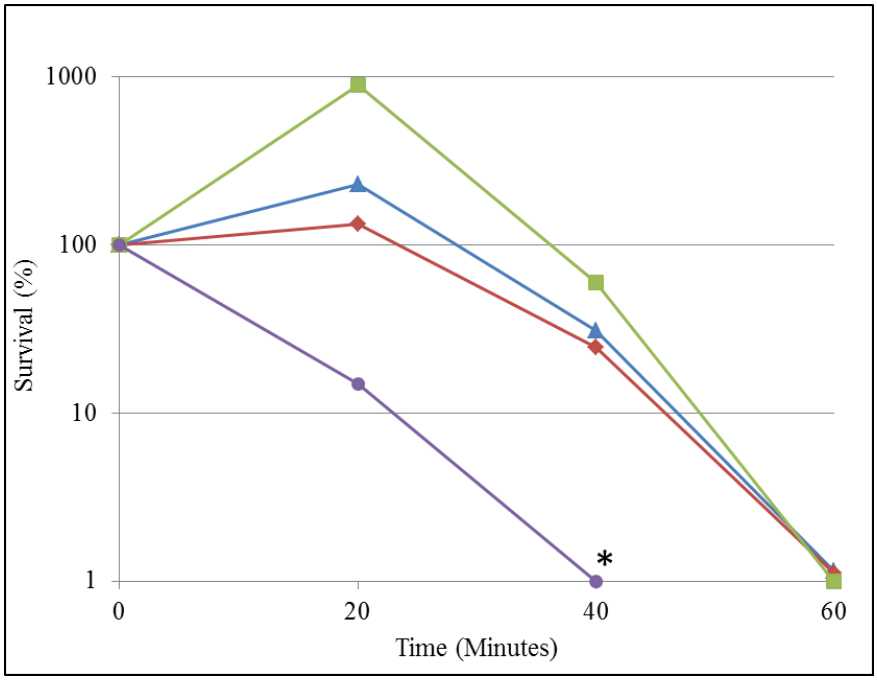

Figure 18. **The Role of PepZ in Response to Elevated Temperatures.** Wild-type strains Newman (■) and USA300 FPR (▲) with their mutant derivatives Newman *pepZ* (●) and USA300 FPR *pepZ* (◆) were characterized for variations in adaptation to heat stress at 55°C. We identified a decreased capacity for survival in the Newman *pepZ* mutant strain compared to the wild-type, whereas the USA300 FPR wild-type and *pepZ* mutant strains lost viability at equivalent rates. Data are represented as an average percent survival from duplicate experiments**.** Significant values (*) were determined using a Student's *t* test ($p<0.05$).

Assessing the Role of PepZ in Response to Oxidative Stresses. Many stresses the bacterial cell encounters can result in protein denaturing and damage; one such being oxidative stress. We therefore sought to explore the potential role of PepZ in protein stability and turnover in response to oxidative stress induced by hydrogen peroxide. This was explored in the wild-type strains Newman and USA300 FPR, and their mutant derivatives. We performed this assay using PBS washed cells resuspended in sterile PBS containing 7.5mM H_2O_2. Cultures were incubated with shaking at 37°C, and monitored at 20 minute intervals by viable cell counts, performed in PBS containing 10 mg ml^{-1} catalase for H_2O_2 inactivation [Watson et al., 1998]. We identified decreased cell

viability for all strains, with no variation between the wild-types and mutants (data not shown). These results suggest no role for PepZ in the cellular response to oxidative stress, at least under the conditions tested.

General Stress Profiling of *pepZ* mutant Strains using a Modified Kirby-Bauer Assay. We examined the role of PepZ in cellular survival using a variety of chemical stressors. This was explored using disk diffusion assays to identify changes in susceptibility of *pepZ* mutants and their parent strains. Disk diffusion assays were performed in triplicate as described above, without the addition of X-Gal [Peng et al., 1988]. Zones of inhibition were measured in mm to identify changes in susceptibility to the various chemical compounds (Table 3). In doing so we identified increased menadione resistance in the USA300 FPR *pepZ* mutant (15.6 mm) when compared to the parent (36 mm), resulting in a 2.3-fold change. Further analysis revealed the average minimum inhibitory concentration of menadione in the USA300 FPR strain was 1.46 µg ml^{-1}, whilst the mutant was 5.1 µg ml^{-1}. In the Newman strain, a limited increase in susceptibility to hydrogen peroxide was identified in the Newman *pepZ* mutant (51 mm) when compared to the parent (46.3 mm). Additionally, limited increased menadione susceptibility in the Newman *pepZ* mutant (17 mm) was identified when compared to the parent (21 mm).

Characterization of the Subcellular Localization of PepZ. Subsequent to the nutritional analysis of PepZ in *S. aureus*, we sought to explore a role for PepZ in protein stability using proteomic analysis. The analysis of preliminary mass spectrometry data

obtained in our laboratory had previously identified PepZ in secreted protein fractions from 15 hour cultures harvested from the SH1000 wild-type. This identified extracellular localization of PepZ may be the result of stationary phase cell lysis, or legitimate secretion. Therefore we sought to investigate further the subcellular localization of this aminopeptidase, as it is predicted to be an intracellular protein. To examine this, we constructed wild-type strains of *S. aureus* USA300 FPR and Newman containing a *pepZ* gene bearing a 6-His tag, using the shuttle vector pMK4. We then purified both intracellular and secreted proteomes from these strains at hours 5 and 15, to monitor the levels of PepZ both inside and outside of the cell. Extracting proteomes at these time points corresponds to post exponential and stationary phase growth, respectively, allowing us to clarify the potential for PepZ secretion during earlier growth stages that would not be associated with cell lysis. We used Western blot detection methods, targeting the 6-His tag, to identify levels of PepZ expression using a SuperSignal West HisProbe Kit. Using this method, we identified PepZ in intracellular and secreted protein fractions extracted from USA300 FPR and Newman cultures at hours 5 and 15. Protein fractions collected from the Newman background at hours 5 (Fig.19A) and 15 (Fig. 19B) identified a 55 kDa band corresponding to the expected size of PepZ at both of the time points in the cytoplasmic and secreted fractions.

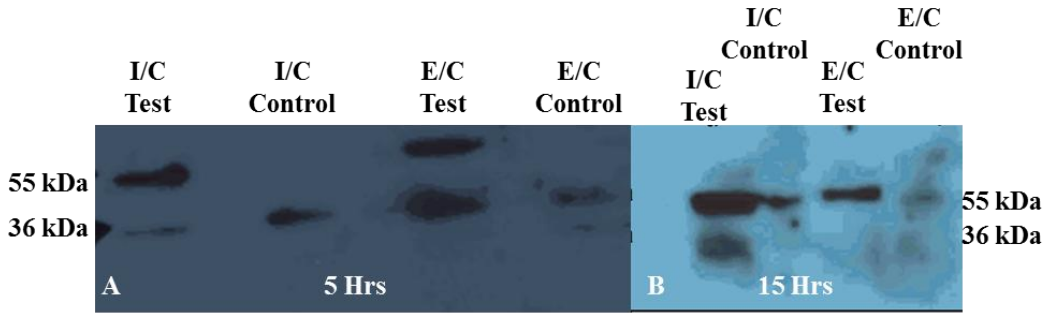

Figure 19. Western Blot Detection of PepZ in Strain Newman. Western blot analysis of Newman pMK4::*pepZ* 6-His and empty vector controls detected a 55 kDa protein band in both intracellular (I/C) and secreted (E/C) protein samples collected at (**A**) 5 and (**B**) 15 hours. Empty vector controls are labeled as control. Protein samples were standardized to 1 µg of total protein per lane.

Further, a pMK4 empty vector was run concurrently as a negative control from intracellular and secreted protein samples collected from 5 and 15 hour cultures, which did not detect protein bands at 55 kDa. Similarly, a 55 kDa band was identified in the USA300 FPR background at hours 5 (Fig. 20A) and 15 (Fig. 20B) from both intracellular and secreted protein fractions. Again, a pMK4 empty vector was run concurrently as a negative control from intracellular and secreted protein samples collected from 5 and 15 hour cultures, which did not detect protein bands at 55 kDa. Including the pMK4 negative control ensured the produced 55 kDa band was not a false positive produced from protein samples collected from the pMK4 vector, which was used to construct the 6-His strains.

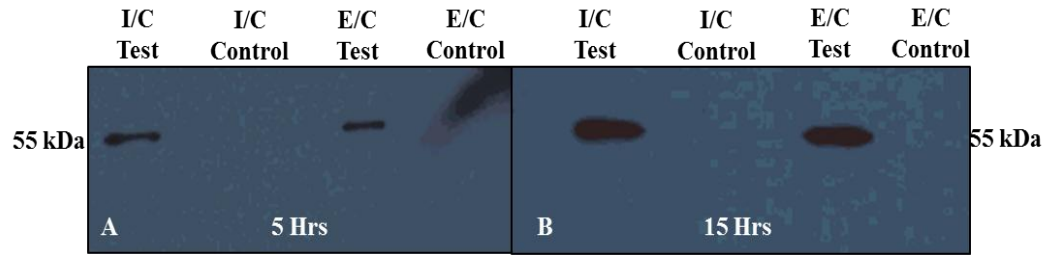

Figure 20. Western Blot Detection of PepZ in Strain USA300 FPR. Western blot analysis of USA300 FPR pMK4::*pepZ* 6-His and empty vector control detected a 55 kDa protein band in both intracellular (I/C) and secreted (E/C) protein samples collected at (**A**) 5 and (**B**) 15 hours. Empty vector controls are labeled as control. Protein samples were standardized to 1 µg of total protein per lane.

Proteomes were further explored for cellular localization patterns of PepZ from intracellular and secreted protein samples collected hourly for eight hours from synchronized cultures in the Newman background. Protein samples demonstrated an increased abundance of PepZ in cytoplasmic fractions at hours two through four, which decreased at later time points (Fig. 21A). In comparison, PepZ detection in the secretome remained relatively consistent through the eight hour period, with a 55 kDa band detected at similar levels of protein abundance at hours three through eight (Fig. 21B). From these experiments, we have identified the potential for PepZ secretion in *S. aureus*, suggesting a possible extracellular role for this aminopeptidase.

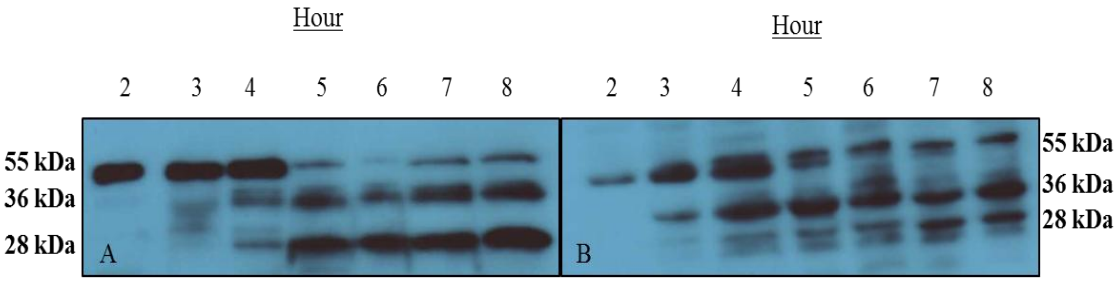

Figure 21. Detection of PepZ during Continuous Growth of Strain Newman. Western blot analysis of Newman bearing a *pepZ*::6-His identified changes in PepZ (55 kDa) abundance over an eight hour period from intracellular (**A**) and extracellular samples (**B**). Samples collected at hour 1 failed to identify any detectable protein, and are not shown. Protein samples were standardized to 1 µg of total protein per lane.

Exploring Potential Substrates for the PepZ Enzyme using 2D Difference Gel Electrophoresis (DIGE) and Tandem Mass Spectrometry. Experimental data collected thus far demonstrates an important role for PepZ in *S. aureus* virulence. Additionally, we have shown that PepZ is capable of being externalized during the growth of *S. aureus* strains. We therefore sought to clarify how PepZ fulfills its enzymatic role at the level of protein stability. Accordingly, we probed the proteomes of

pepZ mutant and parental strains to identify alterations in the stability of proteins both within, and outside, the cell. Proteome profiling of secreted and intracellular proteomes from USA300 FPR wild-type and *pepZ* mutant strains using 2D-DIGE coupled with mass spectrometry was performed in collaboration with the ICBR facility at the University of Florida. 2D-DIGE analysis provides the ability to quantify sample specific changes in protein abundance using a single gel and fluorescent labeling. Protein samples are mixed and run together with an internal standard, allowing protein samples to be resolved to the same intensity and measured relative to the internal reference. Gels can then them be visualized for changes in color, indicating altered protein abundance levels or changes in proteolytic processing. As such, this method of analysis was selected to identify the effect of PepZ on changes in the protein profile of *S. aureus*. Briefly, intracellular and secreted proteomes were collected in triplicate from USA300 FPR wild-type and *pepZ* mutant strains from three hour cultures, corresponding to peak expression of *pepZ*. Protein fractions were then purified and transferred to the ICBR facility at the University of Florida. Protein spots determined with increased or decreased protein levels of 1.2-fold or more were then extracted and analyzed for identification using mass spectrometry and MASCOT software.

Differential analysis of intracellular fractions identified eleven protein spots that demonstrated fold changes ranging from -7 to 1.74 in at least six of nine 2-D protein map images ($p<0.05$) between the wild-type and mutant strains (Fig. 22). From the eleven spots identified from in gel analysis, mass spectrometry identified 30 total proteins with two unique peptides and a 95% protein identification probability as determined by protein

Prophet using Scaffold software, in which multiple proteins were identified for each spot (Table 5). Additionally, protein spots 1425, 1780, 1806, 1818, 1831, 2046 and 2139 identified variations in protein molecular weight, which may be due to altered protein cleavage in the absence of PepZ (Table 6). These proteins include: autolysin, alpha-hemolysin, N-acetylmuramoyl-L-alanine amidase domain protein, 50s ribosomal proteins, 30s ribosomal proteins, elastin binding proteins, staphopain A, foldase, Alkaline shock protein, putative lipoprotein and ATP-dependent Clp protease.

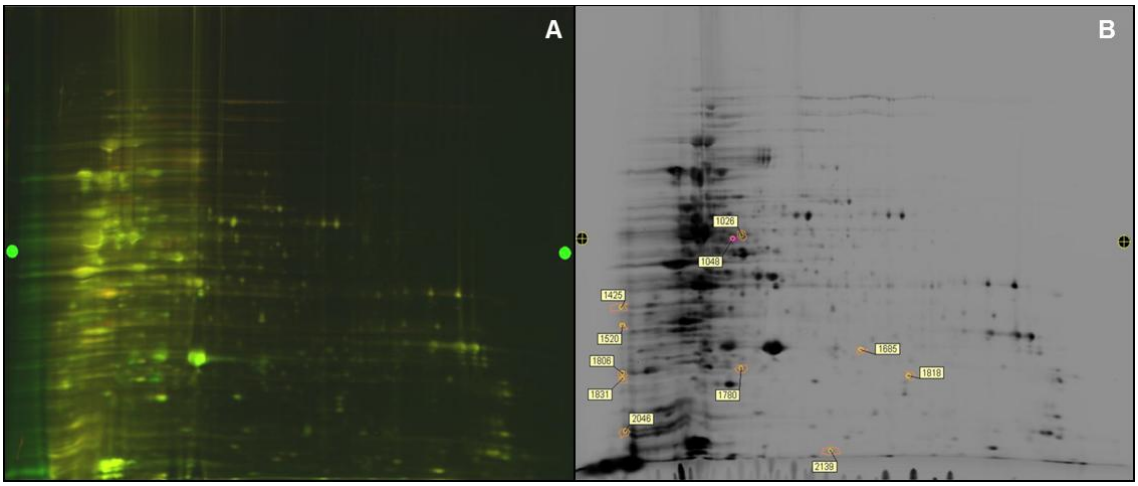

Figure 22. Intracellular Proteome Analysis of *S. aureus* USA300 FPR and its *pepZ* mutant using 2D-DIGE. (A) Differential analysis of intracellular proteins from the USA300 FPR wild-type and *pepZ* mutant strains following isoelectric focusing using a 24 cm pH 3 to 10 non linear IPG strip at 10 k volts. USA300 FPR wild-type proteins are indicated by the green fluorescent color and *pepZ* mutant proteins are shown in red. (**B**) In gel analysis identified 11 proteins with varied levels of abundance by at least 1.5 fold ($p<0.05$), which were further characterized using mass spectrometry analysis.

Table 5. Intracellular Proteome Analysis of *S. aureus* USA300 FPR and its *pepZ* mutant using Mass Spectrometry

Spot	Protein [A]	Peptides [A]	Protein [B]	Peptides [B]	Protein [C]	Peptides [C]	Protein [D]	Peptides [D]	Protein [E]	Peptides [E]	Protein [F]	Peptides [F]	Fold Δ
1831	50S ribosomal protein L4 RplD (USA300)	4	Uncharacterized leukocidin-like protein 2 SAUSA300_1975	3	50S ribosomal protein L6 RplF (USA300)	2							-7
1806	50S ribosomal protein L6 RplF (USA300)	4	50S ribosomal protein L4 RplD (USA300)	3	Staphopain A SAUSA300_1890	3	ATP-dependent Clp protease proteolytic subunit (USA300)	2	Uncharacterized leukocidin-like protein 2 SAUSA300_1975	2			-5.37
1520	5'-nucleotidase, lipoprotein e(P4) family SAUSA300_0307	6	ABC transporter, substrate-binding protein SAUSA300_0618	3	Secretory antigen SsaA (USA300)]	2	Uncharacterized leukocidin-like protein 2 SAUSA300_1975	2					-5.01
1425	N-acetylmuramoyl-L-alanine amidase Sle1(USA300)	3	Foldase protein PrsA (USA300)	2	50S ribosomal protein L25 PlY (USA300)	2	30S ribosomal protein S2 RpsB (USA300)	2					-3.68
2046	50S ribosomal protein L19 RplS (USA300)	5	50S ribosomal protein L14 RplN (USA300)	4	50S ribosomal protein L21 RplU (USA300)	4	Putative uncharacterized protein SAUSA300_0602	3	30S ribosomal protein S11 RpsK (USA300)	3			-3.22
2139	Alkaline shock protein 23 Asp23 (USA300)	3											-2.34
1818	ATP synthase subunit delta AtpH (USA300)	3	Elastin-binding protein EbpS (USA300)	2									-1.54

1685	50S ribosomal protein L1 RplA (USA300)	4	Uridylate kinase PyrH (USA300)	2									-1.54
1780	50S ribosomal protein L6 RplF (USA300)	7	Putative lipoprotein SAUSA300_0372	4	50S ribosomal protein L4 rplD (USA300)	3	Uncharacterized leukocidin-like protein 2 SAUSA300_1975	2	ATP-dependent Clp protease proteolytic subunit (USA300)	2			-1.49
1026	Enolase Eno (USA300)	3	Autolysin Atl (USA300)	3	NAD-specific glutamate dehydrogenase GudB (USA300)	2							1.51
1048	Protein RecA (USA300)	9	3-oxoacyl-[acyl-carrier-protein] synthase 2 FabF (USA300)	7	Enolase Eno (USA300)	4	Autolysin Atl (USA300)	3	Immunoglobulin-binding protein Sbi (USA300)	3	Adenylosuccinate lyase PurB (USA300)	2	1.74

**Mass spectrometric analysis identified 30 proteins from the 11 protein spots having fold changes of 1.5 fold or greater ($p<0.05$) between the USA300 FPR and pepZ mutant intracellular proteomes. Proteins were identified by unique peptide values of two or more and a 95% protein identification probability as determined by protein Prophet for each spot using Scaffold software.*

Table 6. Intracellular Protein Spots Identified by 2D-DIGE and Mass Spectrometry Analysis to Have Altered Protein Stability

Spot	2D MW	Protein [A]	Expected MW [A]	Protein [B]	Expected MW [B]	Protein [C]	Expected MW [C]	Protein [D]	Expected MW [D]
1425	33 kDa	Foldase protein PrsA (USA300)	36 kDa	N-acetylmuramoyl-L-alanine amidase Sle1 (USA300)					
1780	18 kDa	50S ribosomal protein L6 RplF (USA300)	20 kDa	Putative lipoprotein SAUSA300_0372	21 kDa	ATP-dependent Clp protease proteolytic subunit ClpP (USA300)	22 kDa	Uncharacterized leukocidin-like protein 2 SAUSA300_1975	40 kDa
1806	17 kDa	50S ribosomal protein L6 RplF (USA300)	20 kDa	ATP-dependent Clp protease proteolytic subunit ClpP (USA300)	22 kDa	Uncharacterized leukocidin-like protein 2 SAUSA300_1975	40 kDa	Staphopain A SAUSA300_1890	44 kDa
1818	18 kDa	ATP synthase subunit delta AtpH (USA300)	20 kDa	Elastin-binding protein EbpS (USA300)	53 kDa				
1831	181 kDa	50S ribosomal protein L6 RplF (USA300)	20 kDa	50S ribosomal protein L4 RplD (USA300)	22 kDa	Uncharacterized leukocidin-like protein 2 SAUSA300_1975	40 kDa		
2046	10 kDa	50S ribosomal protein L21 RplU (USA300)	11 kDa	50S ribosomal protein L14 RplN (USA300)	13 kDa	30S ribosomal protein S11 RpsK (USA300)	14 kDa	Putative uncharacterized protein SAUSA300_0602	19 kDa
2139	9 kDa	Alkaline shock protein 23 Asp23 (USA300)	19 kDa						

**In the absence of PepZ, protein spots 1425, 1780, 1806, 1818, 1831, 2046 and 2139 were identified to have variations in 2D-DIGE predicted molecular weight values compared to mass spectrometry predicted protein molecular weight values. These results indicate potential changes in intracellular protein processing events in the absence of PepZ. Protein cleavage was determined by +/- 2 kDa in protein molecular weight changes, determined between the two analyses.*

2D-DIGE performed on the secreted protein fractions produced 83 protein spots that demonstrated fold changes ranging from -1.33 to 15.05 ($p<0.05$) between the USA300 FPR wild-type and *pepZ* mutant strains (Fig. 23). Mass spectrometry and Scaffold software analysis identified 43 proteins from the 83 spots shown to vary in protein intensity and abundance between the *pepZ* mutant and wild-type secretomes (Table 7).

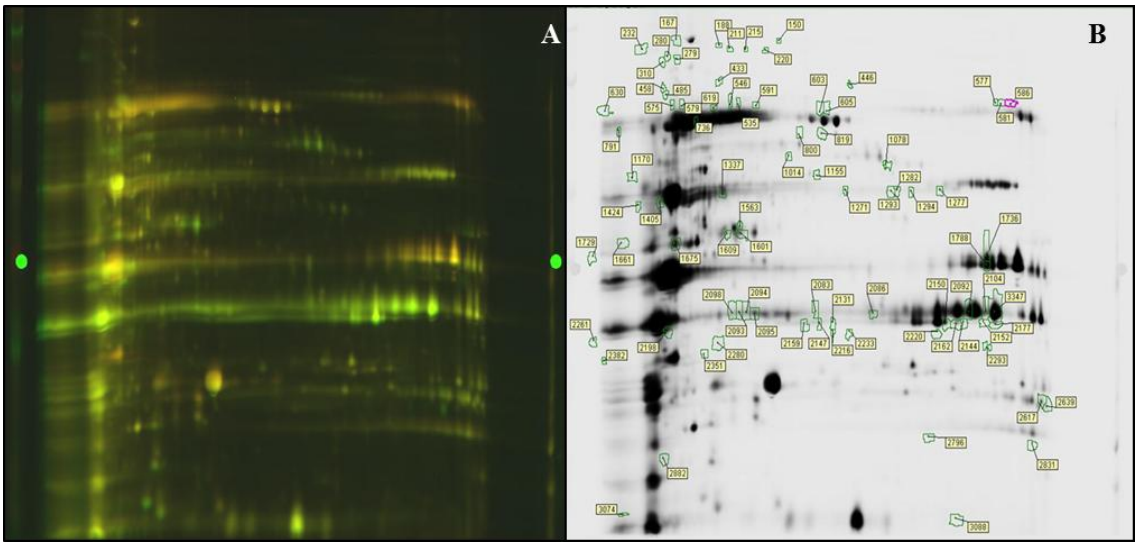

Figure 23. Secretome Analysis of *S. aureus* USA300 FPR and its *pepZ* mutant using 2D-DIGE. (A) Differential analysis of secreted proteins from the USA300 FPR wild-type and *pepZ* mutant strains following isoelectric focusing using a 24 cm pH 3 to 10 non linear IPG strip at 10 k volts. USA300 FPR wild-type proteins are indicated by the green fluorescent color and *pepZ* mutant proteins are shown in red. (**B**) In gel analysis identified 83 proteins with varied levels of abundance by at least 1.5 fold ($p<0.05$), which were further characterized using mass spectrometry analysis. Mass spectrometry analysis failed to identify proteins for 28 of the 83 spots, which are listed in appendix 1.

Scaffold software analysis identified the proteins according to unique peptide sequences, in which to two unique peptides and a 95% protein identification probability as determined by protein Prophet was used for protein identification. Based on these parameters, proteomic analysis failed to identify proteins in 28 of the 83 protein spots. Additionally, protein spots 3074, 591, 535, 630, 586, 2351, 579, 575, 736, 819, 619, 1788, 791, 1337, 1282, 1405, 1271, 2639, 2095, 2083, 1675, 2159, 2831, 3347, 2617,

Table 7. Secretome Analysis of *S. aureus* USA300 FPR and its *pepZ* mutant using Mass Spectrometry

Spot	Protein [A]	Peptides [A]	Protein [B]	Peptides [B]	Protein [C]	Peptides [C]	Protein [D]	Peptides [D]	Fold Δ
581	Triacylglycerol lipase SAUSA300_0320	2							-2.41
577	Triacylglycerol lipase SAUSA300_0320	7							-2.38
3074	Thermonuclease Nuc (USA300)	5							-2.15
546	Triacylglycerol lipase SAUSA300_0320	8							-2.12
591	Triacylglycerol lipase SAUSA300_0320	15	Autolysin Atl (USA300)	13					-2
535	Autolysin Atl (USA300)	22	Triacylglycerol lipase SAUSA300_0320	10					-1.94
630	Autolysin Atl (USA300)	7	Triacylglycerol lipase SAUSA300_0320	4					-1.9
586	Triacylglycerol lipase SAUSA300_0320	11	Autolysin Atl (USA300)	3					-1.88
211	Triacylglycerol lipase SAUSA300_0320	2							-1.88
1736	Uncharacterized leukocidin-like protein 1 SAUSA300_1974	7							-1.83
280	Serine-aspartate repeat-containing protein E SdrE (USA300)	5							-1.83
2351	Uncharacterized leukocidin-like protein 1 SAUSA300_1974	4							-1.74
579	Autolysin Atl (USA300)	7	Triacylglycerol lipase SAUSA300_0320	3	Elongation factor G (USA300)	2			-1.73
603	Triacylglycerol lipase SAUSA300_0320	9	N-acetylmuramoyl-L-alanine amidase domain protein SAUSA300_2579	5					-1.72
575	Autolysin Atl (USA300)	13	Triacylglycerol lipase SAUSA300_0320	7					-1.66
736	Triacylglycerol lipase SAUSA300_0320	17	N-acetylmuramoyl-L-alanine amidase domain protein SAUSA300_2579	4	Dihydrolipoamide acetyltransferase SAUSA300_0995	3			-1.65
819	N-acetylmuramoyl-L-alanine amidase domain protein SAUSA300_2579	4							-1.64
619	Triacylglycerol lipase SAUSA300_0320	10	Triacylglycerol lipase SAUSA300_0320	10	Autolysin Atl (USA300)	5			-1.62

1788	Uncharacterized leukocidin-like protein 1 SAUSA300_1974	8	N-acetylmuramoyl-L-alanine amidase domain protein SAUSA300_2579	2					-1.61
605	Triacylglycerol lipase SAUSA300_0320	6	N-acetylmuramoyl-L-alanine amidase domain protein SAUSA300_2579	6					-1.59
791	Triacylglycerol lipase SAUSA300_0320	15	Dihydrolipoamide acetyltransferase SAUSA300_0995	6	N-acetylmuramoyl-L-alanine amidase domain protein SAUSA300_2579	2			-1.58
433	Triacylglycerol lipase SAUSA300_0320	3							-1.58
1337	Autolysin Atl (USA300)	16	Putative cell wall surface anchor family protein SAUSA300_2436	8	Glycerol phosphate lipoteichoic acid synthase ItaS (USA300)	8	Triacylglycerol lipase SAUSA300_0320	3	-1.57
1170	Dihydrolipoyl dehydrogenase IpdA (USA300)	4							-1.57
1282	Putative cell wall surface anchor family protein SAUSA300_2436	13	Glycerol phosphate lipoteichoic acid synthase ItaS strain USA300)	3					-1.56
1405	Putative cell wall surface anchor family protein SAUSA300_2436	10	Autolysin Atl (USA300)	3	Enolase Eno (USA300)	2			-1.55
1293	Putative cell wall surface anchor family protein SAUSA300_2436	17							-1.55
1294	Putative cell wall surface anchor family protein SAUSA300_2436	12							-1.53
1424	Putative cell wall surface anchor family protein SAUSA300_2436	10	Autolysin Atl (USA300)	5					-1.51
232	Clumping factor A ClfA (USA300)	9	Clumping factor B ClfB (USA300)	7					-1.51
1271	Putative cell wall surface anchor family protein SAUSA300_2436	7	Autolysin Atl (USA300)	6					-1.5
2639	Serine protease SplE (USA300)	6	Serine protease SplF (USA300)	3					1.46
2095	Alpha-hemolysin SAUSA300_1058	14	N-acetylmuramoyl-L-alanine amidase Sle1 (USA300)	3	Panton-Valentine leukocidin, LukS-PV (USA300)	2			1.49
2083	Alpha-hemolysin SAUSA300_1058	5							1.51
1675	Triacylglycerol lipase SAUSA300_0320	8	Immunoglobulin-binding protein Sbi (USA300)	3					1.52
2159	Alpha-hemolysin SAUSA300_1058	2							1.54
2831	Staphopain A SAUSA300_1890	8							1.55
3347	Alpha-hemolysin SAUSA300_1058	20	Panton-Valentine leukocidin, LukS-PV (USA300)	2					1.56
2617	Serine protease SplE (USA300)	2	Serine protease SplF (USA300)	3					1.57

2198	Alpha-hemolysin SAUSA300_1058	14	Panton-Valentine leukocidin, LukS-PV (USA300)	9	1-phosphatidylinositol phosphodiesterase Plc (USA300)	4	Leukotoxin LukE (USA300)	2	1.57
2094	Alpha-hemolysin SAUSA300_1058	13	N-acetylmuramoyl-L-alanine amidase Sle1 (USA300)	4					1.58
2098	Alpha-hemolysin SAUSA300_1058	8	Panton-Valentine leukocidin, LukS-PV (USA300)	3	N-acetylmuramoyl-L-alanine amidase Sle1 (USA300)	2			1.59
2150	Alpha-hemolysin SAUSA300_1058	8	1-phosphatidylinositol phosphodiesterase Plc (USA300)	6					1.61
2162	Alpha-hemolysin SAUSA300_1058	13	1-phosphatidylinositol phosphodiesterase Plc (USA300)	2					1.63
2092	Alpha-hemolysin SAUSA300_1058	18							1.64
2882	Staphopain A SAUSA300_1890	2							1.65
2147	Alpha-hemolysin SAUSA300_1058	10	1-phosphatidylinositol phosphodiesterase Plc (USA300)	2					1.7
2152	Alpha-hemolysin SAUSA300_1058	12	Panton-Valentine leukocidin, LukS-PV (USA300)	3	Uncharacterized leukocidin-like protein 1 SAUSA300_1974	6			1.75
2131	Alpha-hemolysin SAUSA300_1058	6							1.77
2177	Alpha-hemolysin SAUSA300_1058	20	Panton-Valentine leukocidin, LukS-PV (USA300)	3					1.82
2144	Alpha-hemolysin SAUSA300_1058	16							1.82
2093	Alpha-hemolysin SAUSA300_1058	6							1.82
2086	Alpha-hemolysin SAUSA300_1058	7	1-phosphatidylinositol phosphodiesterase Plc (USA300)	2					1.93
2220	1-phosphatidylinositol phosphodiesterase Plc (USA300)	7							2.74
2261	Alpha-hemolysin SAUSA300_1058	5	1-phosphatidylinositol phosphodiesterase Plc (USA300)	3					15.05

** Mass spectrometric analysis identified 43 proteins from the 83 protein spots having fold changes of 1.5 fold or greater ($p<0.05$) in the USA300 FPR and pepZ mutant secretomes. Proteins were identified by unique peptide values of two or more and a 95% protein identification probability as determined by protein Prophet for each spot using Scaffold software.*

2198, 2094, 2098, 2150, 2162, 2092, 2882, 2147, 2152, 2131, 2177, 2144, 2093, 2086, 2220 and 2261 identified variations in protein molecular weight size due to potential altered protein stability in the absence of PepZ (Table 8). These proteins include: autolysin, alpha-hemolysin, N-acetylmuramoyl-L-alanine amidase domain protein, glycerol phosphate lipoteichoic acid synthase, serine proteases SplE and SplF, immunoglobulin-binding protein, staphopain A, 1-phosphatidylinositol phosphodiesterase, thermonuclease, uncharacterized leukocidin-like protein 1, triacylglycerol lipase and Panton-Valentine leukocidin, LukS-PV.

Table 8. Secreted Protein Spots Identified by 2D-DIGE and Mass Spectrometry Analysis to Have Altered Protein Stability

Spot	2D MW	Protein [A]	Expected MW [A]	Protein [B]	Expected MW [B]	Protein [C]	Expected MW [C]	Protein [D]	Expected MW [D]
535	86 kDa	Autolysin Atl (USA300)	137 kDa						
575	85 kDa	Autolysin Atl (USA300)	137 kDa						
579	84 kDa	Autolysin Atl (USA300)	137 kDa						
586	86 kDa	Autolysin Atl (USA300)	137 kDa						
591	84 kDa	Autolysin Atl (USA300)	137 kDa						
619	82 kDa	Autolysin Atl (USA300)	137 kDa						
630	77 kDa	Autolysin Atl (USA300)	137 kDa						
736	68 kDa	Triacylglycerol lipase SAUSA300_0320	76 kDa						
791	65 kDa	N-acetylmuramoyl-L-alanine amidase domain protein SAUSA300_2579	69 kDa	Triacylglycerol lipase SAUSA300_0320	76 kDa				

819	64 kDa	N-acetylmuramoyl-L-alanine amidase domain protein SAUSA300_2579	69 kDa						
1271	52 kDa	Autolysin Atl (USA300)	137 kDa						
1282	52 kDa	Glycerol phosphate lipoteichoic acid synthase ItaS (USA300)	74 kDa						
1337	52 kDa	Glycerol phosphate lipoteichoic acid synthase ItaS (USA300)	74 kDa	Triacylglycerol lipase SAUSA300_0320	76 kDa	Autolysin Atl (USA300)	137 kDa		
1405	51 kDa	Autolysin Atl (USA300)	137 kDa						
1675	41 kDa	Immunoglobulin-binding protein Sbi (USA300)	50 kDa	Triacylglycerol lipase SAUSA300_0320	76 kDa				
1788	41 kDa	N-acetylmuramoyl-L-alanine amidase domain protein SAUSA300_2579	69 kDa						
2083	33 kDa	Alpha-hemolysin SAUSA300_1058	36 kDa						
2086	32 kDa	Alpha-hemolysin SAUSA300_1058	36 kDa	1-phosphatidylinositol phosphodiesterase Plc (USA300)	37 kDa				
2092	33 kDa	Alpha-hemolysin SAUSA300_1058	36 kDa						
2093	33 kDa	Alpha-hemolysin SAUSA300_1058	36 kDa						
2094	33 kDa	Alpha-hemolysin SAUSA300_1058	36 kDa						

2095	32 kDa	Panton-Valentine leukocidin, LukS-PV (USA300)	35 kDa	Alpha-hemolysin SAUSA300_1058	36 kDa				
2098	32 kDa	Panton-Valentine leukocidin, LukS-PV (USA300)	35 kDa	Alpha-hemolysin SAUSA300_1058	36 kDa	Autolysin Atl (USA300)	137 kDa		
2131	29 kDa	Alpha-hemolysin SAUSA300_1058	36 kDa						
2144	29 kDa	Alpha-hemolysin SAUSA300_1058	36 kDa						
2147	29 kDa	Alpha-hemolysin SAUSA300_1058	36 kDa	1-phosphatidylinositol phosphodiesterase Plc (USA300)	37 kDa				
2150	29 kDa	Alpha-hemolysin SAUSA300_1058	36 kDa,	1-phosphatidylinositol phosphodiesterase Plc (USA300)	37 kDa				
2152	29 kDa	Panton-Valentine leukocidin, LukS-PV (USA300)	35 kDa	Alpha-hemolysin SAUSA300_1058	36 kDa	Uncharacterized leukocidin-like protein 1 SAUSA300_1974	39 kDa		
2159	29 kDa	Alpha-hemolysin SAUSA300_1058	36 kDa						
2162	29 kDa	Alpha-hemolysin SAUSA300_1058	36 kDa	1-phosphatidylinositol phosphodiesterase Plc (USA300)	37 kDa				
2177	29 kDa	Panton-Valentine leukocidin, LukS-PV (USA300)	35 kDa	Alpha-hemolysin SAUSA300_1058	36 kDa				

2198	28 kDa	Panton-Valentine leukocidin, LukS-PV (USA300)	35 kDa	Alpha-hemolysin SAUSA300_1058	36 kDa	1-phosphatidylinositol phosphodiesterase Plc (USA300)	37 kDa	Autolysin Atl (USA300)	137 kDa
2220	28 kDa	1-phosphatidylinositol phosphodiesterase Plc (USA300)	37 kDa						
2261	28 kDa	Autolysin Atl (USA300)	36 kDa	1-phosphatidylinositol phosphodiesterase Plc (USA300)	37 kDa				
2351	29 kDa	Uncharacterized leukocidin-like protein 1 SAUSA300_1974	40 kDa						
2617	23 kDa	Serine protease SplE (USA300)	26 kDa	Serine protease SplF (USA300)	26 kDa				
2639	22 kDa	Serine protease SplE (USA300)	26 kDa	Serine protease SplF (USA300)	26 kDa				
2831	18 kDa	Staphopain A SAUSA300_1890	44 kDa						
2882	17 kDa	Staphopain A SAUSA300_1890	44 kDa						
3347	33 kDa	Panton-Valentine leukocidin, LukS-PV (USA300)	35 kDa	Alpha-hemolysin SAUSA300_1058	36 kDa				
3074	12 kDa	Thermonuclease Nuc (USA300)	25 kDa						

****** *In the absence of PepZ, the listed proteins were identified to have variations in 2D-DIGE predicted molecular weight values compared to mass spectrometry predicted protein molecular weight values. These results indicate potential changes in secreted protein cleavage, maturation and or activation events in the absence of PepZ. Protein cleavage was determined by +/- 2 kDa protein molecular weight change determined between the two analyses.*

Exploring the Role of PepZ in the Formation of Biofilms. Biofilms are sessile microbial aggregates assembled in an adhesive structural matrix composed of polysaccharides, DNA and proteins [Lawrence et al., 1991]. The switch of infectious states from adhesion to invasion has been suggested to be primarily driven by the interplay of proteases, and cell adhesion and colonization factors [McGavin et al., 1997]. Indeed, a number of recent studies [Boles and Horswill, 2008; Beenken et al., 2003; and Tsang et al., 2008] have identified the modification of protein profiles via proteases during the detachment stages of *S. aureus* biofilm formation. As such, we decided to explore the role of PepZ on the formation of a biofilm. This experiment was performed in triplicate in the wild-type strains, Newman and USA300 FPR, and their associated *pepZ* mutants. The *S. aureus* strain RN6390 was used as a negative control in the biofilm assays. From this experiment, we identified a minor defect in the ability the USA300 FPR *pepZ* mutant to form a biofilm, where the average absorbance readings from eluted crystal violet at 595 nm for the wild-type was determined to be 0.94 and 0.81 for the *pepZ* mutant, which was measured using a BioTek Synergy2 96-well plate reader (Fig. 24). These results overall suggest a limited role for PepZ in the formation of a biofilm under the conditions tested.

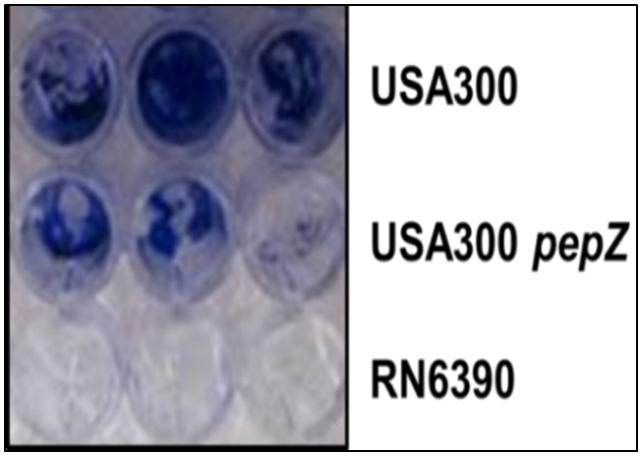

Figure 24. The Role of PepZ in the Formation of an *S. aureus* Biofilm. Biofilm formation assays performed in triplicate detected a slight reduction in the biofilms formed by the USA300 FPR *pepZ* mutant strain when compared to the USA300 FPR parent strain. Biofilm formation was determined by crystal violet absorbance readings at 595 nm using a 96-well BioTek Synergy-2 plate reader, identified to be 0.94 for the wild-type and 0.81 for the *pepZ* mutant. RN6390 was used as a negative control, with an average biofilm absorbance reading of 0.088.

Analysis of the Importance of PepZ during Interaction with Components of the Human Immune System. Evasion of host immune factors is vital to the survival and persistence of pathogens within the host. Thus, experiments exploring the role of PepZ in response to interactions with the human immune system were performed in collaboration with Dr. Jan Potempa from the Jagiellonian University, Krakow, Poland. A human model of macrophage survival and clearance was performed with the Newman wild-type and its *pepZ* mutant strain in two independent experiments. Cell viability was monitored by quantitative plating at hours 0, 2, 24, 48, 72 and 96 post-inoculum, yielding reduced levels of survival in the Newman *pepZ* mutant strain. Viable counts identified a 15-fold decrease in survival at 2 hours for the *pepZ* mutant when compared to the wild-type (Fig. 25). This was followed by further declines in mutant survival of 240-fold at 24 hours and 129-fold at 48 hours. These results suggest PepZ is important for host immune system interaction, and evasion.

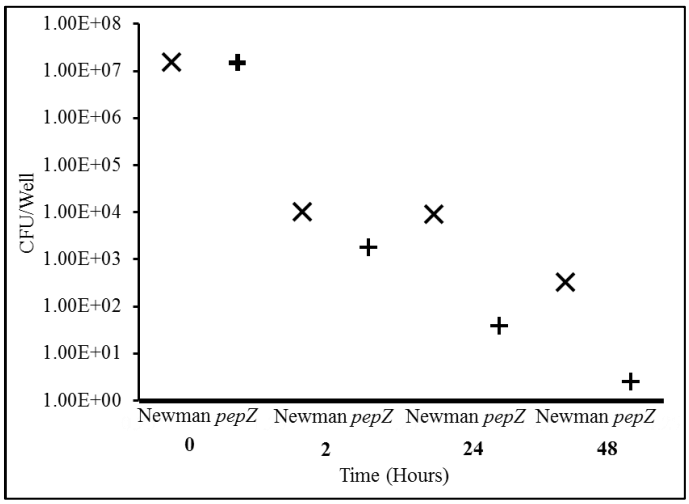

Figure 25. Characterization of the Role of PepZ in Human Immune System Interactions. Human models of macrophage survival and clearance was performed in strains Newman (**X**) and Newman *pepZ* (+). The *pepZ* mutant showed a consistent impairment in viability while interacting with components of the human immune system. Data is represented as CFU/well measured at the indicated time intervals from 2 independent experiments.

Further Characterization of the Role of PepZ in *S. aureus* Virulence using a Murine Model of Wound Formation. We sought to corroborate our findings of alterations in systemic virulence of *pepZ* mutant strains by investigating the role of this enzyme in localized infections, using a murine model of abscess formation. Ten hairless, SKH-1 immunocompetent mice were inoculated subcutaneously in the right flank with 1 x 10^8 CFU of either the USA300 FPR wild-type or *pepZ* mutant. Infections were monitored for seven days and any abscesses formed were harvested following animal euthanasia [Bunce et al., 1992; Chan and Foster, 1998]. The bacterial load per abscess was determined by recovery from abscess homogenates, and yielded 8.10 x 10^7 CFU per abscess for the wild-type, or 85% of the original inoculum (Fig. 26). In contrast, 35% of the *pepZ* mutant inoculum was recovered, or 3.51 x 10^7 CFU per abscess. This resulted in a 2.3-fold reduction in bacterial load of the USA300 FPR *pepZ* mutant, which was found to be

statistically significant ($p<0.03$). This further suggests that PepZ is required for full virulence of *S. aureus*, and is not confined to a single strain or lineage.

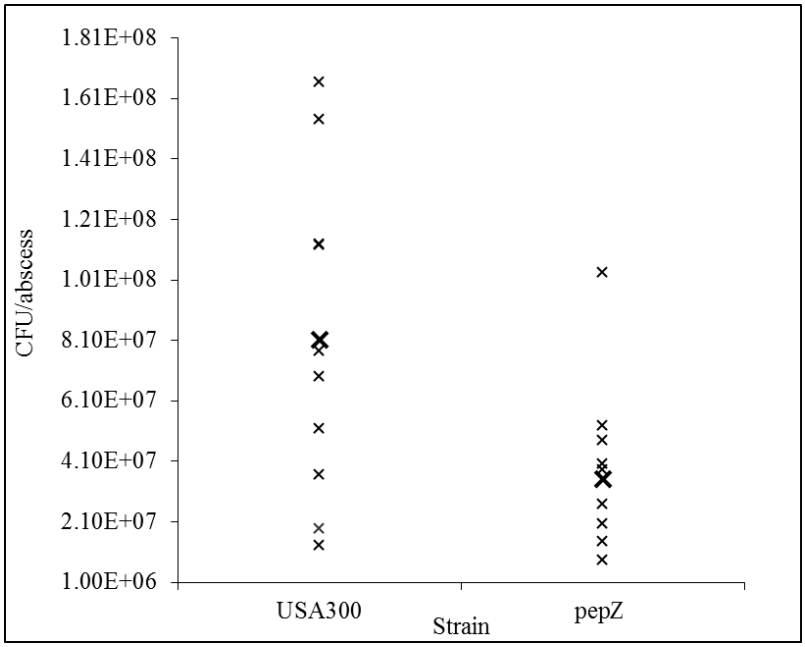

Figure 26. PepZ is Required for Full Virulence of CA-MRSA Strains in a Murine Model of Wound Formation. The USA300 FPR wild-type and *pepZ* mutant were used to subcutaneously inoculate 10 mice each with a bacterial load of 1×10^8. A 2.3-fold ($p<0.03$) bacterial load reduction of the USA300 FPR *pepZ* mutant was identified Results are represented as CFU/abscess. The average CFU/abscess is indicated by a bold marker for both wild-type and mutant.

Evaluating the Role of *pepZ* in CA-MRSA Sepsis using a Mouse Model. We next set out to characterize the role of PepZ in *S. aureus* virulence using a CA-MRSA model of murine sepsis. Ten CD-1 immunocompetent mice were inoculated via tail vein injection with 100 µl of 1.00×10^8 CFU ml^{-1} USA300 FPR wild-type or *pepZ* mutant cells. Strikingly, all mice inoculated with the USA300 FPR wild-type strain died within 24 hours following injection. In comparison, two of the ten mice injected with the USA300 FPR *pepZ* mutant strain died two days post inoculation, with the remaining eight surviving the seven day experimental period (Fig. 27). These results are in accordance

with all former virulence assays performed; further substantiating that PepZ is required for full virulence of *S. aureus*.

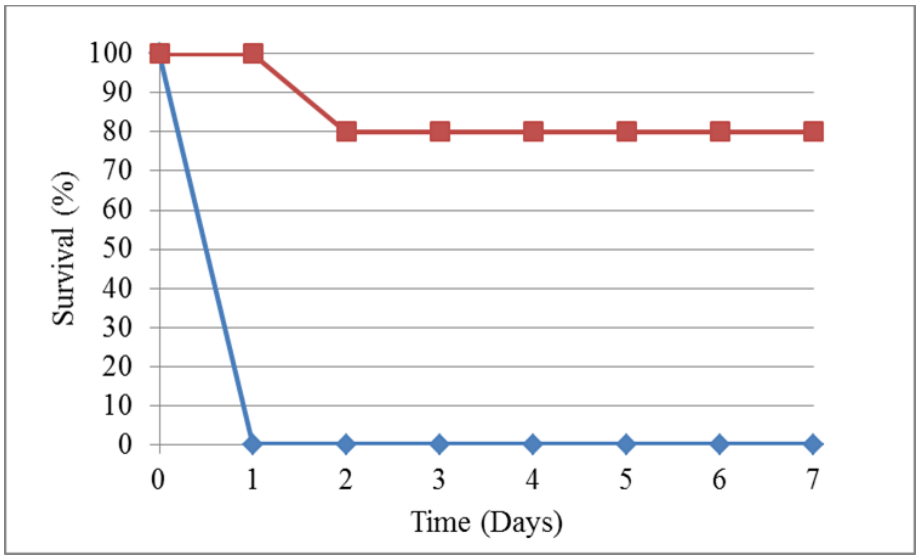

Figure 27. The Role of *pepZ* in CA-MRSA Sepsis. Ten mice each were tail vein inoculated with either the USA300 FPR (◆) wild-type or USA300 FPR *pepZ* (■) mutant. All mice inoculated with the USA300 FPR wild-type strain died within 24 hours following injection, compared to only two deaths for mice injected with *pepZ* mutant cells. Data is represented as percent survival over time.

Discussion

During a previous screen in our laboratory focused on the role of proteases in *S. aureus* virulence, we identified a mutant in aminopeptidase Z as being attenuated in disease causation. This phenotype, as determined using a murine model of septic arthritis, led us to begin the initial characterization of PepZ to determine the role(s) it fulfills in *S. aureus* physiology, nutrition and pathogenesis. BLAST analysis of the PepZ protein sequence PepZ revealed homology to the cytoplasmic aminopeptidase M17 family of exopeptidases (Fig. 28). Aminopeptidases serve an array of functions in the microbial cell ranging from the degradation of damaged proteins, to providing sources of energy and nutrition [Taylor, 1993, Chandu and Nandi, 2003; Patil et al., 2007; Miller, 1978]. It has been speculated that the primary role of externalized aminopeptidases is to liberate free amino acids from exogenous peptides, which are required for nutritional purposes and continual cell growth [Maeda et al., 1996]. In addition to roles in nutrition, aminopeptidase activity may be important in proteolytic cleavage events in a variety of organisms [Gonzales and Robert-Baudouy, 1996]. Proteomic analysis using CA-MRSA strains identified aminopeptidase PepV in early exponential and stationary phase secretomes, as well as aminopeptidases PepS, PepP and $PepT_2$ in stationary phase secretomes [Burlak et al., 2007], suggesting a role for aminopeptidases beyond the confines of the cell membrane. Thus, the basis of this study is driven by two

hypothesized roles for PepZ in *S. aureus*; the first being in the processing of exogenous oligopeptides for nutrition, and the second in protein stability, activation and degradation.

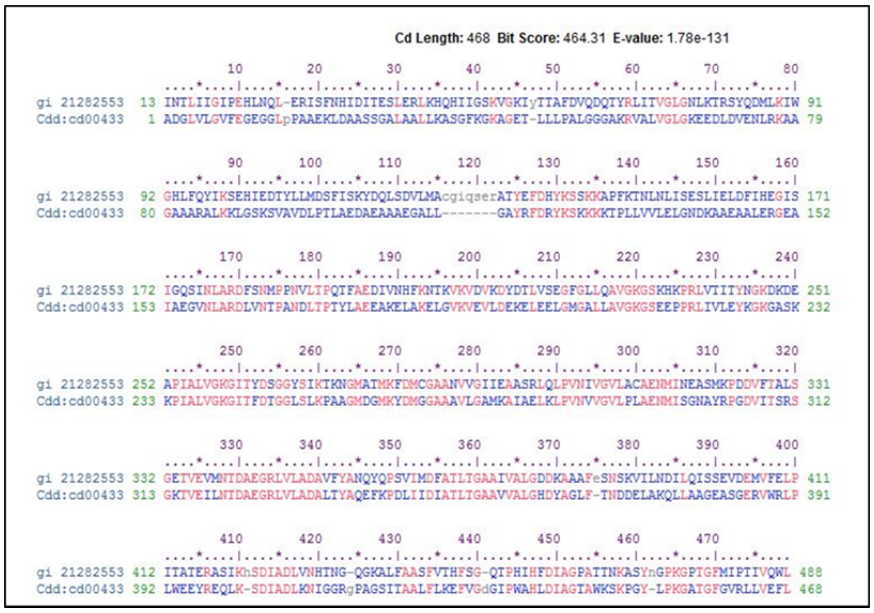

Figure 28. BLAST Analysis of PepZ Reveals Homology to Intracellular Leucine Specific Aminopeptidases from Other Organisms. BLAST analysis of the amino acid sequence of PepZ demonstrates homology to N-terminal cytoplasmic exopeptidases from the aminopeptidase family M17. The M17 family of aminopeptidases includes the hexametric leucine aminopeptidases, which contain metal ions within their catalytic domain.

The proteolytic processing of imported oligopeptides by cellular aminopeptidases is important for nutrition and continued cell viability [Linderstrom-Lang, 1929; McDonald, 1986; Rawlings, 2004]. As such, we sought to investigate the role of PepZ in *S. aureus* nutrition, using both peptide rich (milk) media and TSB. Growth analysis performed in milk media using wild-type strains Newman and USA300 FPR, and their respective *pepZ* mutants, identified similar growth profiles, with only one distinct phase of exponential growth, indicating the use of free peptides only [Borezee-Durant et al., 2009]. Conversely, previous observations identified decreased growth for *Lactobacillus lactis* cells lacking aminopeptidase PepN when provided casein as a carbon source, necessitating the

proteolytic activity of this aminopeptidase when grown in peptide rich media [Mierau et al., 1996]. We therefore contend that PepZ is dispensable for growth in media where peptides form the sole nitrogen source, possibly resulting from the redundant activities of cellular peptidases or a potential function for growth in other specialized conditions or environmental niches [Yen et al., 1980; Conlin and Miller, 1995].

Starvation analysis performed using cultures grown in aerated TSB also failed to identify any changes in cell viability. This dispensable role for PepZ under these conditions reflects previous observations in *Salmonella typhimurium*, which found that aminopeptidase PepN did not contribute to growth in nutrient rich media [Patil et al., 2007]. Conditions of growth were performed both static and shaking, to monitor the effects of oxygen tension on PepZ, in accordance with previous observations associating increased levels of oxygen with protease maturation and activation [Lindsay and Foster, 1999]. We found reduced survivability for *pepZ* mutant cells grown in milk under static conditions after four weeks, or aerobic growth after one week. These results indicate the aminopeptidase activity of PepZ is most important during the initial periods of long-term starvation; consistent with the abundance of nutrients present during early time periods, which dissipates over time as they are used by the cell. Indeed, nutritional analysis in *L. lactis* identified that the starvation response is limited to the first few hours following media carbohydrate exhaustion, which may indicate the presence of additional mechanisms for cell survival under conditions of starvation in *S. aureus* [Otto et al., 1983; Poolman and Konings, 1988]. Further, decreased growth rates of *pepZ* mutants cells grown in milk possibly indicates reduced activities of oligopeptide transport systems, due

to the intracellular pooling of peptides in the absence of the peptidase [Mierau et al., 1996]. In response to decreased protease activities for PepZ deficient cells, an intracellular accumulation of unprocessed peptides is likely, reflecting a nutrient surplus and decrease in the activities of oligopeptide transport systems. This type of regulation has been observed in *S. aureus*, in which CodY, a negative regulator of genes involved in amino acid synthesis and transport, was shown to repress oligopeptide transporters due to the intracellular accumulation of branched-chain amino acids and GTP [Pohl et al., 2009]. A potential regulatory role for CodY on *pepZ* is supported in a study by Majerczyk et al., 2010, which showed decreased expression of *pepZ* in a *codY* deficient *S. aureus* strain [Majerczyk et al., 2010]. Interestingly, CodY has been shown to regulate the activation of various virulence determinants as well, potentially associating PepZ with virulence. Cells deficient in *pepZ* were also grown competitively in cocultures with their respective parent strains, in either milk or TSB. The *pepZ* mutants showed decreased fitness in both backgrounds when cultured either statically or while shaking, in peptide based media or TSB. The impaired ability of *pepZ* mutant strains to compete for nutrients while in coculture with *S. aureus* wild-types, suggests a possible intracellular proteolytic role for PepZ and increased cellular fitness. Additionally, *pepZ* mutant cells grown in static cocultures compared to shaking cocultures showed a greater ability to compete for nutrients while in competition with the parent strain, possibly due to increased oxidative stresses, associated with the greater oxygen levels. Therefore, one can conclude that PepZ may negatively affect the ability of *S. aureus* to counteract oxidative stress. This hypothesis is in accordance with our general stress analysis experiments, which identified increased menadione resistance in a USA300 FPR *pepZ* mutant (15.6 mm) when

compared to the parent (36 mm). Of note, previous research has shown that organisms deficient in aminopeptidase activity are better placed for survival when some cellular stresses are incurred. In *E. coli*, it was shown that aminopeptidase PepN negatively regulates sodium-salicylate-induced stress, and the protease activity of PepN on certain peptides may result in a decreased ability of the organism to resist such conditions [Chandu and Nandi, 2003].

The role of PepZ during anaerobic growth was investigated using chemically defined media, in accordance with previous observations that both oxygen and nutrient limiting conditions impact aminopeptidase expression [Strauch et al., 1985; Jamieson and Higgins, 1984]. The inability to proliferate when limited for amino acids in the absence of oxygen was observed for both the Newman and USA300 FPR *pepZ* mutant strains compared to the wild-type. Interestingly, NAD-specific glutamate dehydrogenase, a protein that functions in amino acid degradation, was identified in our proteomic analysis to be of greater abundance in USA300 FPR PepZ deficient intracellular proteomes compared to the wild-type. Additionally, aminopeptidase PepA has been hypothesized to maintain housekeeping roles, including amino acid recycling in *E. coli* and *S. typhimurium* [Miller, 1996]. As such, these results suggest a potential intracellular role for PepZ in peptide turn over and amino acid recycling during nutrient limiting conditions.

Further, the USA300 FPR *pepZ* mutant showed impairment when grown under anaerobic conditions limited for phosphate, compared to the wild-type. These results are similar to

the reported increase in the transcription of aminopeptidase *pepN* in *E. coli* when subjected to conditions of phosphate starvation, anaerobiosis, and growth in minimal media [Gharbi et al., 1985]. In addition, the same study identified a slight impact on the expression of aminopeptidase *pepN* by an alkaline phosphatase (AP) encoded in the *pho* operon [Gharbi et al., 1985]. Alkaline phosphatase activity has previously been shown to increase under phosphate limiting conditions [Horiuchi et al., 1959]. Indeed, AP is typically synthesized during conditions of low phosphate, and repressed when it is abundant. It is also produced by bacteria limited for organic carbon substrates, which are the end product of phosphodiester hydrolysis [Hoppe, 2003; Hoppe and Ullrich, 1999]. Thus, it would be expected that alkaline phosphatase would be induced when grown on chemically defined media and limited for various nutrients. It is therefore tempting to speculate that *pepZ* expression is controlled by nutrient sensing regulators (such as CodY and CcpA) in *S. aureus* and contributes to cell viability in environments deficient in phosphate.

Interestingly, the failure of a USA300 FPR *pepZ* mutant to grow on MSA media under conditions of anaerobiosis suggests either a role for PepZ in the utilization of mannitol or osmotic stress. In *Listeria monocytogenes,* large accumulations of certain peptides resulted from either high or low levels of osmolarity, with the accumulated peptides found to contribute to osmoregulation [Maria-Rosario et al., 1995]. As such, the failure of a *pepZ* mutant to grown on media containing elevated sodium chloride levels, MSA, tends to suggest a possible role for PepZ in osmotic stress, resulting from an increase in

intracellular peptides due to a deficiency in aminopeptidase activity, or in the utilization of mannitol as a carbon source for nutrition.

The role of PepZ in protein degradation and turnover in response to protein denaturing conditions was investigated using heat shock and adaptation experiments. We identified a decreased capacity for survival in the Newman *pepZ* mutant strain compared to the wild-type strain, which suggests a role for PepZ at higher temperatures in the Newman background. A previous study identified mutants defective in aminopeptidase PepS produced a similar phenotype in response to elevated temperatures in *Streptococcus thermophilus,* resulting from of decreased degradation of malformed proteins, negatively affecting growth [Thomas et al., 2010].

Western blot analysis performed using proteomes collected from wild-type and *pepZ* mutant strains at hours 5 and 15, identified PepZ in the secretome during both exponential and post exponential growth. This subcellular localization of PepZ beyond the cytoplasm indicates a probable extracellular role for this enzyme. The lack of an identifiable signal sequence for PepZ does not preclude its potential for secretion and possible extracellular activity. Specifically, Ess, a type VII-like secretion system identified in *S. aureus* has been implicated in the development of staphylococcal infections, and deficiencies in the Ess system demonstrated reduced virulence in mice [Burts et al., 2008; Anderson et al., 2011]. As such, it appears that PepZ, while lacking an identifiable signal sequence, could potentially be externalized by the Ess system, in which the externalized protease activity could contribute towards virulence in *S. aureus*

by potentially degrading host factors. Future work could seek to characterize the potential for PepZ secretion by the Ess pathway using various methods of proteomic analysis to identify potential protein-protein interactions.

Profiling of secreted and intracellular proteomes from USA300 FPR wild-type and *pepZ* mutant strains using 2D-DIGE was performed on three hour cultures to elucidate how PepZ fulfills its enzymatic role at the level of protein stability. 2D-DIGE secretome analysis identified variations in protein molecular weight due to altered protein stability in the absence of PepZ. Many of the proteins identified were found to be involved in cell wall turnover and maintenance, nucleic acid processing and virulence [Fischer et al., 1981; Oshida et al., 1995; Cuatrecasas et al., 1967; Tucker et al., 1978; Gillett et al., 2002; Dunman et al., 2001]. A protein involved in the synthesis of the cell wall, lipoteichoic acid synthase, was reduced in two spots by 1.57-fold and 1.56-fold, and differentially processed in the absence of PepZ. It has been shown previously [Gründling and Schneewind, 2007] that *S. aureus* cells lacking lipoteichoic acid synthase result in defects in cell envelope and cell division. Further, a proposed function of lipoteichoic acid includes targeting of autolysins to the bacterial envelope [Fischer et al., 1981]. Our 2D-DIGE analysis also found the major autolysin (Atl) to be reduced by 1.57 to 1.94-fold in five different spots, with modified stability in the absence of PepZ. In *S. aureus*, Atl is a bifunctional protein that must undergo proteolytic processing to release two functional, lytic enzymes that participate in cell division and separation, cell lysis, and the release of peptidoglycan at the cell surface [Foster, 1995; Oshida et al., 1995]. Interestingly, the N-terminal domain of Atl, an N- acetylmuramoyl-L-alanine amidase, was determined to be

reduced by 1.49-fold to 1.72-fold from nine different spots in our 2D-DIGE analysis, and have modified protein stability in PepZ deficient strains. Thus, it appears possible that PepZ aids in cell wall turnover, corroborating our data from cell lysis experiments, which demonstrate decreased membrane stability under lytic conditions for cells deficient in PepZ.

2D-DIGE analysis performed on the cytoplasmic proteomes identified changes in protein abundance and stability for various proteins involved in protein synthesis, amino acid transport and metabolism, protein folding and degradation, peptide transport, and virulence [Kuroda et al., 2001; Frees et al., 1999; Gaillot et al., 2000; Park et al., 1999; Golonka et al., 2004, Highlander et al., 2007]. The wide range of functional roles for the identified proteins, as well as the abundance of proteins (30) identified from only eleven spots, demonstrates the limitations of this method of analysis. Image analysis performed following the first method for protein separation, isoelectric focusing, produced suboptimal protein separation patterns, with protein clustering at the acidic regions. As a result, protein overlapping and clustering was observed due to incomplete separation. This lack of protein separation can be attributed to the use of a broad pH range immobilized pH gradient (IPG) strip for protein separation during isoelectric focusing. IPG strips provide stable pH gradients for protein focusing according to the isoelectric points of the proteins [Bjellqvistn et al., 1982]. Therefore, the use of narrow range IPG strips allows proteins with similar isoelectric points to separate over a greater distance, resulting in enhanced protein resolution, and added specificity for mass spectrometry based protein identification [Issaq and Veenstra, 2008]. As such, the analysis of USA300

FPR wild-type and PepZ mutant intracellular proteomes could be optimized with the use of a narrow range IPG strip for greater specificity of proteins in the acidic pH range.

Strains deficient in *pepZ* were identified to be attenuated in both *in vivo* and *in vitro* models of virulence. *In vitro* analysis performed using murine models of wound formation and bacterial sepsis and dissemination, both demonstrated a significantly attenuated ability of *pepZ* mutants to sustain infection. Further, Newman wild-type and *pepZ* mutant cells were used to infect human macrophages, and a reduced survivability was observed for cells lacking *pepZ* by 240-fold following 24 hours of incubation, and 129-fold following 48 hours, when compared to the parent strain. These results conflict with a previous observation for aminopeptidase activity in *S. typhimurium*, in which a *pepN* mutant was impaired in its ability to interact with components of the immune system [Patil et al., 2007]. Collectively, these results suggest that the novel aminopeptidase activity of PepZ is important for host immune system interaction and evasion, and is required for full virulence in *S. aureus,* regardless of strain lineage. This was determined using strain USA300 FPR, a CA-MRSA clinical strain and strain Newman, a methicillin sensitive, MSSA, clinical strain, in the models of infections. The use of a CA-MRSA model, USA300 FPR, allowed for the analysis of PepZ using a current clinically relevant strain for analysis. The data we present herein suggests a possible role for PepZ in the degradation of host factors that may control bacterial growth, or potentially cleave a variety of secreted staphylococcal proteins that directly stimulate and maintain intracellular infections. Proteases function in a wide variety of essential regulatory and housekeeping functions, and secreted proteases regulate protein

maturation and activation events. In *S. aureus*, proteases are secreted in a temporal manner, many of which have been shown to contribute towards the progression of disease [Chan and Foster, 1998; Karlsson and Arvidson, 2002; Lindsay and Foster, 1999; McAleese et al., 2001; McGavin et al., 1997; Rice et al., 2001; Shaw et al., 2004].

S. aureus is a highly ubiquitous organism that has been implicated in a wide spectrum of diseases ranging from skin and soft tissue infections to life threatening septicemia [Lowry, 1998]. These manifestations of disease are the result of virulence factors expressed by the organism, and include toxins, hemolysins, and proteases [Novick, 2006]. Typically, these are secreted factors which directly interact with the host during infection, and facilitate invasion and colonization [Cheung et al., 1992, 2008; Janzon et al., 1989; Peng et al., 1988]. In this study, we have demonstrated that PepZ, a novel leucine-specific aminopeptidase is essential for pathogenesis in *S. aureus*, with no direct role in *S. aureus* nutrition. The data presented here suggests that PepZ may function in the degradation of host factors that may control bacterial growth, or potentially cleave a variety of secreted staphylococcal proteins that directly stimulate and maintain intracellular infections. Phenotypic characterization of PepZ has shown that *S. aureus* strains deficient in the aminopeptidase have a decreased capacity for survival under stress conditions associated with protein denaturing. These phenotypes tend to indicate a role for PepZ in protein stability, activation and degradation, which could be associated with the nutritional status of the cell via various regulatory proteins. This is in accordance with transcriptional regulators such as CcpA and CodY that have been shown to link cell

metabolism to the regulation of virulence determinants in *S. aureus* [Iyer et al., 2005; Seidel et al., 2006; Abranches et al., 2008; Majerczyk et al., 2008].

Future Directions

Future approaches for further elucidating the role of aminopeptidase PepZ in *S. aureus* virulence could explore potential alterations in the global metabolism of wild-type and *pepZ* deficient strains. This method of analysis would seek to identify potential substrates of PepZ according to cellular metabolites. Additional characterization may seek to explore the roles of the remaining twelve aminopeptidases in *S. aureus* for further insight into the role of PepZ by virtue of the activity of the remaining peptidases. This method of investigation could be performed through the construction of single and multiple peptidase mutants, followed by nutritional analysis and phenotypic characterization experiments. Future directions may also include the investigation of oligopeptide transport systems to identify specific substrates for PepZ or peptide cleavage sites, according to imported peptides and their subsequent processing by PepZ. Again, the investigation of the transport systems could be performed through the construction of single and multiple mutants in their respective genes, followed by nutritional analysis and phenotypic characterization experiments. Further analysis of *pepZ* regulation by CodY under conditions of limited nutrients could potentially clarify a role for the aminopeptidase in *S. aureus* virulence. This method of analysis could be carried out using murine models of infection to investigate the impact of a *pepZ*/*codY* double mutant on the ability of *S. aureus* to cause infection. In addition, the construction of *pepZ-lacZ* reporter fusion strains deficient in *codY* could explore the regulatory effects of CodY on *pepZ*

expression, which could also be investigated using RT-PCR. Exploring the potential for regulation of PepZ by CodY may identify regulatory roles for PepZ in transcription, in accordance with previous reports that PepA, a M17 leucine specific aminopeptidase, was found to regulate pyrimidine biosynthesis at the transcriptional level in *E. coli* [Charlier et al., 2000].

References

1. (1944) Discussion on Penicillin. Proc R Soc Med. 37(3): 101-12.

2. (1999) Four Pediatric Deaths From Community-Acquired Methicillin-Resistant *Staphylococcus aureus*—Minnesota and North Dakota, 1997-1999. JAMA: The Journal of the American Medical Association 282: 1123-1125.

3. Abranches, J., M. M. Nascimento, et al., (2008). CcpA regulates central metabolism and virulence gene expression in *Streptococcus mutans*. J. Bacteriol. 190(7), 2340-2349.

4. Aiello AE, Lowy FD, Wright LN, Larson E.L. (2006). Methicillin-resistant *Staphylococcus aureus* among US prisoners and military personnel: review and recommendations for future studies. Lancet Infect Dis; 6:335–41.

5. Akiyama Y, Kanehara K, Ito K. (2004). RseP (YaeL), an *Escherichia coli* RIP protease, cleaves transmembrane sequences. EMBO J 23: 4434-4442.

6. Anderson M, Chen Y-H, Butler EK, Missiakas D.M. (2011). EsaD, a Secretion Factor for the Ess Pathway in *Staphylococcus aureus*. J. Bacteriol. 193, 1583-1589.

7. Barber, M., and M. Rozwadowska-Dowzenko (1948). Infection by penicillin-resistant staphylococci. Lancet ii: 641-644.

8. Bauman SJ, Kuehn M.J. (2006). Purification of outer membrane vesicles from *Pseudomonas aeruginosa* and their activation of an IL-8 response. Microbes and Infection 8: 2400-2408.

9. Batchelor, F.R., Doyle F.P., Nayler, J.H.C., Rolinson, G.N. (1959). Synthesis of Penicillin: 6-Aminopenicillanic Acid in Penicillin Fermentations. Nature (London) 183: 257-8.

10. Bazan, J. F., Weaver, L. H., Roderick, S. L., Huber, R., and Matthews, B.W. (1994). Proc. Natl. Acad. Sci. U.S.A. 91, 2473–2477.

11. Beenken, K. E., J. S. Blevins, et al., (2003). Mutation of *sarA* in *Staphylococcus aureus* Limits Biofilm Formation. Infect. Immun. 71(7): 4206-4211.

12. Beenken KE, Mrak LN, Griffin LM, Zielinska AK, Shaw LN, et al., (2010). Epistatic Relationships between *sarA* and *agr* in *Staphylococcus aureus* Biofilm Formation. PLoS ONE *5*(5): e10790.

13. Behari J, Stagon L, Calderwood S.B. (2001). *pepA*, a Gene Mediating pH Regulation of Virulence Genes in *Vibrio cholerae*. J. Bacteriol. 183, 178-188.

14. Ben-Bassat A, Bauer K, Chang SY, Myambo K, Boosman A., et al., (1987). Processing of the initiation methionine from proteins: properties of the *Escherichia coli* methionine aminopeptidase and its gene structure. J. Bacteriol. 169, 751-757.

15. Bjellqvist, B., K. Ek, P.G. Righetti, E. Gianazza, A.Gorg, R.Westermeier, and W. Postel (1982). Isoelectric focusing in immobilized pH gradients: principle, methodology and some applications. J. Biochem. Biophys. Methods 6:317-339.

16. Boles BR, Horswill A.R. (2008). Agr-mediated dispersal of *Staphylococcus aureus* biofilms. PLoS Pathog 4 (4).

17. Borezee-Durant E, Hiron A, Piard J-C, Juillard V. (2009). Dual Role of the Oligopeptide Permease Opp3 during Growth of *Staphylococcus aureus* in Milk. Appl.

18. Brown, M.S., Ye, J., Rawson, R.B., and Goldstein, J.L. (2000). Regulated Intramembrane Proteolysis: A control mechanism conserved from bacteria to humans. Cell 100: 391–398.

19. Bunce C, Wheeler L, Reed G, Musser J, Barg N. (1992). Murine Model of Cutaneous Infection with Gram-Positive Cocci. Infect Immun. 60: 2636–2640.

20. Burlak C, Hammer CH, Robinson M-A, Whitney AR, McGavin M.J., et al., (2007). Global analysis of community-associated methicillin-resistant Staphylococcus.

21. Burts, M. L., DeDent, A. C. and Missiakas, D. M. (2008). EsaC substrate for the ESAT-6 secretion pathway and its role in persistent infections of *Staphylococcus aureus*. Molecular Microbiology, 69: 736–746.

22. Calander A-M, Jonsson I-M, Kanth A, Arvidsson S, Shaw L., et al., (2004). Impact of staphylococcal protease expression on the outcome of infectious arthritis. Microbes and Infection 6: 202-206.

23. Cao M, Wang T, Ye R, Helmann J.D. (2002). Antibiotics that inhibit cell wall biosynthesis induce expression of the *Bacillus subtilis* σ^W and σ^M regulons. Molecular Microbiology 45(5): 1267-1276.

24. Cassat JE, Dunman PM, McAleese F, Murphy E, Projan S.J., et al., (2005). Comparative genomics of *Staphylococcus aureus* musculoskeletal isolates. J. Bacteriol. 187, 576–592.

25. Chambers, H. F. (2001). The changing epidemiology of *Staphylococcus aureus*? Emerg Infect Dis. 7(2): 178–182.

26. Chambers, H. F. and F. R. DeLeo (2009). Waves of resistance: *Staphylococcus aureus* in the antibiotic era. Nat Rev Micro 7(9): 629-641.

27. Chan PF, Foster S.J. (1998). The role of environmental factors in the regulation of virulence-determinant expression in *Staphylococcus aureus* 8325-4. Microbiology 144: 2469-2479.

28. Chandu D, Nandi D. (2003). PepN is the major aminopeptidase in *Escherichia coli* insights on substrate specificity and role during sodium-salicylate-induced stress. Microbiology 149: 3437-3447.

29. Chang, S. Y., McGary, E. C. & Chang, S. (1989). Methionine aminopeptidase gene of *Escherichia coli* is essential for cell growth. J. Bacteriol. 171, 4071–4072.

30. Charlier D, Gigot D, Huysveld N, Roovers M, Piérard A., et al., (1995). Pyrimidine Regulation of the *Escherichia coli* and *Salmonella typhimurium carAB* Operons: CarP and Integration Host Factor (IHF) Modulate the Methylation Status of a GATC Site Present in the Control Region. Journal of Molecular Biology 250: 383-391.

31. Cheung AL, Koomey JM, Butler CA, Projan SJ, Fischetti V.A. (1992). Regulation of exoprotein expression in *Staphylococcus aureus* by a locus (*sar*) distinct from *agr*. Proc Natl Acad Sci U.S.A. 89: 6462–6466.

32. Cheung, A. L., K. A. Nishina, et al., (2008). The SarA protein family of *Staphylococcus aureus*. The International Journal of Biochemistry & Cell Biology 40(3): 355-361.

33. Christensen JE, Dudley EG, Pederson JA, Steele J.L. (1999). Peptidases and amino acid catabolism in lactic acid bacteria. Antonie Van Leeuwenhoek 76:217-246.

34. Chung, C. H., and A. L. Goldberg (1981).The product of the lon (*capR*) gene in *Escherichia coli* is the ATP dependent protease, protease La. Proc. Natl. Acad. Sci. U.S.A. 78:4931–4935.

35. Conlin, C. A. & Miller, C. G. (1995). Dipeptidyl carboxypeptidase and oligopeptidase A from *Escherichia coli* and *Salmonella typhimurium*. Methods Enzymol. 248, 567–579.

36. Crosse, A.-M., Greenway, D. and England, R. (2000). Accumulation of ppGpp and ppGp in *Staphylococcus aureus* 8325-4 following nutrient starvation. Letters in Applied Microbiology, 31: 332–337.

37. Cui, L., H. M. Neoh, M. Shoji, and K. Hiramatsu (2009). Contribution of *vraSR* and *graSR* point mutations to vancomycin resistance in vancomycin intermediate *Staphylococcus aureus*. Antimicrob. Agents Chemother. 53:1231–1234.

38. Cuatrecasas P, Fuchs S, Anfinsen C.B. (1967). Catalytic Properties and Specificity of the Extracellular Nuclease of *Staphylococcus aureus*. Journal of Biological Chemistry 242: 1541-1547.

39. Cuypers HT, van Loon-Klaassen LA, Egberts WT, de Jong WW, Bloemendal H. (1982). The primary structure of leucine aminopeptidase from bovine eye lens.

40. Dancer, B. N., and J. Mandelstam (1975). Production and possible function of serine protease during sporulation of *Bacillus subtilis*. J. Bacteriol. 121, 406–410.

41. Deresinski, S. (2005). Methicillin-Resistant *Staphylococcus aureus*: An Evolutionary, Epidemiologic, and Therapeutic Odyssey. Clinical Infectious Diseases 40(4): 562-573.

42. Diep BA, Stone GG, Basuino L, Graber CJ, Miller A., et al., (2008). The Arginine Catabolic Mobile Element and Staphylococcal Chromosomal Cassette *mec* Linkage: Convergence of Virulence and Resistance in the USA300 Clone of Methicillin-Resistant *Staphylococcus aureus*. Journal of Infectious Diseases 197: 1523-1530.

43. Diep BA, Otto M. (2008). The role of virulence determinants in community-associated MRSA pathogenesis. Trends in Microbiology 16: 361-369.

44. Drapeau GR, Boily Y, Houmard J. (1972). Purification and Properties of an Extracellular Protease of *Staphylococcus aureus*. Journal of Biological Chemistry.

45. Dunman PM, Murphy E, Haney S, Palacios D, Tucker-Kellogg G., et al., (2001). Transcription Profiling-Based Identification of *Staphylococcus aureus* Genes Regulated by the *agr* and/or *sarA* Loci. J. Bacteriol. 183, 7341-7353.

46. Evers S, Quintiliani R Jr, Courvalin P. (1996). Genetics of Glycopeptides Resistance in Enterococci. Microb Drug Resist. 2(2): 219-23.

47. Fischer W, Rosel P, Koch H.U. (1981). Effect of alanine ester substitution and other structural features of lipoteichoic acids on their inhibitory activity against autolysins of *Staphylococcus aureus.* J. Bacteriol. 146, 467-475.

48. Foster, S. J. (1995). Molecular characterization and functional analysis of the major autolysin of *Staphylococcus aureus* 8325/4. J. Bacteriol.177, 5723-5725.

49. Fowler VG, Miro JM, Hoen B, Cabell CH, Abrutyn E., et al., (2005). *Staphylococcus aureus* Endocarditis. JAMA: The Journal of the American Medical Association 293: 3012-3021.

50. Franzetti B, Schoehn G, Hernandez JF, Jaquinod M, Ruigrok R.W.H., et al., (2002). Tetrahedral aminopeptidase: a novel large protease complex from archaea. EMBO J 21: 2132-2138.

51. Frees, D., Qazi, S. N. A., Hill, P. J. and Ingmer, H. (2003). Alternative roles of ClpX and ClpP in *Staphylococcus aureus* stress tolerance and virulence. Molecular Microbiology, 48: 1565–1578.

52. Fridkin SK, Hageman JC, Morrison M, Sanza LT, Como-Sabetti K., et al., (2005). Methicillin-Resistant *Staphylococcus aureus* Disease in Three Communities. New England Journal of Medicine 352: 1436-1444.

53. Fujimoto DF, Bayles K.W. (1998). Opposing Roles of the *Staphylococcus aureus* Virulence Regulators, Agr and Sar, in Triton X-100 and Penicillin-Induced Autolysis. J. Bacteriol. 180, 3724-3726.

54. Gaillot, M. Wetsch, N. Fortineau and P. Berche (2000). Evaluation of CHROM agar *Staphylococcus aureus*, a new chromogenic medium for isolation and presumptive identification of *Staphylococcus aureus* from human clinical isolates. J. Clin. Microbiol., 38, pp. 1587–1591.

55. Gharbi S, Belaich A, Murgier M, Lazdunski A. (1985). Multiple controls exerted on *in vivo* expression of the *pepN* gene in *Escherichia coli*: studies with *pepN-lacZ* operon and protein fusion strains. J. Bacteriol. 163, 1191-1195.

56. Gill SR, Fouts DE, Archer GL, Mongodin EF, DeBoy R.T., et al., (2005). Insights on Evolution of Virulence and Resistance from the Complete Genome Analysis of an Early Methicillin-Resistant *Staphylococcus aureus* Strain and a Biofilm-Producing Methicillin-Resistant *Staphylococcus epidermidis* Strain. J. Bacteriol. 187, 2426-2438.

57. Gillet Y, Issartel B, Vanhems P, Fournet J-C, Lina G., et al., (2002). Association between *Staphylococcus aureus* strains carrying gene for Panton Valentine leukocidin and highly lethal necrotizing pneumonia in young immunocompetent patients. The Lancet 359: 753-759.

58. Golonka E, Filipek R, Sabat A, Sinczak A, Potempa J. (2004). Genetic characterization of staphopain genes in *Staphylococcus aureus*. Biological Chemistry 385: 1059-1067.

59. Girish TS, Gopal B. (2010). Crystal Structure of *Staphylococcus aureus* Metallopeptidase (Sapep) Reveals Large Domain Motions between the Manganese-bound and Apo-states. Journal of Biological Chemistry 285: 29406-29415.

60. Graber CJ, Wong MK, Carleton HA, Perdreau-Remington F, Haller BL, Chambers H.F. Intermediate vancomycin susceptibility in a community-associated MRSA clone. Emerg Infect Dis 13: 491-3.

61. Grundling A, Schneewind O. (2007). Genes Required for Glycolipid Synthesis and Lipoteichoic Acid Anchoring in *Staphylococcus aureus*. J. Bacteriol. 189, 2521-2530.

62. Gonzales, T. and Robert-Baudouy, J. (1996). Bacterial aminopeptidases: Properties and functions. FEMS Microbiology Reviews, 18: 319–344.

63. H. J. Issaq and T. D. Veenstra (2008). Two-dimensional polyacrylamidegel electrophoresis (2D-PAGE): advances and perspectives, BioTechniques, vol. 44, no. 5, pp. 697–700.

64. Highlander S, Hulten K, Qin X, Jiang H, Yerrapragada S., et al., (2007). Subtle genetic changes enhance virulence of methicillin resistant and sensitive *Staphylococcus aureus*. BMC Microbiology 7: 99.

65. Horiuchi T, Horiuchi S, Mizuno D. (1959). A Possible Negative Feedback Phenomenon controlling Formation of Alkaline Phosphomonoesterase in *Escherichia coli*. Nature 183: 1529-1530.

66. Hoppe, H.G. (2003). Phosphatase activity in the sea. Hydrobiologia, 493, 187–200.

67. Hoppe, H.G.; Ullrich, S. (1999). Profile of ectoenzymes in the Indian Ocean: phenomena of phosphatase activity in the mesopelagic zone. Aquat. Microb. Ecol. 19, 139–148.

68. Imamura T, Tanase S, Szmyd G, Kozik A, Travis J., et al., (2005). Induction of vascular leakage through release of bradykinin and a novel kinin by cysteine proteinases from *Staphylococcus aureus*. The Journal of Experimental Medicine 201: 1669-1676.

69. Inaoka, T., K. Takahashi, et al., (2003). Guanine nucleotides guanosine 5' diphosphate 3'-diphosphate and GTP co-operatively regulate the production of an antibiotic bacilysin in *Bacillus subtilis*. J Biol Chem 278(4): 2169-2176.

70. Ito T, Katayama Y, Hiramatsu K. (1999). Cloning and nucleotide sequence determination of the entire *mec* DNA of pre-methicillin-resistant *Staphylococcus aureus* N315. Antimicrob Agents Chemother 43: 1449–1458.

71. Iyer, R., N. S. Baliga, et al., (2005). Catabolite control protein A (CcpA) contributes to virulence and regulation of sugar metabolism in *Streptococcus pneumoniae*. J. Bacteriol. 187(24), 8340-8349.

72. Jamieson, D. J., and C. F. Higgins (1984). Anaerobic and leucine-dependent expression of a peptide transport gene in *Salmonella typhimurium.* J. Bacteriol. 160, 131-136.

73. Janzon L, Lofdahl S, Arvidson S. (1989). Identification and nucleotide sequence of the delta-lysin gene, *hld*, adjacent to the accessory gene regulator *agr* of *Staphylococcus aureus*. Mol Gen Genet 219: 480–485.

74. Jevons, M. P. (1961). Br. Med. J. 1, 124–125.

75. Kanayama N, Kajiwara Y, Goto J, el Maradny E, Maehara K., et al., (1995). Inactivation of interleukin-8 by aminopeptidase N (CD13). Journal of Leukocyte Biology 57: 129-134.

76. Kaplan S.L., et al., (2005). Three-year surveillance of community-acquired *Staphylococcus aureus* infections in children. Clin Infect Dis; 40:1785–91.

77. Karlsson, A. and S. Arvidson (2002). Variation in Extracellular Protease Production among Clinical Isolates of *Staphylococcus aureus* Due to Different Levels of Expression of the Protease Repressor *sarA*. Infect. Immun. 70(8): 4239-4246.

78. Kerr J F R, Wyllie A H, Currie A. R. (1972). Apoptosis: a basic biological phenomenon with wide-ranging implications in tissue kinetics. Br J Cancer; 26:239–257.

79. Kim, H., and Lipscomb, W. N. (1993). Proc. Natl. Acad. Sci. U.S.A. 90, 5006–5010.

80. Kirby W.M. (1944). Extraction of a Highly Potent Penicillin Inactivator from Penicillin Resistant Staphylococci. Science 99(2579): 452-453.

81. Klein, J.O. and Finland M. (1963). The New Penicillins. N Engl J Med. 269: 1074-1082.

82. Klevens R.M., et al., (2007). Invasive methicillin-resistant *Staphylococcus aureus* infections in the United States. Jama; 298:1763–71.

83. Kobayashi, S. D. and F. R. DeLeo (2009). An update on community-associated MRSA virulence. Current Opinion in Pharmacology 9(5): 545-551.

84. Koziel J, Maciag-Gudowska A, Mikolajczyk T, Bzowska M, Sturdevant DE, et al., (2009). Phagocytosis of *Staphylococcus aureus* by Macrophages Exerts Cytoprotective Effects Manifested by the Upregulation of Antiapoptotic Factors. PLoS ONE 4: e5210.

85. Kumagai Y, Konishi K, Gomi T, Yagishita H, Yajima A., et al., (2000). Enzymatic Properties of Dipeptidyl Aminopeptidase IV Produced by the Periodontal Pathogen *Porphyromonas gingivalis* and Its Participation in Virulence. Infect Immun 68: 716-724.

86. Kumagai Y, Yagishita H, Yajima A, Okamoto T, Konishi K. (2005). Molecular Mechanism for Connective Tissue Destruction by Dipeptidyl Aminopeptidase IV Produced by the Periodontal Pathogen *Porphyromonas gingivalis*. Infect Immun 73: 2655-2664.

87. Kuroda M, Ohta T, Uchiyama I, Baba T, Yuzawa H., et al., (2001). Whole genome sequencing of methicillin-resistant *Staphylococcus aureus*. Lancet 357:1225-1240.

88. Lawrence, J R, Korber, D R, Hoyle, B D, Costerton, J W, Caldwell, D. E. (1991). Optical sectioning of microbial biofilms. J. Bacteriol. 173, 6558-6567.

89. Li M, Diep BA, Villaruz AE, Braughton KR, Jiang X., et al., (2009). Evolution of virulence in epidemic community-associated methicillin-resistant *Staphylococcus aureus*. Proc. Natl. Acad. Sci. U.S.A. 106: 5883-5888.

90. Linderstrom-Lang, Y. K. (1929). Uber Darmerepsin. HoppeSeyler's Z PhysioL Chern. 182, 151-174.

91. Lindsay JA, Foster S.J. (1999). Interactive regulatory pathways control virulence determinant production and stability in response to environmental conditions in *Staphylococcus aureus.* Molecular and General Genetics 262: 323-331.

92. Lowy, F. D. (1998). *Staphylococcus aureus* Infections. New England Journal of Medicine 339(8): 520-532.

93. Majerczyk CD, Dunman PM, Luong TT, Lee CY, Sadykov M.R., et al., (2010). Direct Targets of CodY in *Staphylococcus aureus*. J. Bacteriol. 192, 2861-2877.

94. Maeda, H., and T. Yamamoto (1996). Pathogenic mechanisms induced by microbial proteases in microbial infections. Biol. Chem. Hoppe-Seyler 377: 217–226.

95. Mani, N, Tobin, P, Jayaswal, R.K. (1993). Isolation and characterization of autolysis-defective mutants of *Staphylococcus aureus* created by Tn917-*lacZ* mutagenesis. J. Bacteriol. 175, 1493-1499.

96. Maria-Rosario A, Davidson I, Debra M, Verheul A, Abee T., et al., (1995). The role of peptide metabolism in the growth of *Listeria monocytogenes* ATCC 23074 at high osmolarity. Microbiology 141: 41-49.

97. Matsui, M., Fowler, J. H. & Walling, L. (2006). Leucine aminopeptidases: diversity in structure and function. Biological Chemistry 387, 1535-1544.

98. McAleese, F.M., E.J. Walsh, M. Sieprawska, J. Potempa, and T.J. Foster (2001). Loss of Clumping factor B fibrinogen binding activity by *Staphylococcus aureus* involves cessation of transcription, shedding and cleavage by metalloprotease. J Biol. Chem. 276:29969-78.

99. McDonald, J. K. (1986). A brief history of the study of mammalian exopeptidases. In Mammalian Proteases (McDonald, J. K., and Barrett, A. J., eds.) 2, 7-19, Academic Press, New York.

100. McGavin, M. J., C. Zahradka, R. Kelly, and J. E. Scott (1997). Modification of the *Staphylococcus aureus* fibronectin binding phenotype by V8 protease. Infect. Immun. 65:2621–2628.

101. Meehl, M., S. Herbert, F. Gotz, and A. Cheung (2007). Interaction of the GraRS two-component system with the VraFG ABC transporter to support vancomycin-intermediate resistance in *Staphylococcus aureus*. Antimicrob. Agents Chemother. 51:2679–268.

102. Miller CG, Schwartz G. (1978). Peptidase-deficient mutants of *Escherichia coli*. J. Bacteriol. 135, 603-611.

103. Miller C. G. Protein degradation and proteolytic modification. In: Neidhardt F C, Curtiss III R, Ingraham J L, Lin E C C, Low K B, Magasanik B, Reznikoff W S, Rilley M, Schaechter M, Umbarger H.E., editors. *Escherichia coli* and Salmonella: cellular and molecular biology. 2nd ed. Vol. 1. Washington, D.C.: American Society for Microbiology; 1996. pp. 938–954.

104. Mierau I, Kunji E, Leenhouts K, Hellendoorn M, Haandrikman A., et al., (1996). Multiple-peptidase mutants of *Lactococcus lactis* are severely impaired in their ability to grow in milk. J. Bacteriol. 178, 2794-2803.

105. Mwangi, M. M., S. W. Wu, Y. Zhou, K. Sieradzki, H. de Lencastre, P. Richardson, D. Bruce, E. Rubin, E. Myers, E. D. Siggia, and A. Tomasz. (2007). Tracking the *in vivo* evolution of multidrug resistance in *Staphylococcus aureus* by whole-genome sequencing. Proc. Natl. Acad. Sci. U.S.A. 104:9451–9456.

106. Nandi D, Tahiliani P, Kumar A and Chandu D. (2006). The ubiquitin-proteasome system; J. Biosci. 31:137–155.

107. National Nosocomial Infections Surveillance (NNIS) System Report. Data summary from January 1992 through June 2004, issued October 2004. Am J Infect Control. 2004; 32: 470–485.

108. Novick, R. P., H. F. Ross, S. J. Projan, J. Kornblum, B. Kreiswirth, and S. Moghazeh (1993). Synthesis of staphylococcal virulence factors is controlled by a regulatory RNA molecule. EMBO J. 12:3967–3975.

109. Novick R.P. (2006). Staphylococcal Pathogenesis and Pathogenicity Factors: Genetics and regulation. In: Fischetti VA, Novick RP, Ferretti JJ, Portnoy DA, Rood JI, editors. Gram-Positive Pathogens. Washington, D.C.: ASM Press. pp. 496–516.

110. Odintsov SG, Sabala I, Bourenkov G, Rybin V, Bochtler M. (2005). *Staphylococcus aureus* Aminopeptidase S Is a Founding Member of a New Peptidase Clan. Journal of Biological Chemistry 280(30): 27792-27799.

111. Oefner C, Douangamath A, D'Arcy A, Häfeli S, Mareque D., et al., (2003). The 1.15 Å Crystal Structure of the *Staphylococcus aureus* Methionyl-aminopeptidase and Complexes with Triazole Based Inhibitors. Journal of Molecular Biology 332: 13-21.

112. Ogston A. (1984). On Abscesses. Classics in Infectious Diseases. Rev Infect Dis 6(1): 122–28.

113. Oshida T, Sugai M, Komatsuzawa H, Hong Y-M, Suginaka H and Tomasz A. (1995). A *Staphylococcus aureus* autolysin that has an N-acetylmuramoyl-L-alanine amidase domain and an endo-β-*N*-acetylglucosaminidase domain: cloning, sequence analysis and characterization. Proc Natl Acad Sci U.S.A., 92, 285–289.

114. Otto, R., B. Ten Brink, H. Veldkamp, and W. N. Konings. (1983). The relationbetween growth rate and electrochemical proton gradient on *Streptococcus cremoris*. FEMS Microbiol. Lett. 16:69–74.

115. Pan ES, Diep BA, Carleton HA, Charlebois ED, Sensabaugh G.F., et al., (2003). Increasing prevalence of methicillin-resistant *Staphylococcus aureus* infection in California jails. Clin Infect Dis; 37:1384–8.

116. Park PW, Broekelmann TJ, Mecham BR, Mecham R.P. (1999). Characterization of the Elastin Binding Domain in the Cell-surface 25 kDa Elastin-binding Protein of *Staphylococcus aureus* (EbpS). Journal of Biological Chemistry 274: 2845-2850.

117. Patil V, Kumar A, Kuruppath S, Nandi D. (2007). Peptidase N encoded by *Salmonella enterica* serovar *typhimurium* modulates systemic infection in mice. FEMS Immunology & Medical Microbiology 51: 431-442.

118. Peng, H. L., Novick, R. P., Kreiswirth, B., Kornblum, J. & Schlievert, P. (1988). Cloning, characterization, and sequencing of an accessory gene regulator *agr* in *Staphylococcus aureus*. J. Bacteriol. 170, 4365-4372.

119. Pohl K, Francois P, Stenz L, Schlink F, Geiger T., et al., (2009). CodY in *Staphylococcus aureus*: a Regulatory Link between Metabolism and Virulence Gene Expression. J. Bacteriol. 191, 2953-2963.

120. Poolman, B., and W. N. Konings (1988). Relation of growth of *Streptococcus lactis* and *Streptococcus cremoris* to amino acid transport. J. Bacteriol. 170, 700–707.

121. Piriz-Duran, S., F. H. Kayser, and B. Berger-Bachi (1996). Impact of *sar* and *agr* on methicillin resistance in *Staphylococcus aureus*. FEMS Microbiol. Lett. 141:255–260.

122. Rawlings ND, O'Brien E, Barrett A.J. (2002). MEROPS: the protease database. Nucleic Acids Research 30: 343-346.

123. Rawlings, N.D. and Barrett, A.J. (2004). Introduction: Metallopeptidases and their clans. In: Handbook of Proteolytic Enzymes, 2nd Edition, A.J. Barrett, N.D. Rawlings, and J.F. Woesner, eds. (San Diego, USA: Elsevier/Academic Press), pp. 231–263.

124. Rawlings ND, Barrett A.J. (1995). Families of aspartic peptidases, and those of unknown catalytic mechanism. In: Alan JB, editor. Methods in Enzymology: Academic Press. pp. 105-120.

125. Reduced susceptibility of *Staphylococcus aureus* to vancomycin--Japan, 1996. MMWR Morb Mortal Wkly Rep. 1997 Jul 11; 46(27):624-6.

126. Rice K, Peralta R, Bast D, de Azavedo J, McGavin M.J. (2001). Description of Staphylococcus Serine Protease (*ssp*) Operon in *Staphylococcus aureus* and Nonpolar Inactivation of *sspA*-Encoded Serine Protease. Infect Immun 69: 159-169.

127. Ridley M, Barrie D, Lynn R, Stead K. (1970). Antibiotic-Resistant *Staphylococcus aureus* and Hospital Antibiotic Policies. Lancet; i: 230-3.

128. Russo S, Baumann U. (2004). Crystal Structure of a Dodecameric Tetrahedral-shaped Aminopeptidase. Journal of Biological Chemistry 279: 51275-51281.

129. Sambrook, J, Fritsche, E, Maniatis T. (2001). Molecular Cloning (a laboratory manual). New York: Cold Spring Harbour Laboratory.

130. Schenk S, Laddaga R.A. (1992). Improved method for electroporation of *Staphylococcus aureus.* FEMS Microbiol Lett.; 73:133.

131. Schneewind, O Mihaylova-Petkov, D. and Model P. (1993). Cell wall sorting signals in surface proteins of Gram-positive bacteria. The EMBO Journal; 1: (2)4803–4811.

132. Schneewind, O., Model, P. and Fischetti, V.A. (1992). Cell, 70, 267-281.

133. Seidl, K., M. Stucki, et al., (2006). *Staphylococcus aureus* CcpA affects virulence determinant production and antibiotic resistance. Antimicrob Agents Chemother 50(4): 1183-1194.

134. Shaw L, Golonka E, Potempa, J., Foster S.J. (2004). The role and regulation of the extracellular proteases of *Staphylococcus aureus*. Microbiology 150: 217-228.

135. Shaw LN, Golonka E, Szmyd G, Foster SJ, Travis J., et al., (2005). Cytoplasmic Control of Premature Activation of a Secreted Protease Zymogen: Deletion of Staphostatin B (SspC) in *Staphylococcus aureus* 8325-4 Yields a Profound Pleiotropic Phenotype. J. Bacteriol. 187, 1751-1762.

136. Shaw LN, Lindholm C, Prajsnar TK, Miller HK, Brown M.C., et al., (2008). Identification and Characterization of σ^S, a Novel Component of the *Staphylococcus aureus* Stress and Virulence Responses. PLoS ONE 3: e3844.

137. Sobral, R. G., Jones, A. E., Des Etages, S. G., Dougherty, T. J., Peitzsch, R. M., Gaasterland, T., Ludovice, A. M., de Lencastre, H., Tomasz, A. (2007). Extensive and Genome-Wide Changes in the Transcription Profile of *Staphylococcus aureus* Induced by Modulating the Transcription of the Cell Wall Synthesis Gene *murF*. J. Bacteriol.189, 2376-2391.

138. Sorsa, T Ingman, K Suomalainen, M Haapasalo, Y.T Konttinen, O Lindy, H Saari and V.J Uitto (1992). Identification of proteases from periodontopathogenic bacteria as activators of latent human neutrophil and fibroblast-type interstitial collagenases. Infect. Immun., 60, pp. 4491–4495.

139. Spoering, A. L., and M. S. Gilmore (2006). Quorum sensing and DNA release in bacterial biofilms. Curr. Opin. Microbiol. 9:133–137.

140. *Staphylococcus aureus* resistant to vancomycin–United States, 2002. MMWR Morb Mortal Wkly Rep. 2002; 51:565–56.

141. Staub, L and Sieber, S.A. (2009). J. Am. Chem. Soc. 131, 6271-6276.

142. Stirling, V.J., Colloms, S.D., Collins, J.F., Szatmari, G. and Sherratt, D. J. (1989). *xerB*, an *Escherichia coli* gene required for plasmid ColE1 site-specific recombination, is identical to *pepA*, encoding aminopeptidase A, a protein with substantial similarity to bovine lens leucine aminopeptidase. The EMBO J. 8, (5) 1623-1627.

143. Strater, N., Sherratt, D.J., and Colloms, S.D. (1999). X-ray structure of aminopeptidase A from *Escherichia coli* and a model for the nucleoprotein complex in Xer site-specific recombination. EMBO J. 18, 4513–4522.

144. Strauch, K. L., J. B. Lenk, B. L. Gamble, and C. G. Miller (1985). Oxygen regulation in *Salmonella typhimurium*. J. Bacteriol. 161, 673-680.

145. Sussman AJ, Gilvarg C. (1971). Peptide Transport and Metabolism in Bacteria. Annual Review of Biochemistry 40: 397-408.

146. Taylor A. (1993). Aminopeptidases: structure and function. The FASEB Journal 7: 290-298.

147. Tenover F.C. (2008). Vancomycin-Resistant *Staphylococcus aureus*: A Perfect but Geographically Limited Storm? Clinical Infectious Diseases 46: 675-677.

148. Thomas, S., Besset, C., Courtin, P. & Rul, F. (2010). The role of aminopeptidase PepS in the growth of *Streptococcus thermophilus* is not restricted to nitrogen nutrition. Journal of Applied Microbiology 108, 148-157.

149. Tsang LH, Cassat JE, Shaw LN, Beenken KE, Smeltzer M.S. (2008). Factors Contributing to the Biofilm-Deficient Phenotype of *Staphylococcus aureus sarA* Mutants. PLoS ONE 3(10): e3361.

150. Tucker PW, Hazen JrEE, Cotton F.A. (1978). Staphylococcal nuclease reviewed: A prototypic study in contemporary enzymology. I. Isolation, physical and enzymatic properties. Mol Cell Biochem, 22, 67–77.

151. Vancomycin-resistant *Staphylococcus aureus*–Pennsylvania, 2002. MMWR Morb Mortal Wkly Rep.; 51:902.

152. Wang Y, Dang Y, Wang X, Lu H, Wang X., et al., (2011). Comparative Proteomic Analyses of *Streptococcus suis* Serotype 2 Cell Wall-Associated Proteins. Current Microbiology 62: 578-588.

153. Watson, S. P., Clements, M. O. & Foster, S. J. (1998). Characterization of the Starvation Survival Response of *Staphylococcus aureus*. J. Bacteriol. 180, 1750-1758.

154. Wertheim HFL, Vos MC, Ott A, van Belkum A, Voss A., et al., (2004). Risk and outcome of nosocomial *Staphylococcus aureus* bacteremia in nasal carriers versus non-carriers. The Lancet 364: 703-705.

155. Woolwine SC, Wozniak D.J. (1999). Identification of an *Escherichia coli pepA* Homolog and Its Involvement in Suppression of the *algB* Phenotype in Mucoid *Pseudomonas aeruginosa*. J. Bacteriol. 181, 107-116.

156. Wu SW, Lencastre H, Tomasz A. (2001). Recruitment of the *mecA* Gene Homologue of *Staphylococcus sciuri* into a Resistance Determinant and Expression of the Resistant Phenotype in *Staphylococcus aureus.* J. Bacteriol. 183(8), 2417-2424.

157. Yaron, A. & Naider, F. (1993). Crit. Rev. Biochem. Mol. Biol. 28, 31–81.

158. Yarwood JM, McCormick JK, Schlievert P.M. (2001). Identification of a Novel Two-Component Regulatory System That Acts in Global Regulation of Virulence Factors of *Staphylococcus aureus*. J. Bacteriol. 183, 1113-1123.

159. Yen, C., Green, L. & Miller, C. G. (1980). Degradation of intracellular protein in *Salmonella typhimurium* peptidase mutants. J Mol Biol 143, 21–33.

160. Yinduo Ji, Barbara Zhang, Stephanie F. Van, Horn, Patrick Warren, Gary Woodnutt, Martin K. R. Burnham, and Martin Rosenberg (2001). Identification of Critical Staphylococcal Genes Using Conditional Phenotypes Generated by Antisense RNA. Science 293(5538): 2266.

Appendices

Appendix 1. Secreted Spots Determined by Mass Spectrometry Analysis to Have Undetectable Protein Levels

Spot	Fold Δ
2382	-6.31
220	-2.22
150	-1.84
215	-1.8
1155	-1.69
279	-1.69
310	-1.66
188	-1.66
458	-1.63
2280	-1.56
1277	-1.55
2293	-1.51
800	-1.5
167	-1.5
485	-1.33
1661	1.41
2796	1.53
1609	1.54
2104	1.59
1601	1.71
1563	1.71
1078	1.92
3088	2.02
2216	2.72
2233	2.89
446	3.26
1729	7.8

**USA300 FPR wild-type and pepZ mutant 2D-DIGE secreted protein spots that mass spectrometry analysis failed to detect protein for.*